Available online at www.sciencedirect.com
ScienceDirect
Coordination Chemistry Reviews 251 (2007) 2622–2664
COORDINATION CHEMISTRY REVIEWS
www.elsevier.com/locate/ccr

Review

Magnetic assemblies based on Mn(III) salen analogues

Hitoshi Miyasaka [a,b,*], Ayumi Saitoh [c], Satoshi Abe [c]

[a] *Department of Chemistry, Graduate School of Science, Tohoku University, 6-3 Aramaki-Aza-Aoba, Aoba-ku, Sendai, Miyagi 980-8578, Japan*
[b] *CREST, Japan Science and Technology Agency (JST), 4-1-8 Honcho, Kawaguchi, Saitama 332-0012, Japan*
[c] *Department of Chemistry, Graduate School of Science, Tokyo Metropolitan University, 1-1 Minami-ohsawa, Hachioji, Tokyo 192-0397, Japan*

Received 29 January 2007; accepted 28 July 2007
Available online 22 August 2007

Contents

Abbreviations: salen, *N*,*N*′-ethylene-bis(salicylideneiminate); 3-MeOsalen, *N*,*N*′-ethylene-bis(3-methoxysalicylideneiminate); 5-Brsalen, *N*,*N*′-ethylene-bis(5-bromosalicylideneiminate); 5-Clsalen, *N*,*N*′-ethylene-bis(5-chlorosalicylideneiminate); 3,5-Brsalen, *N*,*N*′-ethylene-bis(3,5-dibromosalicylideneiminate); naphen, *N*,*N*′-ethylene-bis[(2-hydroxy-1-naphthyl)methaniminate]; salpn, *N*,*N*′-(1,3-propylene)bis(salicylideneiminate); 5-Brsalpn, *N*,*N*′-(1,3-propylene)bis(5-bromosalicylideneiminate); 3-MeOsalpn, *N*,*N*′-(1,3-propylene)bis(3-methoxysalicylideneiminate); 2-OH-salpn, *N*,*N*′-disalicylidene-2-hydroxypropylenediaminate; *rac*-salmen, *rac*-*N*,*N*′-(1-methylethylene)bis(salicylideneiminate); saldmen, *N*,*N*′-(1,1-dimethylethylene)bis(salicylideneiminate); *rac*-salcy, *rac*-*N*,*N*′-(1,2-cyclohexanediylethylene)bis(salicylideneiminate); (*R*,*R*)-salcy, (*R*,*R*)-*N*,*N*′-(1,2-cyclohexanediylethylene)bis(salicylideneiminate); (*S*,*S*)-salcy, (*S*,*S*)-*N*,*N*′-(1,2-cyclohexanediylethylene)bis(salicylideneiminate); saltmen, *N*,*N*′-(1,1,2,2-tetramethylethylene)bis(salicylideneiminate); 5-Rsaltmen, *N*,*N*′-(1,1,2,2-tetramethylethylene)bis(5-Rsalicylideneiminate); 5-Brsaltmen, *N*,*N*′-(1,1,2,2-tetramethylethylene)bis(5-bromosalicylideneiminate); 5-Clsaltmen, *N*,*N*′-(1,1,2,2-tetramethylethylene)bis(5-chlorosalicylideneiminate); 5-MeOsaltmen, *N*,*N*′-(1,1,2,2-tetramethylethylene)bis(5-methoxysalicylideneiminate); 5-TMAMsaltmen, *N*,*N*′-(1,1,2,2-tetramethylethylene)bis(5-trimethylamminiomethylsalicylideneiminate); naphtmen, *N*,*N*′-(1,1,2,2-tetramethylethylene)bis(naphthylideneiminate); acphen, bis(*o*-hydroxyacetophenone)ethylenediiminate; acphmen, *N*,*N*′-bis(2-hydroxyacetophenylidene)-1,2-diaminopropane; salacen^{2-}, *N*-(acetylacetonylidene)-*N*′-(α-methylsalicylidene)ethylenediaminate; 3,6-Mesalphen, 1,3-bis(3,6-dimethylsalicylideneamino)benzenate; acacen, *N*,*N*′-ethylene-bis(acetylacetonylideneaminate); salenox, 3-{2-[(2-hydroxy-benzylidene)amino]-2-methyl-propylimino}butan-2-one oximate; H_3DCBI, dicarboxyimidazole; phth, terephthalate; TCNQ, tetracyanoquinodimethane; TCNE, tetracyanoethylene; DCNNQI, *N*,*N*′-dicyano-1,4-naphthoquinonediiminate; TCEA, tricyanoethenolate; H_2A, 4-(6-methyl-8-oxo-2,5-diazanonane-1,5,7-trienyl)imidazole; H_2bpmb, 1,2-bis(pyridine-2-carboxamido)-4-methylbenzene; H_2bpb, 1,2-bis(pyridine-2-carboxamido)benzene; acimen, 4-(6-methyl-8-oxo-2,5-diazanonane-1,5,7-trienyl)imidazolate; Tp, hydrotris(pyrazolyl)borate; pao, pyridine-2-aldoximate; miao, 1-methylimidazole-2-aldoximate; eiao, 1-ethylimidazole-2-aldoximate; Him, imidazole; 1-CH_3im, 1-methylimidazole; *N*-Meim, *N*-methylimidazole; py, pyridine; 4-pic, 4-picoline; *t*-Bupy, 4-*tert*-butylpyridine; bpy, 2,2′-bipyridine; dppe, 1,2-bis(diphenylphosphino)ethane; Cp, cyclopentadiene; 18-cr-6, 18-crown-6-ether.

* Corresponding author. Tel.: +81 22 795 6545; fax: +81 22 795 6548.
E-mail address: miyasaka@agnus.chem.tohoku.ac.jp (H. Miyasaka).

0010-8545/$ – see front matter
doi:10.1016/j.ccr.2007.07.028

Abstract

Assembled Mn(III) salen-type quadridentate Schiff-base (SB) complexes, $[Mn^{III}(SB)]^{n+}$, with various metal-containing/non-metal building blocks and their synthetic strategies are summarized. With the Mn(III) salen-type complexes, it is possible to have two coordination labile sites in *trans*- or *cis*-position as the SB ligand takes a *quasi-planar chelate* form and a *stereoscopic chelate* form, respectively, being a coordination-acceptor building block. Particularly in the quasi-planar form, the coordination labile sites face the direction of the Jahn–Teller elongated axis occupying the d_{z^2} orbital with an unpaired electron. Due to this characteristic orbital arrangement, the activity and magnetic–electronic properties of the Mn(III) salen-type complexes can be tuned, at will, by modulating the SB ligand that is equatorially located around the Mn(III) ion and coupled with the empty $d_{x^2-y^2}$ orbital. Both the structural aspects, and magnetic characteristics of assembled compounds are of great interest. This point is the main theme in this review. The high-spin Mn(III) salen-type complexes ($S = 2$) display strong magnetic uniaxial anisotropy, in which the magnetic easy axis can be unambiguously found as the Jahn–Teller axis. Thus, out-of-plane assembly of the quasi-planar Mn(III) salen-type complexes makes it possible to align the easy axes of the Mn(III) ions. This strategy creates unique magnetic systems involving molecular superparamagnets such as single-molecule magnets and single-chain magnets. So far, variously assembled systems employing Mn(III) salen-type complexes as oligomers, one-dimensional chains, and two- or three-dimensional networks have been designed. By following this review, we would know that the Mn(III) salen-type complexes have the potential as a versatile magnetic source for the design of unique magnetic materials with multiple assembling structures.

Keywords: Mn(III) salen-type complexes; Assembled compounds; Magnetic properties; Bulk magnetism; Superparamagnetism

1. Introduction

The current outstanding development in the coordination chemistry of manganese (Mn) is largely a result of the following three research subjects: (i) the design of models of Mn-containing biological systems [1–4] (e.g., photosystem II of green plants [5,6], manganese catalase [7,8], superoxide dismutase [9], ribonucleotide reductase [10], and acid phosphatase of sweet potato [11]), (ii) the development of catalysts for oxidations of organic substrates [12,13] (e.g., epoxidation [14,15] and aziridination of olefins [16,17], oxidation of sulfides [18,19]), and (iii) study on magnetism of Mn complexes and Mn-containing hetero-metallic assemblies [20]. The design (and/or search) for *key ligands* to suit respective needs is the most important process to advance this research. The desired ligands need to have the potential not only to stabilize the coordination of Mn ions but also to modulate ligand fields around Mn ion in order to control the reactivity and operability with reactants or additional ligands and concomitant oxidation states and spin states of the Mn ion. Despite the different purposes of the various (i)–(iii) research subjects, quadridentate Schiff-base ligands such as *N*,*N*′-ethylene-bis(salicylideneiminate) called "*salen*" and its analogues (hereafter, referred to simply as "salen" or as "Schiff-base (SB)") have often been used as a key ligand common to these versatile Mn chemistries (Scheme 1 shows some salen ligands introduced in this review).

The stable quadridentate salen chelate is reminiscent of the porphyrin framework. Indeed, because of their commonality, the substitution of heme-active-site with salen metal complexes has frequently been carried out in bioinorganic chemistry [21]. However, the salen ligands have an open framework for binding metal ions. Assuming octahedral Mn geometry the ligand can flexibly take two coordination modes as a *quasi-planar chelate* or a *stereoscopic chelate*, in which the other two coordination sites are positioned in *trans*- and *cis*-fashions, respectively (Scheme 2). The Mn ion in these coordination modes, can, in general, adopt multiple oxidation states of II, III, IV, and

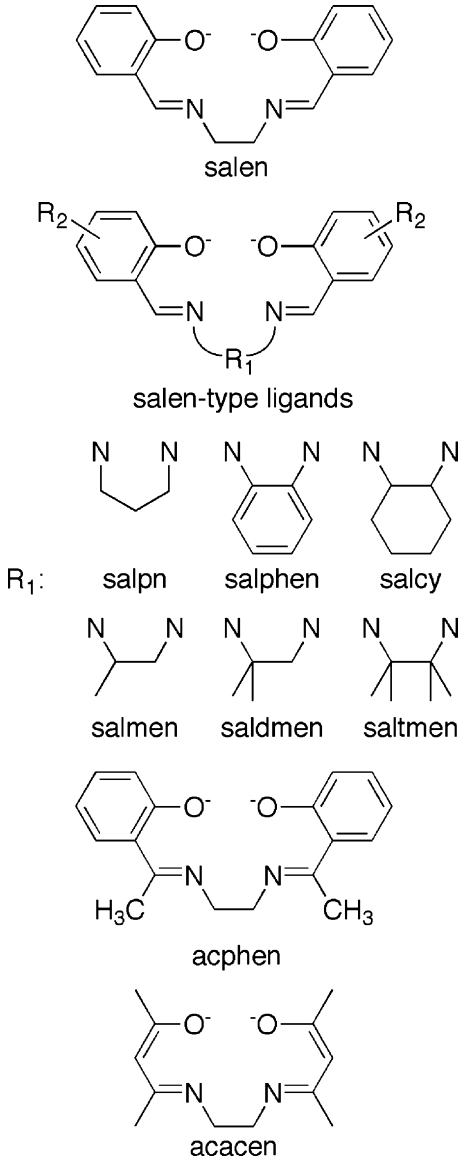

Scheme 1.

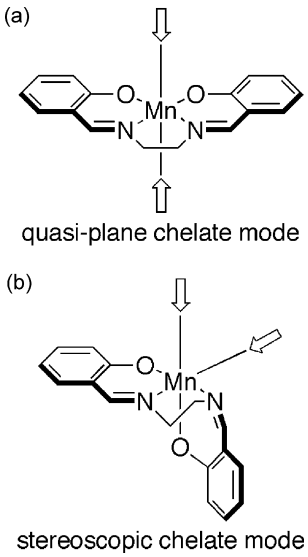

Scheme 2. The arrows show coordination labile sites.

possibly, V. In air or in the reaction with oxidants, the high oxidation states of Mn(III), Mn(IV), and Mn(V) are more stable than the oxidation state of Mn(II). Among these oxidation states, the Mn(III) species can be generally found under common experimental conditions independent of additional ligands, except O^{2-}, OH^{-}, or some oxygen sources, and their binding modes (*trans* or *cis*). The Mn(IV) [22,23] and Mn(V) species are obtained by oxidation of the Mn(III) species (such compounds as di-μ-oxo-Mn(IV) dimers will be described in Section 3). In particular, the Mn(V) species are exceptionally stabilized in two forms as oxo-Mn(V) complexes [24–27] (Scheme 3a) or as nitrido-Mn(V) complexes [28–32] (Scheme 3b). Meanwhile, the Mn(II) species are generally stable in anaerobic conditions [33]. Only salen ligands substituted with strong electron-withdrawing groups such as an $-NO_2$ group tend to stabilize the Mn(II) species in air in the solid state [34].

Thus, the stability in their complexation and flexibility and diversity in coordination modes and oxidation states of Mn ion in the salen ligands allowed multiple uses for various research subjects. Furthermore, it should be emphasized that the introduction of functional groups on the salen ligand (R_1 and R_2 in Scheme 1) makes it possible to tune the ligand field around Mn(III) ion (this effect may be more characteristic for the quasi-planar form). The ligand field influences the versatility for reactivity and availability of oxidation states of the Mn ion in the process of molecular assembly.

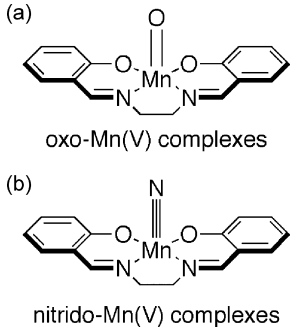

Scheme 3.

As supposed from their many oxidation states, Mn complexes display a diversity of spin states (the research subject of (iii)). Thus, the magnetic behavior of these Mn complexes and Mn-containing hetero-metallic assemblies has been energetically studied. Mn(III) salen complexes are attractive targets, because they promote stable and versatile complexation with themselves or other metal ions to form polynuclear assemblies. Furthermore, the recent interest in molecular superparamagnets such as single-molecule magnets (SMMs) [35] and single-chain magnets (SCMs) [36,37], in which uniaxial anisotropy originating from metal ions fulfill a crucial role, has accelerated investigation of the magnetic properties of Mn(III) salen complexes.

For the past decade, we have investigated Mn(III) salen assemblies from the viewpoint of their assembling activities and magnetic properties. Through our studies, we reaffirmed that Mn(III) salen complexes act as highly useful building blocks for the design of magnetic assemblies not only toward bulk magnets but also toward molecular superparamagnets. Some important results are briefly reviewed in this article.

2. Motivation for the use of Mn(III) salen complexes as a building block

Mn(III) salen complexes can be regarded as a *coordination-acceptor building block*, with two ligand-substitution-labile sites adopting a hexa-coordination mode (Scheme 2), whereas complexes possessing coordinatable ligand group(s) are defined as *coordination-donor building blocks*. The benefits of using such building blocks for assemblies would be (i) its variable magnetic nature (i.e., intrinsic magnetic–electronic aspect) and (ii) flexibility of the coordination-acceptor ability (i.e., structural aspect). Since these aspects are closely related to each other, Mn(III) salen complexes are a useful source of spin for the design of multiple magnetic assemblies. Here, we present a brief discussion, first, on the magnetic–electronic aspect (Section 2.1), and then, on the structural aspect (Section 2.2).

2.1. The intrinsic magnetic nature of Mn(III) ion in octahedral ligand fields

The high-spin free Mn(III) ion with $S = 2$ has a ^5D ground term, which splits in octahedral ligand fields to form $^5T_{2g}$ and ^5E_g terms. Under Jahn–Teller distortion forming a tetragonal geometry (D_{4h} symmetry), these terms split from $^5T_{2g}$ to $^5B_{2g}$ and ^5E_g and from ^5E_g to $^5A_{1g}$ and $^5B_{1g}$. If the complex has an axial-elongated geometry, the ground term is $^5B_{1g}$, while if the complex has a compressed form, $^5A_{1g}$ is the ground term. The spin degeneracy of the ground state is further removed by the second-order spin–orbit coupling, the so-called zero-field splitting (ZFS) (Fig. 1). The ZFS from the ground term, $^5B_{1g}$ or $^5A_{1g}$, produces the lowest magnetization levels of $M_s = \pm 2$ or 0, respectively, with a gap of $4D$ ($=|D|S^2$) between the spin ground state and the highest excited state (when $^5B_{1g}$ is the ground term, D is negative, and conversely,

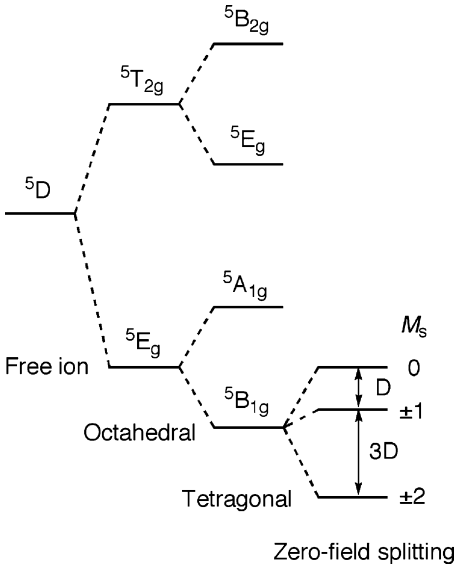

Fig. 1. Splitting of the ^5D term (d^4) by octahedral and tetragonal (axially elongating) fields and by second-order spin–orbit coupling (zero-field splitting).

when $^5A_{1g}$ is the ground term, D is positive with a Hamiltonian of $H = D[\hat{S}^2 - 1/3S(S+1)]$) [38,39]. Gerritsen and Sabinsky [40] have experimentally demonstrated that the anisotropy of the Mn^{III} ion depends greatly on its Jahn–Teller distortion, leading in most cases to a negative ZFS parameter (D). Indeed, Mn(III) salen complexes afford a typical axial-elongated Jahn–Teller distortion, and therefore exhibit a negative D parameter with finite uniaxial anisotropy. In 1985, Mennedy and Murray [41] reported the first experimental study on the anisotropy of several Mn(III) salen complexes and related complexes.

For this reason, Mn(III) salen complexes have recently been attracting much attention as a uniaxial anisotropic magnetic source for the design of molecular superparamagnets. Concrete examples for SMMs or SCMs will be introduced in Sections 4 and 5. Before that, we comment briefly about the self-assembled dimer of Mn(III) salen complexes. The self-assembled out-of-plane dimers have co-linear Jahn–Teller axes and, in many cases, exhibit ferromagnetic coupling between Mn(III) ions via a bi-phenolate bridge to induce an $S_T = 4$ ground state. These dimer complexes are of interest not only in their intrinsic superparamagnetism (Section 4) but also in their use as a bi-coordination-acceptor building block (Section 5).

2.2. Magnetic topology in assembling forms

Another benefit is to be able to easily control the anisotropic direction in assembled structures. As mentioned above, anisotropy is a key ingredient to obtain slow relaxation of the magnetization in SMM and SCM systems. Therefore, control of the building block coordination sphere is very important to produce significant anisotropy in the assembled complex. For example, let us consider an SCM system (i.e., 1D system). As mentioned previously, the Jahn–Teller axis of the Mn(III) salen complexes corresponds to the magnetization easy axis, i.e., the preferential orientation of the magnetic spin on the Mn^{III} complex (Fig. 1). When these complexes are assembled into a chain with a *trans*-bridging ligand or a *trans*-coordination-donor building block with isotropic spins, the individual Mn^{III} Jahn–Teller axes are necessarily aligned to the chain direction (Fig. 2). This topology leads to a simple system with an easy axis of the magnetization parallel to the chain direction.

Thus, in the *quasi-planar chelate* mode, the Jahn–Teller axis (i.e., out-of-plane elongated axis), in which the d_{z^2} orbital contains a spin, is situated in the out-of-plane direction corresponding with sites for additional ligands (see Scheme 2a and Fig. 2). For example, in the assembly with a metal-containing coordination donor building block, the ligands assigned to the

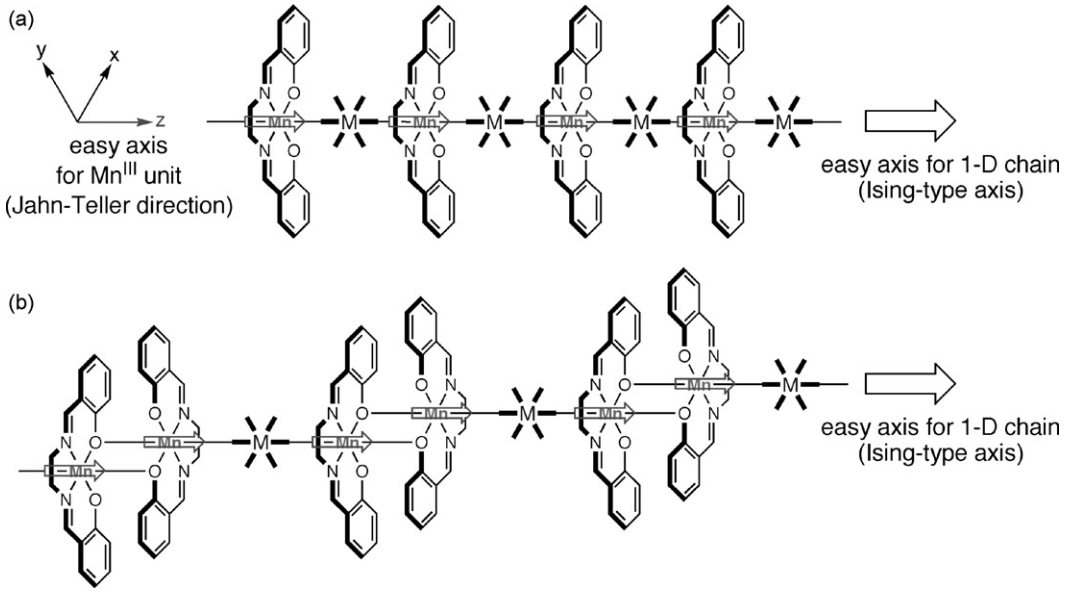

Fig. 2. Schemes of one-dimensional arrangements of Mn^{III} salen units for both monomer (a) and out-of-plane dimer forms (b) with linkers (M). In both cases, the Jahn–Teller axis of Mn^{III} ions is directed along the one-dimensional assembly inducing a unique easy-axis (i.e., Ising-type axis) for a given chain.

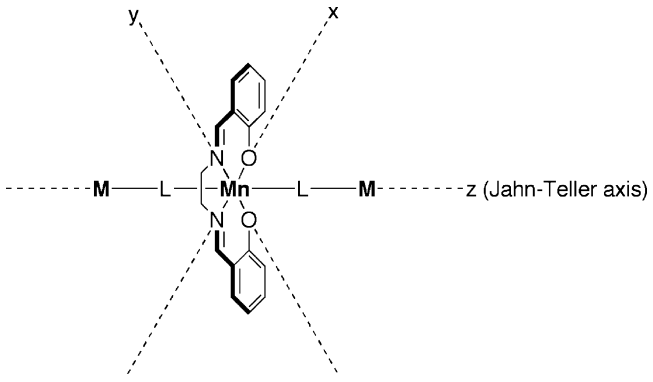

Scheme 4.

Jahn–Teller axis are magnetic mediators (i.e., bridging ligands) between Mn(III) ion and the metal ion of the coordination-donor building block (Scheme 4). At this time, not only the nature of a given bridging ligand but also the nature of the salen ligand modulates the affinity of coordination, the magnetic nature of the Mn(III) ion (e.g., anisotropic nature), and the degree of magnetic interaction between the Mn(III) ion and the metal ion. Namely, the ligand field from the equatorial plane strongly affects the d-orbital ligand field splitting particularly the degree of Jahn–Teller distortion involving the energy difference between the spin-occupying d_{z^2} orbital and the empty $d_{x^2-y^2}$ orbital. In addition, the steric effect of substituent groups influences the packing of the assembled compounds, as shown in later sections. Thus, the choice of the salen ligand is an important factor to determine both structural and magnetic properties of the assembled compounds.

3. Self-assemblies using organic and inorganic bridging ligands

Mn(III) salen complexes can be bound to various additional ligands. With ligands able to cap the residual two coordination sites of octahedral Mn(III) ion (i.e., end-capping ligands), mononuclear Mn(III) salen complexes would be preferentially formed. It is not the main purpose of this review to introduce such mononuclear compounds. In this section, we focus on assembled complexes obtained by reactions of Mn(III) salen complexes with non-metallic bridging ligands. Various organic or inorganic bridging ligands, listed in Fig. 3, formed polynuclear assemblies with Mn(III) salen complexes.

3.1. Discrete Mn complexes

Pecoraro and his group synthesized various dinuclear Mn complexes based on $salpn^{2-}$ and its derivatives (see Scheme 1) mainly with the purpose of mimicking biological Mn-activation sites. Among such dinuclear complexes, the most attractive targets were di-μ-oxo bridged Mn(IV) complexes. Since the first report in 1991 [42], many groups have energetically investigated this type of compound. The di-μ-oxo bridged Mn(IV) complexes exist as two different types with the same chemical formula, $[Mn_2^{IV}(SB)_2(O)_2]$, but are distinguished by their complexation features. One has a structure in which a salen ligand coordinates to each Mn(IV) ion in the *stereoscopic chelating* mode to form a $[Mn^{IV}(SB)]$ moiety, consequently yielding a simple di-μ-oxo-bridging skeleton as $[Mn^{IV}(SB)]$–$(O)_2$–$[Mn^{IV}(SB)]$ (Fig. 4a) [42–47]. The other has a structure in which each salen ligand acts as a bridging ligand to bind two Mn(IV) ions as well as the di-μ-oxo-bridge, producing a formula $[Mn_2^{IV}(\mu\text{-dbsalen})_2(\mu\text{-}O)_2]$ (Fig. 4b) [46–50]. The Mn(IV) ions via the di-μ-oxo bridge (including non-Schiff-base complexes) are strongly antiferromagnetically coupled with an exchange coupling in the range of -80 to $-190\,cm^{-1}$ (-110 to -270 K). Pecoraro et al. investigated a magneto-structural correlation between the exchange interaction and the Mn^{IV}–O–Mn^{IV} angle in these di-μ-oxo bridged Mn(IV) Schiff-base complexes and their related compounds and found a linear correlation between them (Fig. 5) [47].

Note that μ-oxo Mn(IV) dinuclear complexes ($[Mn^{IV}$–O–$Mn^{IV}]^{2+}$) and μ-oxo Mn(III) dinuclear complexes ($[Mn^{III}$–O–$Mn^{III}]$) have also been detected in solution media through oxidation of Mn(III) and Mn(II) salen complexes, respectively, where the former was an intermediate species for the Mn^{V}=O complex, but they have never been characterized by X-ray crystallography [24,51].

Kirk and Pecoraro et al. also synthesized a di-Mn(III) complex and its one-electron oxidized mixed-valent complex (Mn^{III}/Mn^{IV}) using bridging deprotonated H_3DCBI ligands (see Fig. 3), where the di-anionic ligand ($HDCBI^{2-}$, in which one proton would be located on either of the two carboxyl groups) yielded the former and the tri-anionic ligand ($DCBI^{3-}$) yielded the latter (Fig. 6) [52]. In both complexes, the ligands act as chelating/bridging ligands, thus each [Mn(SB)] moiety adopts the *stereoscopic chelating* mode (*cis*-coordination mode). The latter is the first example of a ferromagnetically coupled Mn^{III}/Mn^{IV} dinuclear complex ($J = +1.4\,cm^{-1}$). Incidentally, the use of the H_2DCBI^- ligand, which can act both as monodentate [53] and bidentate [54] end-cap ligands, yielded mononuclear Mn(III) complexes.

Other dinuclear Mn(III) complexes adopting the *stereoscopic chelating* mode in the Mn(III) coordination geometry were synthesized using $salpn^{2-}$: di-μ-MeO [42] and di-μ-OH complexes (note that it is doubtful whether the di-μ-OH complex is true, because the existence of this complex was determined only by X-ray crystallography and the structure obtained was the same as $[Mn^{IV}$–$(O)_2$–$Mn^{IV}]$) [55,56]. Unfortunately, there are no magnetic data for these complexes in the literature.

Looking at Mn(III) salen complexes adopting the *quasi-planar chelating* mode, several discrete complexes are known. A carboxylate-bridged dinuclear Mn(III) complex, in which the opposite coordination sites were capped by H_2O and EtOH, exhibited a weak antiferromagnetic interaction ($4.75\mu_B$ at 300 K, $3.82\mu_B$ at 5 K) [57]. Liu et al. synthesized terephthalate-bridged dinuclear Mn(III) complexes [58]. By capping the opposite coordination sites with a MeOH molecule, discrete di-Mn(III) complexes were obtained: $[\{Mn^{III}(SB)(MeOH)\}_2(\mu\text{-phth})]$ (SB = $salen^{2-}$ and $salpn^{2-}$) (Fig. 7). The corresponding compounds using deuterated terephthalate (p-$C_6D_4(CO_2^-)_2$) were also prepared. The temperature

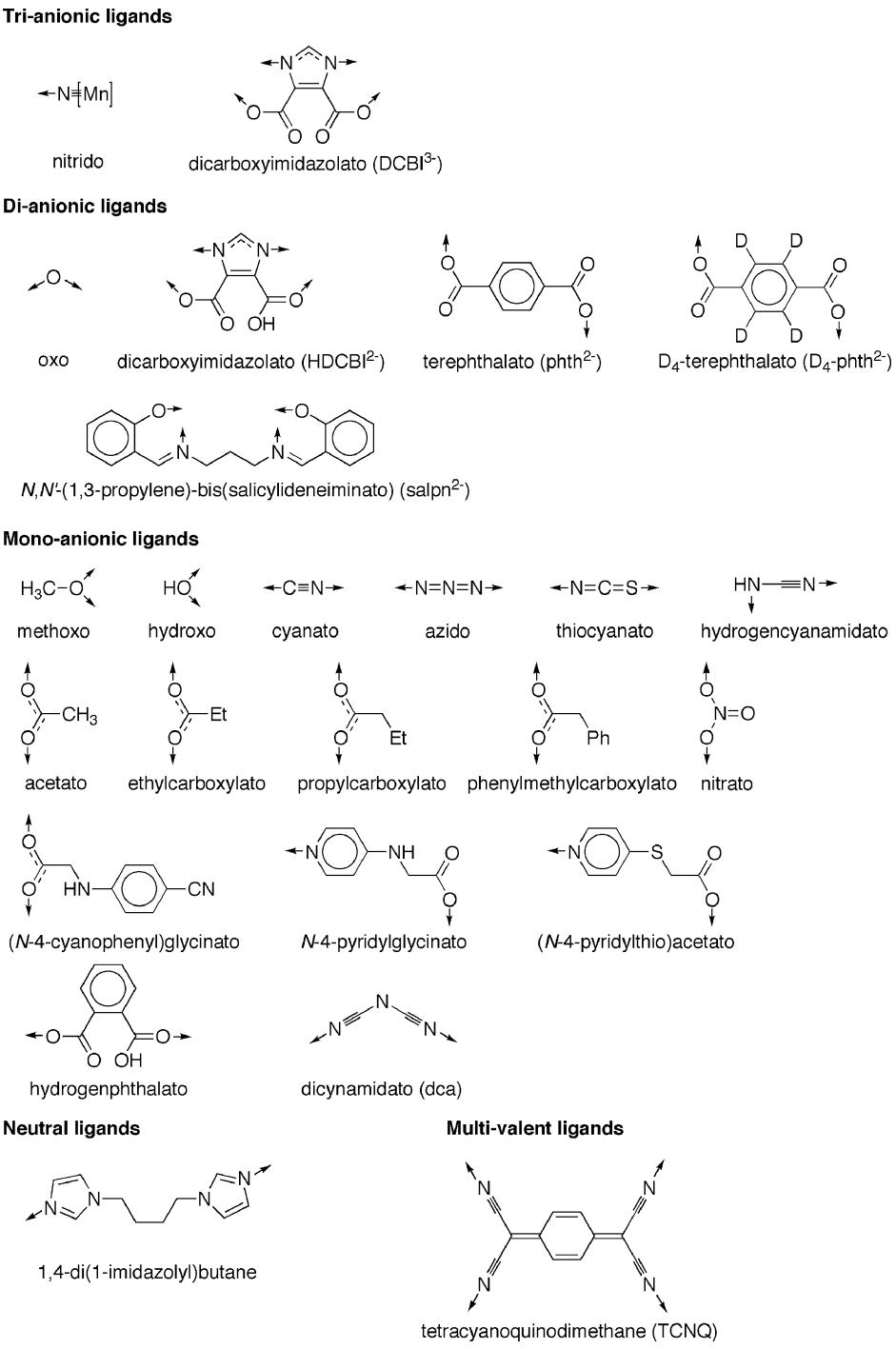

Fig. 3. Bridging ligands connecting Mn(III) salen-type complexes.

dependence of the susceptibility (χ) and χT was simply simulated using a Heisenberg dinuclear model with $S_{Mn1} = S_{Mn2} = 2$. This simulation indicated the presence of a very weak antiferromagnetic interaction ($J \approx -0.2\,cm^{-1}$) via the terephthalate linkage, despite a long Mn···Mn separation. However, due to a lack of more detailed considerations, this conclusion is still ambiguous. For example, the origin of the drop of χT at low temperatures might be due to inter-molecular antiferromagnetic interaction or anisotropy of Mn(III) ion (the ZFS effect was not taken into account) instead of the intra-molecular exchange via the phth bridge. Interestingly, its non-capped unit was also synthesized, which formed a one-dimensional (1D) chain by aggregating in $[Mn(SB)]^+$ moieties of adjacent units (forming an out-of-plane dimeric moiety, $[Mn(SB)]_2^{2+}$). This complex will be described in the next section.

By sandwiching a Na^+ ion between two Mn(III) salpn complexes using phenolate groups of $salpn^{2-}$ and additional carboxyl bridges connecting the Mn(III) and Na^+ ions, trinuclear complexes of $[Mn^{III}–Na^{I}–Mn^{III}]$ were formed. Pecoraro et al. first reported this type of compound using *N*,*N*′-disalicylidene-2-

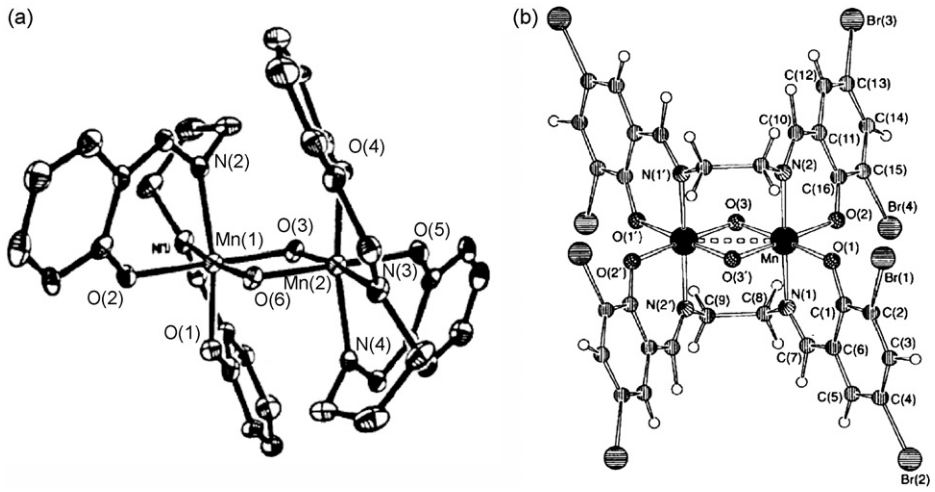

Fig. 4. Structures of two types of di-μ-oxo bridged form: $[Mn^{IV}(salpn)(\mu\text{-}O)]_2$ (a), in which the salpn ligand coordinates to each Mn(IV) ion in the *stereoscopic chelating* mode to form a $[Mn^{IV}(salpn)]$ moiety, yielding a di-μ-oxo bridging skeleton of $[Mn^{IV}(salpn)]$—$(O)_2$—$[Mn^{IV}(salpn)]$, and $[\{Mn(\mu\text{-}3,5\text{-}Brsalen)(\mu\text{-}O)\}_2]$ (b), in which each 3,5-Brsalen ligand is acting as a bridging ligand to bind two Mn(IV) ions as well as the di-μ-oxo-bridge Reproduced with permission from Refs. [42,48].

hydroxypropylenediaminate (Fig. 8) and its magnetic properties: there is a negligible magnetic interaction between the Mn(III) ions via the diamagnetic Na^+ ion, but there is a significant effect of anisotropy attributed to the Mn(III) ion ($D = -6.13\,cm^{-1}$) leading to a drop of χT at low temperature [59]. On the other hand, Liu et al. [58] reported the presence of ferromagnetic exchange in the same core with the $salpn^{2-}$ ligand ($J = +1.74\,cm^{-1}$ as $H = -JS_{Mn1}S_{Mn2}$), where the decrease of χT was treated using the contribution of inter-molecular antiferromagnetic interactions ($zJ' = -0.125\,cm^{-1}$) without taking into account the anisotropy of the Mn(III) ion.

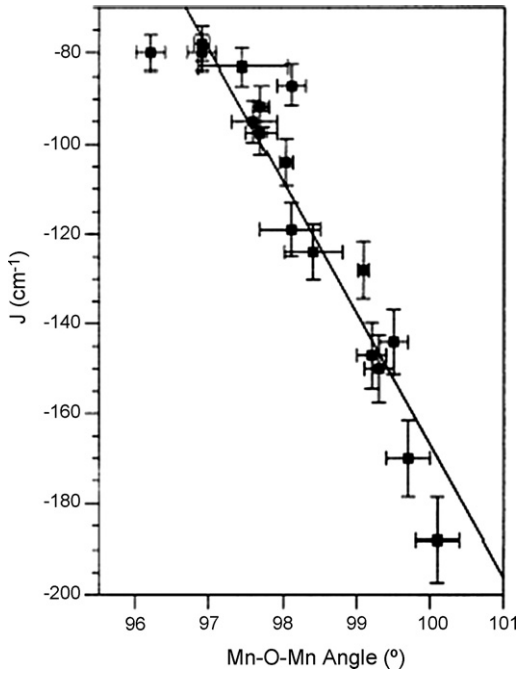

Fig. 5. A plot of the exchange coupling constant between Mn(IV) ions via the bi-μ-oxo bridge, J (cm^{-1}), vs. the Mn—O—Mn angle (°). Reproduced with permission from Ref. [47].

3.2. Mn(III) one-dimensional chains

1D chains are among the most intriguing compounds using assemblies of Mn(III) salen complexes. The *quasi-planar chelating* Mn(III) salen complexes can be used to form a linear-type 1D chain with bridging ligands and coordination-donor building blocks (see Fig. 2). We now used "linear-type" to express this feature of the assembled chains, but it is strongly dependent on the bridging mode and shape of bridging ligands and coordination-donor building blocks used. Assemblies with coordination-donor building blocks will be summarized in Section 5. In this section, we focus on 1D Mn(III) salen assemblies formed using organic and inorganic non-metal bridging ligands. Note that when the *quasi-planar chelating* Mn(III) salen complexes are axially assembled, the half-occupied d_{z^2} orbitals can interact via a bridging group, generally leading to antiferromagnetic coupling except as considered by an accidental orthogonality. Table 1 lists the alternating chain Mn(III) salen complexes with bridging ligands (L), hav-

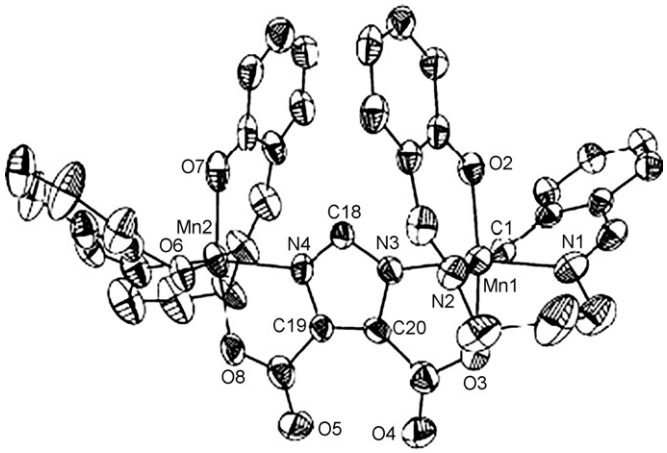

Fig. 6. Structure of $[Mn_2^{III/IV}(dtsalpn)_2(DCBI)]$. Reproduced with permission from Ref. [52].

Table 1
One-dimensional alternating chains of Mn(III) salen complexes with non-metal bridging ligands and their magnetic properties (nd = no data in the literature)

Compound	Bridging ligand	μ_{eff} at 300 K (μ_B)	μ_{eff} at low T (μ_B)	J_{Mn-Mn} (cm^{-1})	D_{Mn} (cm^{-1})	zJ' (cm^{-1})	Additional comments	Reference
[Mn(salen)(O_2CCH_3)]	$CH_3CO_2^-$	4.68	nd	-1.4 ± 0.1	~0	~0		[60]
[Mn(salen)(O_2CCH_3)]	$CH_3CO_2^-$	4.74	nd	−1.8	–	0.1	$J = -1.5 \pm 0.1\ cm^{-1}$, $zJ' = 1.00 \pm 0.05\ cm^{-1}$ from another fitting	[41]
[Mn(salpn)(O_2CCH_3)]·1.5H_2O	$CH_3CO_2^-$	nd	nd	nd	nd	nd		[61]
[Mn(salphen)(O_2CCH_3)]	$CH_3CO_2^-$	nd	1.65 (4.7 K)	−1.32	−0.72	–		[62]
[Mn(salphen)(O_2CCH_3)]	$CH_3CO_2^-$	nd	nd	nd	nd	nd		[63]
[Mn(naphen)(O_2CCH_3)]	$CH_3CO_2^-$	nd	nd	nd	nd	nd		[64]
[Mn(salpn)(O_2CEt)]	$EtCO_2^-$	4.6	nd	nd	nd	nd		[45]
[Mn(5-Brsalpn)(O_2CCH_2Ph)]	$PhCH_2CO_2^-$	4.4	nd	nd	nd	nd		[45]
[Mn(salpn(2-OH))(O_2CCH_3)]	$CH_3CO_2^-$	4.85	nd	−1.72	–	–		[59]
[Mn(salen){(*N*-4-NCPh)glycinate}]	(*N*-4-cyanophenyl)glycinate	nd	nd	nd	nd	nd		[65]
[Mn(salen)(NO_3)]	NO_3^-	4.79	3.80 (4 K)	−0.55	−0.43	–		[66]
[Mn(salpn)(NCS)]	NCS^-	4.75	nd	−3.2	–	–	$T_c = 6.8$ K	[67]
[Mn(salen)(N_3)]	N_3^-	nd	nd	−4.52(4)	–	–	$J = -5.19\ cm^{-1}$ from another fitting	[68]
[Mn(salen)(N_3)]	N_3^-	4.53	nd	-5.42 ± 0.1	-0.18 ± 0.05	–	$J = -4.45 \pm 0.05\ cm^{-1}$, $zJ' = -1.4 \pm 0.2\ cm^{-1}$ from another fitting	[41]
[Mn(salpn)(N_3)]	N_3^-	nd	nd	−4.03	–	–	$\theta = 0.022$ K, $\rho = 0.6\%$	[69]
[Mn(salpn)(N_3)]	N_3^-	5.14	nd	−4.3	–	–	$\chi_{max} = 0.0269\ cm^3\ mol^{-1}$ at 35 K	[70]
[Mn(5-Brsalen)(NCNH)]	$HNCN^-$ (=hydrogencyanamide)	nd	nd	−0.99(3)	–	−1.0(2)	$J = -0.85(2)\ cm^{-1}$, $zJ' = -1.3(1)\ cm^{-1}$ from another fitting $T_N = 7.5$ K, $T_c = 2.8$ K	[71]
[Mn(salen)(dca)]	$NCNCN^-$ (=dicyanamide)	4.70	4.23 (5 K)	−0.24	–	–		[72]
[Mn(3-MeOsalpn)($HO_2CC_6H_4CO_2$)]	$HO_2CC_6H_4CO_2^-$ (=hydrogenphthalate)	4.59	4.65 (150 K)	nd	nd	nd		[75]
[Mn(salen)(biim)]ClO_4	biim (=1,4-di(1-imidazolyl)butane)	nd	nd	nd	nd	nd		[76]
[Mn(salen)(*N*-4-pyridylglycinate)]	*N*-4-pyridylglycinate	nd	nd	nd	nd	nd		[65]
[Mn(salen){(4-pyridylthio)acetate}]	(4-pyridylthio)acetate	nd	nd	nd	nd	nd		[77]

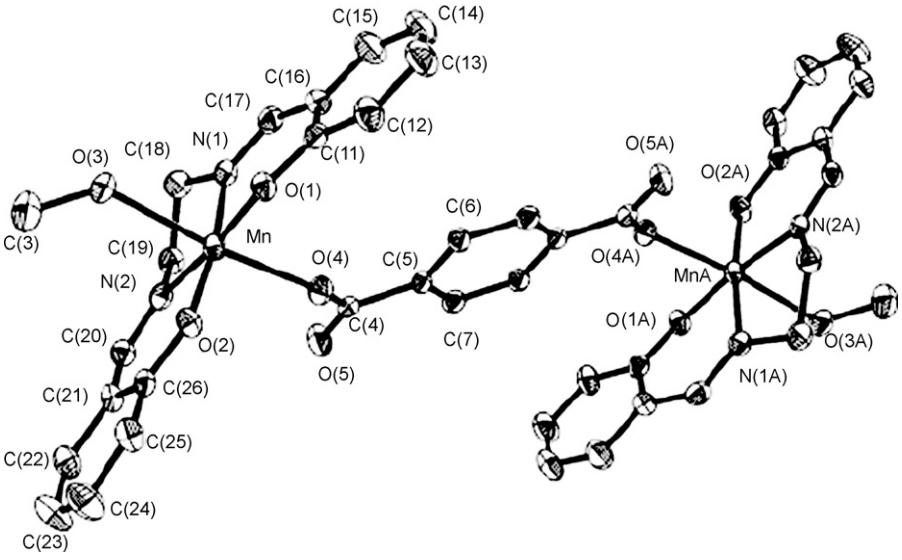

Fig. 7. Structure of [{Mn^{III}(salen)(MeOH)}$_2$(μ-phth)]. Reproduced with permission from Ref. [58].

ing a [–Mn^{III}–L–] repeat unit, together with their magnetic properties.

The carboxylate group such as acetate ($CH_3CO_2^-$) can coordinate to these Mn(III) complexes in several modes. It can act as monodentate [49,45,58] and bidentate end-cap ligands [49,45,57], probably forming discrete complexes in both ligands. Meanwhile, carboxylate-bridged Mn(III) alternating chains having a [–Mn^{III}–O–CR–O–] bridging motif have also been synthesized (Table 1) (discrete compounds with a similar bridging scheme were described in the previous section). Gatehous et al. reported the first example of this type of compound in 1973: [Mn(salen)(μ-O_2CCH_3)] (Fig. 9) [60]. In this compound, the Mn···Mn intra-chain distance is 6.536 Å. The magnetic interaction between the Mn(III) ions via the carboxylate group was estimated as very weak antiferromagnetic with $J = -1.4 \pm 0.1\,cm^{-1}$ by simulating the susceptibility in the temperature range of 300–80 K. Other carboxylate-bridged chains having a similar bridging motif were found in various combinations of salen ligands and carboxylate groups, $CH_3CO_2^-$ [59,61–64], $EtCO_2^-$ [45], $PhCH_2CO_2^-$ [45], (*N*-4-cyanophenyl)glycinate [65] (Table 1). Evidently, the magnetic exchange between the Mn(III) ions via the carboxylate group lies in the range $J \approx -1$ to $-2\,cm^{-1}$.

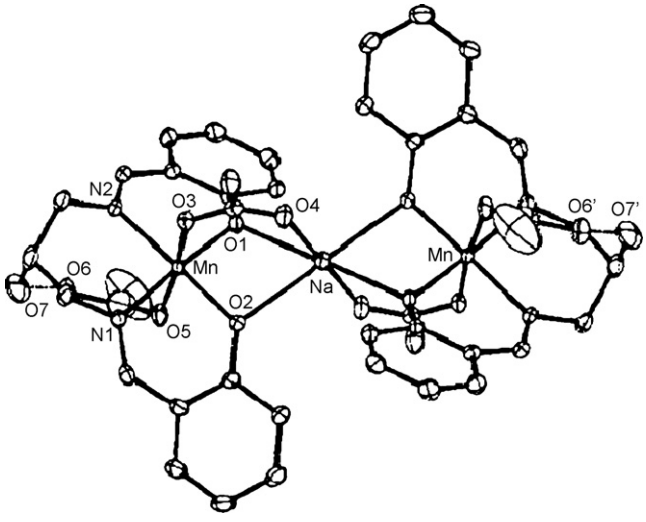

Fig. 8. Structure of the anionic portion of [$C_2H_9O_2$][$NaMn_2^{III}$(2-OH-salpn)$_2$(OAc)$_4$]·2H_2O. Reproduced with permission from Ref. [59].

Three-atom bridged Mn(III) chains can be found in compounds containing inorganic mono-anions such as NO_3^-, NCS^-, N_3^- (end-to-end coordination mode), and hydrogen cyanamide ($HNCN^-$). The NO_3^- linkage complex, having a [–Mn^{III}–O–N–O–] bridging motif, showed weaker Mn···Mn antiferromagnetic exchange ($J = -0.55\,cm^{-1}$) than that of the carboxylate-bridged compounds, despite their similarity [66]. Meanwhile, chains with the NCS^- [67] and N_3^- [68–70,41] linear-type linkages, having [–Mn^{III}–N–C–S–] and [–Mn^{III}–N–N–N–] bridging motives, respectively, yielded exchanges of $J = -3$ to $-5.5\,cm^{-1}$, significantly bigger than those of the carboxylate- or NO_3-bridged chains. While, hydrogen cyanamide is a similar linear-type linkage forming a [–Mn^{III}–NH–C–N–] bridging motif, its chain yielded an exchange of less than $-1.0\,cm^{-1}$ [71]. Compounds with NCS^- and hydrogen cyanamide revealed a three-dimensional (3D) long-range order at $T_c = 6.8$ and 2.8 K, respectively, due to a spin canting arrangement of antiferromagnetically coupled spins.

A five-atom bridged Mn(III) chain was found in a compound of [Mn^{III}(salen)]$^+$ and dicyanamide having a [–Mn^{III}–N–C–N–C–N–] bridging motif, in which the Mn···Mn exchange was estimated as $J = -0.24\,cm^{-1}$ [72]. This small *J* value is compatible with values obtained in other dicyanamide-bridged metal complexes [73,74].

Bigger and longer bridging ligands such as hydrogen phthalate [75], 1,4-di(1-imidazolyl)butane [76], *N*-4-pyridylglycinate [65], and (4-pyridylthio)acetate [65,77] can also form alternating 1D chains with Mn(III) salen complexes. Due to the long distance exchange via these bridging ligands, the intra-chain Mn···Mn interaction would be negligibly small (indeed, no magnetic evaluation was reported in the literature).

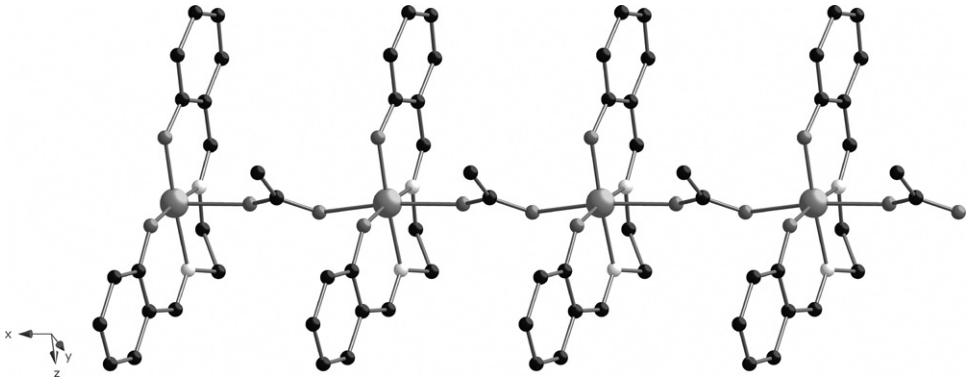

Fig. 9. One-dimensional chain structure of [Mn^{III}(salen)(μ-O_2CCH_3)] [60].

Hereafter, we focus on four interesting chains which are not simple alternating chains as in the compounds mentioned above. The first is [{Mn^{III}(salen)}$_2$(μ-phth)] [58]. The phth ligand bridges two [Mn^{III}(salen)]$^+$ to form a neutral dumbbell-shaped dinuclear Mn(III) unit, [Mn^{III}–phth–Mn^{III}], in which two carboxylate functions of the phth ligand are coordinate to Mn(III) ions in a monodentate fashion. This dinuclear Mn(III) unit interacts with adjacent units by forming an out-of-plane dimer aggregation, constructing a 1D linear chain having a [–Mn^{III}–phth–Mn^{III}–$(O_{Ph})_2$–] repeat unit (where –$(O_{Ph})_2$– is a bi-phenolate bridge in the out-of-plane dimeric moiety) (Fig. 10). The Mn···O^*_{Ph} and Mn···Mn* distances are 2.773 and 3.564 Å, respectively, in the out-of-plane aggregation of the Mn(III) salen molecules. The temperature dependence of μ_{eff} of this compound clearly indicates that a ferromagnetic interaction between Mn(III) ions is dominant. This ferromagnetic interaction is attributed to Mn···Mn coupling via the bi-phenolate bridge. Nevertheless, this magnetic behavior was simulated using a 1D chain model taking into account both the exchanges via the phth ligand (J) and via the bi-phenolate bridge (J'). The least-square fit gave $J = -0.295\ cm^{-1}$ and $J' = +0.329\ cm^{-1}$.

A peculiar 1D chain composed of [Mn(salen)]$^+$ and TCNQ was synthesized by Oshio et al.: [{Mn^{III}(salen)$(TCNQ)_{0.5}$}{Mn^{III}(salen)$(TCNQ)_{0.5}$(MeOH)}]·MeOH·H_2O [78]. This was the first [Mn^{III}(salen)]$^+$–TCNQ assembly (a simple alternating chain was synthesized by Miyasaka et al., and this compound will be described in Section 5.2) [79]. In this compound, two distinct six-coordinate [Mn^{III}(salen)]$^+$ chromophores are bridged by two kinds of $TCNQ^{2-}$ anions (A and B in Fig. 11) in μ_2 and μ_4 fashions to form a 1D structure (Fig. 11). The oxidation state of the TCNQ moieties were determined by their structures and magnetic properties: unfortunately, the interaction between the Mn(III) ions via the diamagnetic $TCNQ^{2-}$ is negligibly small. Note that a complex of Mn(III) salen and TCNE was prepared by Miller et al., but no X-ray structure was reported [80].

Cyano-bridged metal complexes are among the most attractive targets in the field of molecule-based magnetism. Many groups energetically investigate this type of compound, and the assemblies employing Mn(III) salen complexes occupy an important position in this research (see Section 5). The simplest way to obtain cyano-bridged complexes would be to react directly Mn(III) salen complexes with the free CN^- ion. Matsumoto et al. obtained a neutral compound having the formula [Mn^{III}(salen)(CN)] from a methanol/H_2O reaction medium [81]. We suppose, superficially from the formula, that this compound is comprised of one kind of Mn(III) species. However, surprisingly, its magnetic properties deny this general hypothesis outright. The μ_{eff} of 4.09μ_B at room temperature is consistent neither with the spin-only value for high-spin Mn(III) (4.89μ_B for $S = 2$, $g = 2.00$) nor with the spin-only value for low-spin Mn(III) (2.83μ_B for $S = 1$, $g = 2.00$). The temperature dependence of μ_{eff} displays the presence of a ferromagnetic interaction between Mn(III) ions: upon lowering temperature, μ_{eff} increases smoothly from 300 to 25 K and then sharply to reach a maximum value of 10.3μ_B at 6 K, followed by a sudden decrease to 2.75μ_B at 2 K (Fig. 12b). This behav-

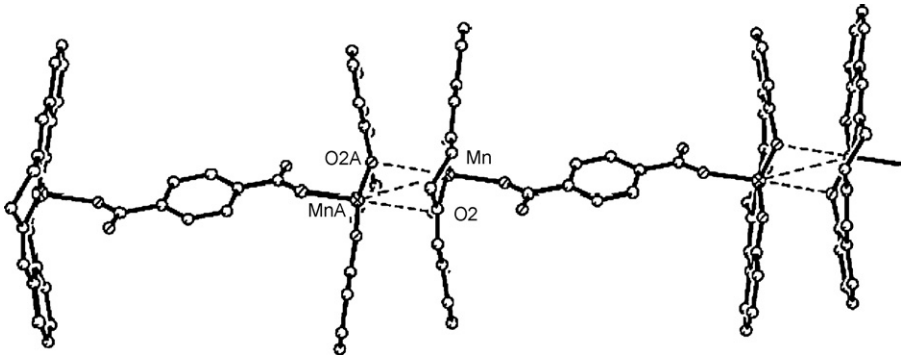

Fig. 10. One-dimensional chain structure of [{Mn^{III}(salen)}$_2$(μ-phth)]. Reproduced with permission from Ref. [58].

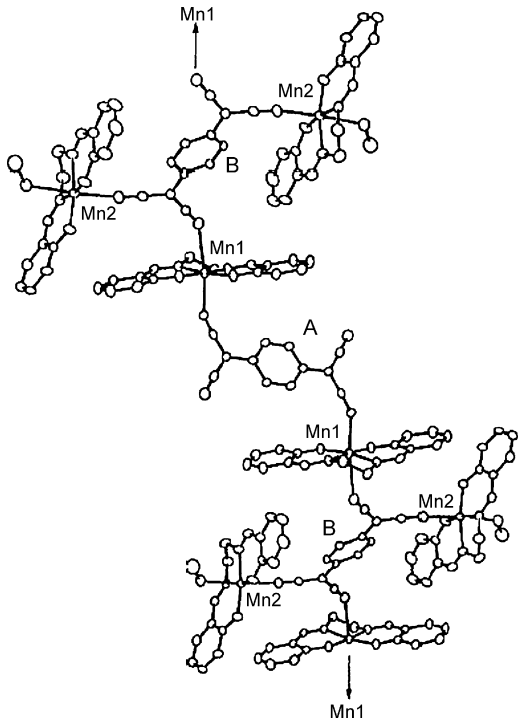

Fig. 11. Structure of $[\{Mn^{III}(salen)(TCNQ)_{0.5}\}\{Mn^{III}(salen)(TCNQ)_{0.5}(MeOH)\}]\cdot MeOH\cdot H_2O$, in which TCNQ (A) and TCNQ (B) make μ_2 and μ_4 bridging fashions, respectively, to form a 1D structure. Reproduced with permission from Ref. [78].

ior is due to the presence of two kinds of Mn(III) species in the compound, i.e., high-spin Mn(III) and low-spin Mn(III). Indeed, the X-ray structure revealed the presence of two independent $[Mn^{III}(salen)]^+$ units, one was axially coordinated with C atoms of two CN^- ions to produce $[Mn^{III}(salen)(CN)_2]^-$ (Mn_B–C = 2.06(3), 2.13(3) Å) and the other was axially coordinated with N atoms from the $[Mn^{III}(salen)(CN)_2]^-$ unit (Mn_A–N = 2.25(3), 2.34(3) Å), constructing a 1D alternating chain having a [–Mn^{III}–NC–Mn^{III}–CN–] repeat unit (Fig. 12a). The Mn^{III} ions of [C–Mn^{III}–C] and [N–Mn^{III}–N] possess a low-spin state ($S = 1$) and a high-spin state ($S = 2$), respectively, and the exchange interaction between these species via CN^- is ferromagnetic. The fact that the exchange between the high-spin Mn(III) ion and the low-spin Mn(III) ion via the CN group is ferromagnetic is known in another example $K[\{Mn^{III}(3\text{-MeOsalen})\}_2\{Mn^{III}(CN)_6\}]$ (see Section 5.3) [82]. Inter-chain antiferromagnetic interactions consequently afforded a metamagnet-type compound. Thus, the simple reaction of $[Mn^{III}(salen)(H_2O)]ClO_4$ with NaCN leads selectively and stoichiometrically to form high-spin and low-spin species in situ and to self-assembly in an alternating arrangement (Scheme 5). Such a peculiar reaction is quite rare.

In the final paragraph of this section, we comment briefly on an assembly of Mn(V)≡N (nitrido-manganese) species. The nitrido-metal complexes are of great interest in research on metal-assisted nitrogen-transfer reactions. To date, several mono-Mn(V) complexes based on salen complexes have been synthesized for this purpose [28–32]. Among these complexes, Tsuchimoto et al. reported a rare 1D chain form repeating a [–Mn^V≡N–] unit: [Mn^V≡N(salpn)] (Fig. 13), where bond distances of Mn≡N and N–Mn* are 1.520(3) and 2.528(3) Å, respectively [83]. Such polymeric nitrido-metal complexes have been observed for V, Mo, W, and Re [84–88]. However, this is the first report of the 1D chain form of Mn(V)≡N. The nitrido-Mn(V) complexes are diamagnetic due to the formation of frontier orbitals between d-orbitals of Mn(V) ion and p-orbitals of nitrogen [29,31,89].

4. Out-of-plane dimers

Cationic Mn(III) salen complexes can be present in solution mainly as a monomer A or as an out-of-plane dimer B depending on the steric characteristics of the Schiff-base ligands (Scheme 6). Inter-conversion between the two forms, depending on the reaction conditions, is probable. The respective species can be isolated in the solid state dependent on their packing stability, and the reaction conditions. Indeed, structural evidence of both species has been obtained from the crystallization of similar reactions: for example, there is a monomer $[Mn^{III}(salen)(Cl)(H_2O)]$ [90,91] and a dimer $[Mn^{III}(salen)(Cl)]_2$ [92]. Additionally, a dimer $[Mn^{III}(5\text{-Brsaltmen})(H_2O)]_2(ClO_4)_2$ first isolated from the reaction of Mn(III) ion with 5-$Brsaltmen^{2-}$ in a MeOH/water medium changed to a monomer $[Mn^{III}(5\text{-Brsaltmen})(H_2O)(MeOH)]ClO_4$ by recrystallization in the same medium [93].

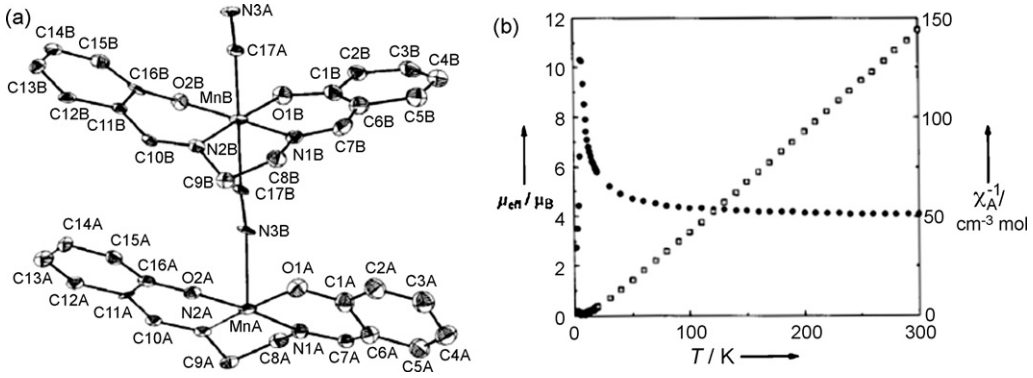

Fig. 12. Structure of the repeat unit of [–Mn^{III}–NC–Mn^{III}–CN–] in a one-dimensional chain compound, [Mn(salen)(CN)] (a), and plots of effective magnetic moment μ_{eff} and the reciprocal magnetic susceptibility χ_A^{-1} of this compound as a function of temperature T (b). Reproduced with permission from Ref. [81].

Table 2
Pertinent bond distances (Å) and Angles (°) for Mn(III) out-of-plane dimeric complexes and magnetic parameters obtained from the simulation of the magnetic susceptibility (F = ferromagnetic interaction, AF = antiferromagnetic interaction, NI = non-interaction, nd = no data in the literature)

Compound	Mn—O	Mn—O*	O—Mn—O*	Mn—O—Mn*	Mn···Mn*	Mn···Mn interaction	g	J (cm^{-1})	D_{Mn} (cm^{-1})	zJ (cm^{-1})	Reference
[Mn(salen)(H_2O)]$_2$(ClO_4)$_2$	1.901(5)	2.412(6)	79.42(21)	100.58(22)	3.334(3)	F	2.0	6.30	−1.70		[66]
[Mn(salen)(NCO)]$_2$	1.8983(14)	2.793(0)	97.82(0)		3.584(1)	F	2.03	0.73	−0.3		[94]
[{Mn(salen)}$_2$(μ-phth)]·2MeOH	1.893(4)	2.773			3.564	F	2.02	0.329			[58]
[Mn(3,5-Brsalen)(3,5-Brsalicylaldehyde)]$_2$	1.918(7)	2.728(2)	100.00(1)		3.597(3)	F	2.00	0.55	−4.1		[94]
[Mn(salpn)(H_2O)]$_2$(ClO_4)$_2$	1.9105(2)	2.3407(2)	80.42(7)	99.58(7)	3.258(5)	F	1.96	1.25	−3.13	−0.06	[109]
[Mn(saltmen)(H_2O)]$_2$(ClO_4)$_2$	1.909(2)	2.434(2)	78.42(10)	101.58(10)	3.381(1)	F	1.93	1.79	−2.53	−0.79	[95]
[Mn(saltmen)(ReO_4)]$_2$	1.913(4)	2.459(4)	81.5(1)	98.5(2)	3.330(1)	F	2.00	1.79	−2.50	(<−0.14)	[96]
[Mn(saltmen)(NCS)]$_2$	1.872(2)	3.441(2)	83.76(8)	96.24(8)	4.0923(8)	F	1.99	0.55	−1.25		[95]
[Mn(saltmen)(O_2CCH_3)]$_2$·2CH_3CO_2	1.8906(13)	2.813(5)	99.57(5)		3.641(5)	F	1.98	1.35	−1.9		[94]
[Mn(saltmen)(N_3)]$_2$	1.863(4)	3.190(2)	98.39(16)		3.922(5)	F	1.98	0.6	−1.0		[94]
[Mn(5-Clsaltmen)(H_2O)]$_2$(ClO_4)$_2$·2H_2O	–	–	–	–	–	F	2.05	1.11	−1.74	−0.21	[93]
[Mn(5-Brsaltmen)(H_2O)]$_2$(ClO_4)$_2$	1.916(3)	2.391(3)	77.7(1)	102.3(1)	3.3681(8)	F	1.95	0.76	−1.81	−0.17	[93]
[Mn(naphtmen)(H_2O)]$_2$(ClO_4)$_2$	1.896(3)	2.662(3)	79.4(1)	100.6(1)	3.541(1)	F	1.96	1.20	−0.38		[95]
[Mn(naphtmen)(NCS)]$_2$	1.877(2)	3.758(3)	83.43(10)	96.57(10)	4.3885(9)	F	2.03	0.12	−1.00		[95]
[Mn(naphtmen)(Cl)]$_2$	1.892(5)	3.505(5)	85.8(2)	94.2(2)	4.102(2)	F	2.04	0.38	−1.87		[95]
[Mn(naphtmen)(TCEA)]$_2$	1.904(3)	2.627(3)	81.1(1)	98.9(1)	3.475(2)	F	2.01	1.50		−0.35	[97]
[Mn(acphen)(N_3)]$_2$	1.88(1)	2.87(1)	83.22	96.76	3.611	F	1.99	1.32			[98]
[Mn(acphmen)(H_2O)]$_2$(ClO_4)$_2$	1.894(3)	2.411(3)		100.4	3.325(1)	F	2.015	1.85		−0.205	[99]
	1.892(3)	2.401(3)		1010.9	3.326(1)						
[Mn(saldmen)(N_3)]$_2$	1.912(4)	2.375(5)	78.17(19)	101.83	3.341(2)	AF	2.00	−0.55			[98]
[Mn(salacen)(H_2O)]$_2$(ClO_4)$_2$	1.912(3)	2.305(2)	76.6(1)	103.4(1)	3.318(1)	AF	2.01	−1.68			[100]
[Mn(5-Brsalen)(H_2O)]$_2$(ClO_4)$_2$	1.906(6)	2.419(7)	–	–	3.350(3)	AF	nd	nd	nd	nd	[48]
[Mn(5-Brsalen)(MeOH)]$_2$(ClO_4)$_2$	1.908(3)	2.395(3)	99.85(11)		3.307(4)	AF	1.96	−0.45	−1.0		[94]
[Mn(salen)(NCS)]$_2$	1.880(6)	2.750(6)	81.3(2)	98.7(2)	3.558(3)	AF	nd	nd	nd	nd	[101,41]
[Mn(salpn)(NCS)]$_2$	1.923(3)	2.539(3)	80.01(12)			NI	nd	nd	nd	nd	[67]
[Mn(salen)(H_2O)]$_2$(ClO_4)$_2$·H_2O	1.891(3)	2.490(3)	80.7(1)	99.3(1)	3.361(2)	nd	nd	nd	nd	nd	[102]
[Mn(salen)(Cl)]$_2$	1.906				3.458	nd	nd	nd	nd	nd	[102]
[Mn(salen)($O_2CC_6H_5$)]$_2$	1.876(3)	3.109				nd	nd	nd	nd	nd	[103]
	1.903(2)	2.803									
[Mn(salen)(*p*-$NO_2C_6H_4S$)]$_2$	1.883(1)				4.14	nd	nd	nd	nd	nd	[11]
[Mn(salen){2-(3-oxobutenyl)phenolate}]$_2$	1.886(4)	2.897(4)			3.644(2)	nd	nd	nd	nd	nd	[104]
[Mn(salpn)(Cl)]$_2$·CH_3CN	1.919(4)	2.487(4)				nd	nd	nd	nd	nd	[49]
[Mn(salpn)(Ph_3PO)]$_2$(CF_3SO_3)$_2$	1.914(3)	2.339(3)	80.48(14)	99.52(14)		nd	nd	nd	nd	nd	[105]
[Mn(salen)(Him)]$_2$(ClO_4)$_2$·2MeOH		2.635(3)				nd	nd	nd	nd	nd	[76]
[Mn(3-MeOsalen)(O_2CEt)]$_2$·EtOH	1.89(1)	2.56(1)			3.485(7)	nd	nd	nd	nd	nd	[45]
[Mn(3-MeOsalen)(O_2CBu^n)]$_2$	1.878(7)	2.765(6)			3.529(4)	nd	nd	nd	nd	nd	[45]
[Mn(3,6-Mesalphen)(H_2O)]$_2$(PF_6)$_2$	1.836(7)	2.780(8)				nd	nd	nd	nd	nd	[51]

Table 3
Pertinent bond distances (Å) and angles (°) for Mn(III) salen out-of-plane dimeric cores in metal-assembled compounds and magnetic parameters obtained from the simulation of the magnetic susceptibility (F = ferromagnetic interaction, AF = antiferromagnetic interaction, NI = non-interaction, nd = no data in the literature)

Compound	Mn—O	Mn—O*	O—Mn—O*	Mn—O—Mn*	Mn···Mn*	Mn···Mn interaction	g_{av}	J_{Mn-Mn} (cm^{-1})	D_{Mn} (cm^{-1})	zJ (cm^{-1})	Reference
$[Mn(salen)Cu(A)]_2(BPh_4)_2$	1.878(9)	3.103(5)	88.9(2)	91.1(2)	3.658(2)	F	nd	nd	nd	nd	[134]
$(NEt_4)[\{Mn(5\text{-}MeOsalen)\}_2\{Fe(CN)_6\}]$	1.913(3)	2.375(3)	91.4(1)	98.6(1)	3.2644(8)	F					[114]
$[\{Mn(saltmen)\}_4\{Fe(CN)_6\}]ClO_4$	1.90(1)	2.85(1)	79.9(5)	100.1(5)	3.693(6)	F	nd	nd	nd	nd	[111]
$[Mn(5\text{-}MeOsaltmen)(DCNNQI)]_2\cdot MeOH$	1.900(4)	2.633(6)	80.6(2)	99.4(2)	3.488(2)	F	1.95	1.39	−2.99	−0.16	[133]
$[Mn(5\text{-}MeOsaltmen)(DCNNQI)]_2\cdot 2CH_2Cl_2\cdot 2CH_3CN$	1.897(5)	2.584(4)	78.7(2)	101.3(2)	3.492(1)	F	1.94	0.56	−2.78	−0.35	[133]
$[\{Mn(saltmen)\}\{Ni(pao)(bpy)_2\}]_2(ClO_4)_4$	–	–	–	–	–	F	2.04	0.63		−0.16	[130]
$[\{Mn(5\text{-}Clsaltmen)\}\{Ni(pao)(bpy)_2\}]_2(ClO_4)_4$	1.925(3)	2.492(3)	79.1(1)	100.9(1)	3.4248(8)	F	2.04	0.49		−0.14	[130]
$[\{Mn(5\text{-}Brsaltmen)\}\{Ni(pao)(bpy)_2\}]_2(ClO_4)_4$	1.929(3)	2.493(3)	79.1(1)	100.9(1)	3.4286(8)	F	2.04	0.56		−0.16	[130]
$[\{Mn(5\text{-}MeOsaltmen)\}\{Ni(pao)(bpy)_2\}]_2(ClO_4)_4$	1.934(3)	2.416(3)	78.5(1)	101.5(1)	3.3826(9)	F	1.96	0.28		−0.13	[130]
$[\{Mn(5\text{-}MeOsaltmen)\}\{Cu(salenox^{2-})\}]_2(CF_3SO_3)_2\cdot 2H_2O$	1.879(3)	3.081(2)	85.11(11)	94.89(12)	3.7436(8)	F	1.994	1.18	−2.50	−0.05	[131]
$[\{Mn(5\text{-}MeOsaltmen)\}\{Cu(salenox^{2-})\}]_2(CF_3SO_3)_2$ (dried sample)	1.876(2)	2.858(2)	82.58(9)	97.42(10)	3.6157(6)	F	2.032	1.95	−2.09	−0.016	[131]
$[\{Mn(5\text{-}MeOsaltmen)\}\{Ni(salenox^{2-})\}]_2(CF_3SO_3)_2\cdot 2H_2O$	1.8715(19)	3.1132(14)	84.04(5)	95.96(6)	3.7953(5)	F	1.995	1.11	−2.50	−0.022	[131]
$[\{Mn(5\text{-}MeOsaltmen)\}\{Ni(salenox^{2-})\}]_2(CF_3SO_3)_2$ (dried sample)	1.8765(19)	2.842(2)	81.48(8)	98.52(9)	3.6305(6)	F	2.05	1.11	−2.50	−0.017	[131]
$[\{Mn(acphmen)\}\{W(bpy)(CN)_6\}]_2\cdot 3H_2O$		2.408(3)		100.7(1)	3.333(1)	F	1.98	0.95			[128]
$[\{Mn(saltmen)\}_2\{Ni(pao)_2(py)_2\}](ClO_4)_2$	1.910(3)	2.551(3)	81.1(1)	98.9(1)		F					[37,138]
$[\{Mn(saltmen)\}_2\{Ni(pao)_2(4\text{-}pic)_2\}](ClO_4)_2$	–	–	–	–	–	F					[138]
$[\{Mn(saltmen)\}_2\{Ni(pao)_2(t\text{-}Bupy)_2\}](ClO_4)_2$	–	–	–	–	–	F					[138]
$[\{Mn(saltmen)\}_2\{Ni(pao)_2(N\text{-}Meim)_2\}](ClO_4)_2$	1.907(5)	2.503(6)	80.7(1)	99.3(2)		F					[138]
$[\{Mn(saltmen)\}_2\{Ni(pao)_2(py)_2\}](BF_4)_2$	–	–	–	–	–	F					[138]
$[\{Mn(saltmen)\}_2\{Ni(pao)_2(py)_2\}](PF_6)_2$	1.903(3)	2.537(3)	80.5(1)	99.5(1)		F					[138]
$[\{Mn(saltmen)\}_2\{Ni(pao)_2(py)_2\}](ReO_4)_2$	1.914(6)	2.470(5)	81.2(2)	98.8(2)		F					[138]
$[\{Mn(saltmen)\}_2\{Ni(miao)_2(py)_2\}](ClO_4)_2$	1.905(3)	2.554(2)	80.72(11)	99.28(12)	3.4238(8)	F					[139]
$[\{Mn(saltmen)\}_2\{Ni(miao)_2(py)_2\}](PF_6)_2$	1.905(2)	2.563(2)	80.54(9)	99.96(10)	3.4357(8)	F					[139]
$[\{Mn(saltmen)\}_2\{Ni(eiao)_2(py)_2\}](PF_6)_2$	1.910(2)	2.552(2)	80.04(10)	99.96(11)	3.4417(8)	F					[139]

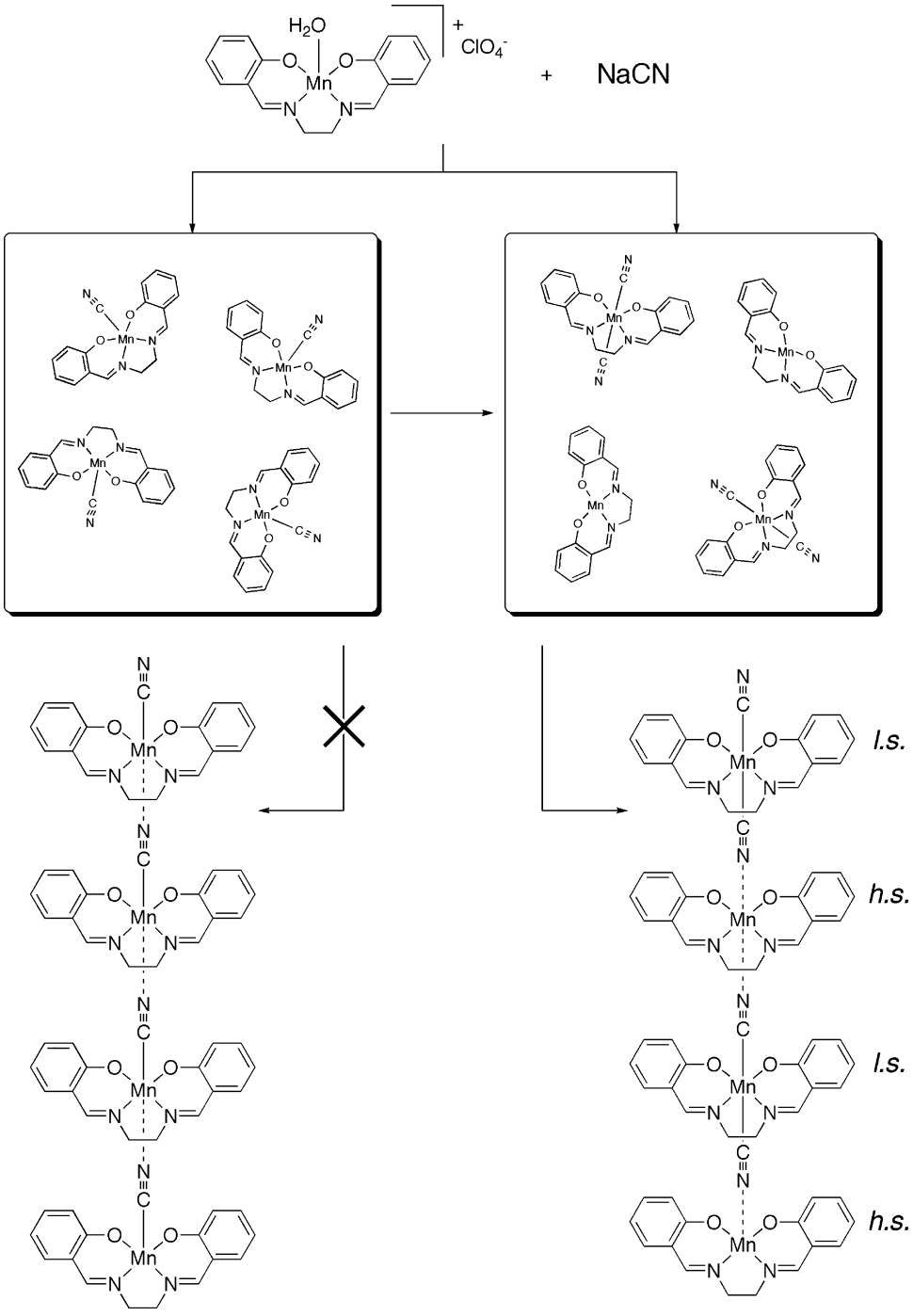

Scheme 5.

The Mn(III) salen out-of-plane dimers are of great interest from a magnetic point of view. A number of such compounds have been structurally characterized and magnetically investigated so far [66,93–105,58,48,41,67,94,11,49,76,45,51]. Furthermore, hetero-metal assembled compounds containing the Mn(III) dimer moiety were also designed (Section 5). Table 2 lists pertinent bond distances and angles for Mn(III) out-of-plane dimers together with their magnetic parameters. Table 3 lists those in metal-assembled compounds. One of the most important aspects is that most dimers exhibit an intra-dimer ferromagnetic exchange coupling, generating an $S_T = 4$ ground state. This ferromagnetic exchange should be due to the accidental orthogonality between the unpaired-electron-occupying d_{z^2} orbital located on the out-of-plane axis (Jahn–Teller axis) and the empty $d_{x^2-y^2}$ orbital located on equatorial Mn–N_2O_2 bonds via the phenolate oxygen, which is explained by the Goodenough–Kanamori rule (Fig. 14) [106]. There are, nevertheless, a few reports of antiferromagnetically coupled dimers. Indeed in some cases, the effective moment (or χT) decreases monotonically at low temperatures and this feature looks like being due to the contribution

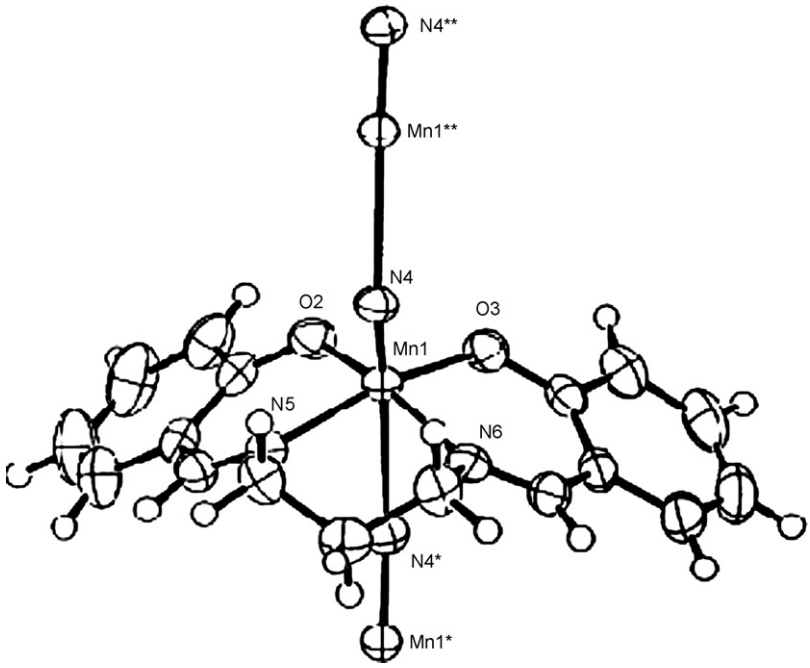

Fig. 13. Structure of a unit of one-dimensional chain [Mn^{V}≡N(salpn)]. Reproduced with permission from Ref. [83].

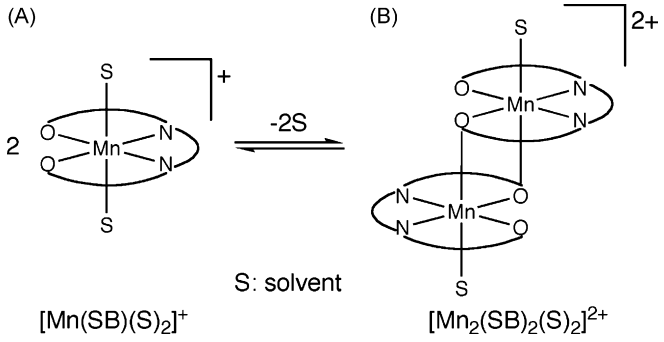

Scheme 6.

of intra-dimer antiferromagnetic coupling. However, in most cases that concluded like that, the contribution of inter-dimer antiferromagnetic interaction and the anisotropic effect, which display as if the decrease of the effective moment was due to

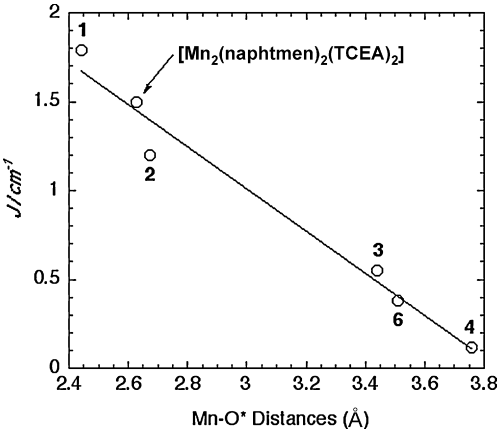

Fig. 15. Correlation between the ferromagnetic exchange parameters J and the Mn—O* distances in Mn(III) out-of-plane dimers with saltmen^{2-} and naphtmen^{2-}. Reproduced with permission from Ref. [95].

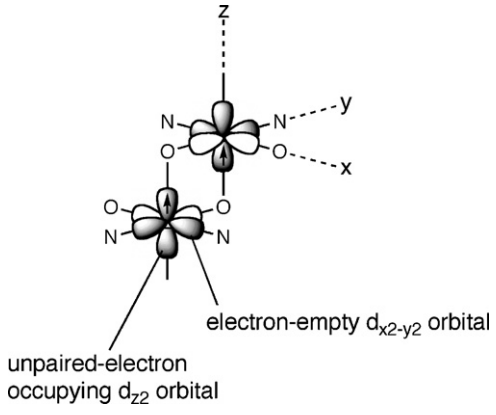

Fig. 14. Orbital arrangements in the out-of-plane dimer of Mn(III) salen-type compounds.

intra-dimer antiferromagnetic coupling despite the actual intra-dimer coupling being ferromagnetic, were undervalued than it is.

Thus, the estimation of magnetic parameters in Mn(III) out-of-plane dimers is sometimes very difficult. Miyasaka et al. first reported a systematic investigation on the correlation between the dimeric core structure and the exchange coupling using a family of Mn(III) saltmen and naphtmen complexes [95]. As mentioned above, the bonding feature Mn^{III}–O^{*}_{Ph}–Mn^{III*} is a key to decide the coupling between Mn^{III} ions. They found a linear correlation between the bond distance of Mn–O^{*}_{Ph} and the exchange coupling constant in this family, where O^{*}_{Ph} is the phenolate oxygen of the neighboring molecule making the out-of-plane dimer and the Mn–O^{*}_{Ph} bond corresponds to the Jahn–Teller axis (Fig. 15). From

these data, $[Mn^{III}(naphtmen)(NCS)]_2$ which has a very long $Mn–O^*_{Ph}$ distance of 3.758 Å still shows ferromagnetic exchange ($J = 0.12\,cm^{-1}$). Not all dimers obey this correlation, but most dimers having the $Mn–O^*_{Ph}$ bond in the range of 2.4–3.76 Å independent of Schiff-base ligand used exhibit ferromagnetic coupling of less than $2\,cm^{-1}$ (note that only a dimer of $[Mn^{III}(salen)(H_2O)]_2(ClO_4)_2$ displayed a strong coupling constant, $J = 6.3\,cm^{-1}$ [66]).

These dimers, albeit with the minimum nuclearity, have the potential themselves to be single-molecule magnets (SMMs) with the $S_T = 4$ ground state. Miyasaka et al. reported the first experimental evidence in 2004 in $[Mn^{III}(saltmen)(ReO_4)]_2$ (Fig. 16) [96]. Before getting down to the specifics of this complex, we give a brief explanation about SMM. The SMM system is a size-defined superparamagnet, which exhibits slow relaxation of the magnetization induced by the combination of a high-spin ground state (S_T) and uniaxial anisotropy (D_{ST}: zero-field splitting parameter). These two intrinsic characteristics create an energy barrier, $D = |D_{ST}|S_T^2$, between spin-up and spin-down states leading to hysteresis phenomena for reversal of the magnetization similar to those observed in bulk magnets. When a magnetic field is applied to magnetize this complex and then removed, the magnetization decays with a relaxation time τ, which follows an Arrhenius law ($\tau = \tau_0 \exp(\Delta_{eff}/k_BT)$) with an effective activation energy equal to Δ_{eff}. At lower temperatures, τ may saturate as the thermally activated relaxation pathway becomes slower than quantum tunneling through the energy barrier.

The simulation of χT and field dependence of the magnetization (MH curve) of $[Mn^{III}(saltmen)(ReO_4)]_2$ gave $D_{ST} = -1.13\,cm^{-1}$ ($D_{ST}/k_B = -1.63$ K) as $g = 2.00$, providing an estimate of the theoretical energy barrier, $D = |D_{ST}|S_T^2/k_B$, of 26 K. Experimental evidence for its SMM behavior was observed in the temperature dependence of relaxation time measured by ac and dc magnetic measurements and an MH curve on an oriented single crystal. At the high temperature range between 4 and 1.9 K, relaxation follows the Arrhenius law with $\Delta_{eff}/k_B = 16$ K and a pre-exponential factor $\tau_0 = 8 \times 10^{-9}$ s (inset of Fig. 17a). Below 1.9 K, τ starts to saturate and becomes temperature independent at 1.9×10^{-4} s below 0.6 K (Fig. 17a). This feature is characteristic of SMM behavior when quantum tunneling of the magnetization (QTM) is dominant [107]. The smaller Δ_{eff} than the expected value of 26 K indicates that the QTM is operative even at higher temperatures. Indeed, the value of Δ_{eff} measured at different dc fields increased up to 23 K at 800 Oe.

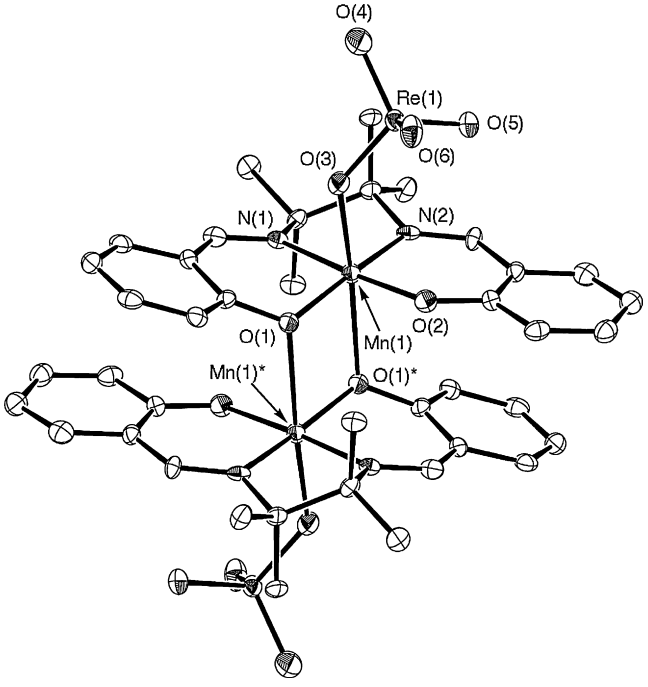

Fig. 16. Structure of an out-of-plane dimeric structure in [Mn(saltmen)$(ReO_4)]_2$. Reproduced with permission from Ref. [96].

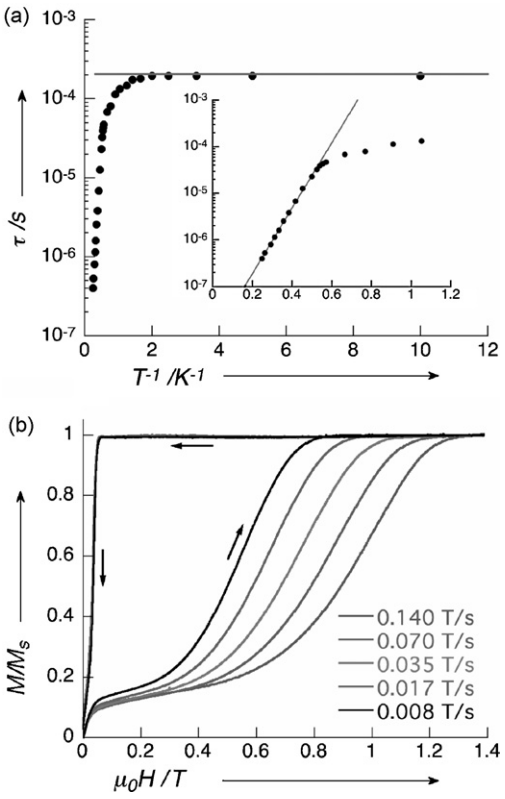

Fig. 17. (a) Plot of the relaxation time τ vs. $1/T$ (a) and the field dependence of the normalized magnetization measured at 0.04 K and several field sweep rates for $[Mn(saltmen)(ReO_4)]_2$. Inset of (a): enlarged view of the high-temperature region of the plot to emphasize the Arrhenius behavior. Reproduced with permission from Ref. [96].

The magnetization hysteresis on an oriented single crystal in the temperature range between 0.04 and 7 K shows a typical butterfly-type hysteresis co-exhibiting fast tunneling between $m_{ST} = \pm 4$ at approximately zero field (Fig. 17b). Hysteresis appeared at temperatures below about 2 K (for field sweep rates of 0.14 T/s) that became temperature independent below 0.6 K but is strongly time dependent, proving the QTM effect. Note that the presence of very small antiferromagnetic intermolecular coupling of about −0.2 K (0.035 T) was observed from these hysteresis data: While the QTM between the ground states $m_{ST} = \pm S_T$ should appear at zero field when inter-SMM

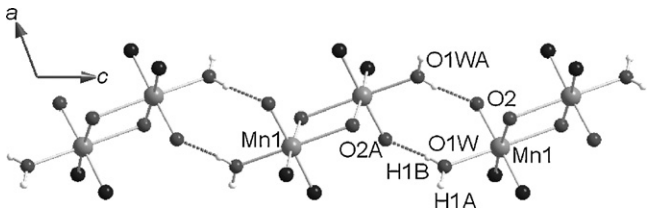

Fig. 18. View of the one-dimensional hydrogen-bond network of $[Mn_2^{III}(salpn)_2(H_2O)_2]^{2+}$ along the *c* axis and the formation of a supramolecular chain motif. Reproduced with permission from Ref. [109].

interactions were negligible, systems with any coexisting inter-SMM interaction have a small shift from zero field, so-called exchange bias field H_{ex} [108]. These magnetic data confirm that the Mn(III) salen dimer is a SMM. Gao et al. confirmed this SMM behavior in several Mn(III) salen dimers [94].

Although more relevant to Section 5.2 on SCMs, one specific case of a Mn(III) out-of-plane dimer will be introduced here. The compound is a SMM system regarded as an intermediate species between ideal SMM system and SCM system. Clérac et al. investigated an out-of-plane dimer, $[Mn^{III}(salpn)(H_2O)]_2(ClO_4)_2$, the cationic dimer of which was linked through weak hydrogen bonds as $OH_{water}\cdots O_{Ph}$ in *one dimension* (Fig. 18) [109]. In the crystal packing, two $[Mn_2^{III}(sapln)(H_2O)_2]^{2+}$ orientations are identified and form an angle (α) of 31° between the respective Jahn–Teller axes. The dimer itself is ferromagnetically coupled to derive the $S_T = 4$ ground state; $J/k_B = 1.8(1)$ K, $D_{Mn}/k_B = -4.5(2)$ K, $J'/k_B = -0.04$ K and $g = 1.96(1)$, where J' is inter-dimer interaction likely mediated by the hydrogen bonds. The D_{ST} was estimated as −1.65 K, therefore, $|D_{ST}|S_T^2 =$ 26.4 K. As a typical case of SMM, we can see a stepwise hysteresis (at 0 and ±0.32 T ($\pm H_1$)) in its *MH* curve measured on an oriented single crystal (Fig. 19a), but at the same time, we realize the occurrence of QTM at zero field despite that the SMM units mutually interact through the hydrogen bonds. This three-step feature including QTM at zero field has never been observed in interaction SMM systems reported previously, but can be explained by taking into account the 1D arrangement of the SMM.

Each magnetic unit (SMM unit) experiences an effective magnetic field (H_{eff}) that results from the applied field (H) and the exchange fields ($\sum H_{ex}$) created by magnetic interactions with its neighbors: $H_{eff} = H + \sum H_{ex}$. In general, when $\sum H_{ex} = 0$, the QTM should be observed at zero field (this is applied to ideal SMMs). Meanwhile, when $\sum H_{ex} \neq 0$, the QTM at $m_{ST} = \pm S_T$ would be shifted by the field to cancel $\sum H_{ex}$, so we can no longer see it at zero field. In the regular case of a 1D arrangement with a weak antiferromagnetic interaction, the sum of the exchange field for one unit can be assumed to be $2H_{ex}$. In such spin units QTM occurs at H_1, but some of the units are *trapped* in the initial m_{ST} state under the experimental conditions, dependent on temperature and field scan rate. Thus, the trapped spin units have the sum of the exchange field of $\sum H_{ex} = (+H_{ex}) + (-H_{ex}) = 0$ (Fig. 19b). Therefore, in the trapped spin units QTM occurs at zero field. This phenomenon is a special case for 1D arranged SMMs with weak intra-chain antiferromagnetic interactions, and should be distinguished from SCM described in Section 5.2. Nevertheless, the observed relaxation of the magnetization is evaluated rather as that for the SCM case ($\Delta = 2\Delta_\xi + \Delta_A$, where $\Delta_\xi = 4|J'|S_T^2\cos(\alpha)/k_B$ and $\Delta_A = |D_{ST}|S_T^2/k_B$) than

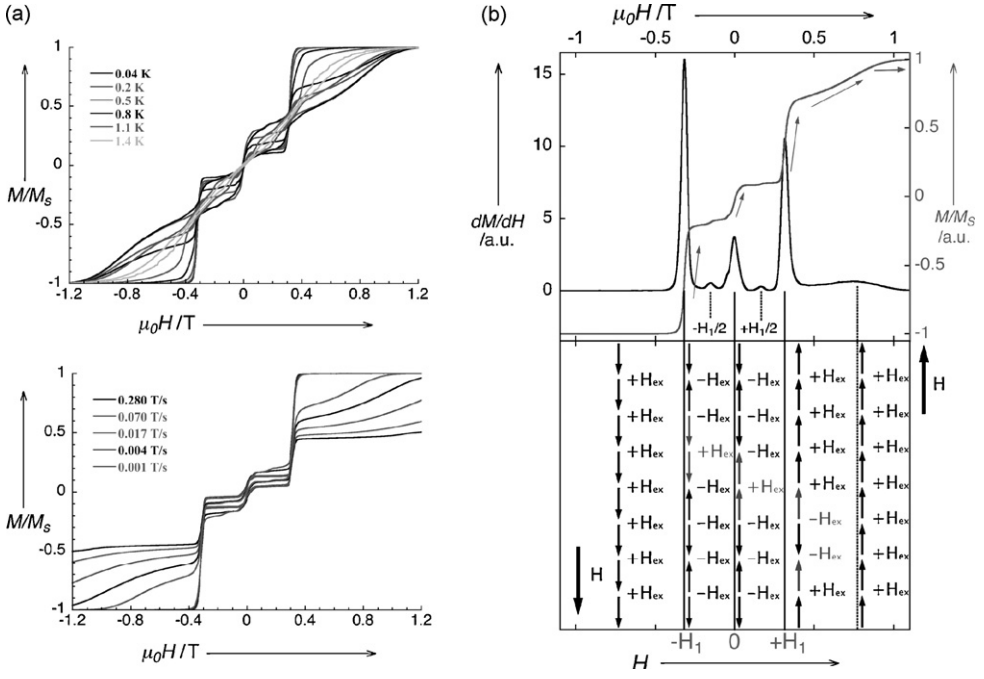

Fig. 19. Field dependence of the normalized magnetization performed on an oriented single crystal of $[Mn_2^{III}(salpn)_2(H_2O)_2]^{2+}$ at different temperatures with a sweep-field rate of 0.002 T/s and with different sweep-field rate at 0.04 K (a) and M/M_S and dM/dH vs. H data at 0.04 K with an increasing sweep-field rate of 0.001 T/s and scheme of the spin chain topology illustrating the observed dynamics (b), where arrows representing the spin projection along the dc field. In these experiments, the field was applied in the easy direction of the crystal. Reproduced with permission from Ref. [109].

that for ideal SMM ($\Delta = |D_{ST}|S_T^2/k_B$): The observed Arrhenius parameters are $\tau_0 = 2 \times 10^{-8}$ s and $\Delta_{eff} = 31.0$ K.

5. Hetero-metallic assemblies with coordination-donor metal complexes

The Mn(III) salen complexes which act as a coordination-acceptor building block led to various hetero-metal assemblies in the reaction with coordination-donor metal complexes. Most assembled compounds are of great interest for their magnetic properties including topics of bulk magnets involving long-range magnetic order, single-molecule magnets (SMMs), and single-chain magnets (SCMs). This section focuses on such hetero-metallic assemblies. Fig. 20 displays coordination-donor metal complexes so far used in the assembly reactions with Mn(III) salen complexes.

5.1. Oligomers including single-molecule magnets

Oligomeric hetero-metallic assemblies based on Mn(III) salen complexes reported so far can be roughly classified into three groups: cyano-bridged compounds, oximate-bridged

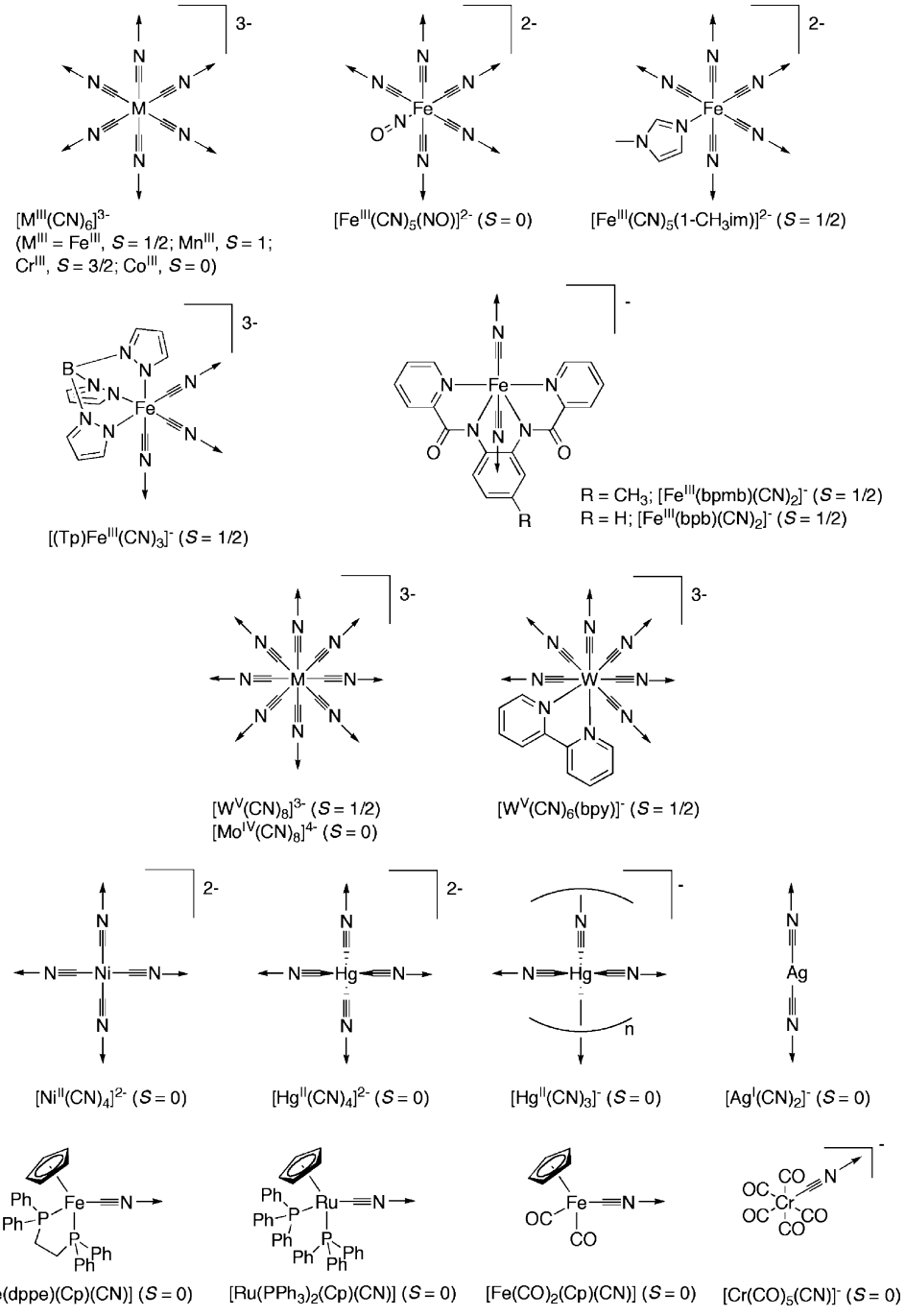

Fig. 20. Coordination-donor building blocks connectable to Mn(III) salen-type complexes.

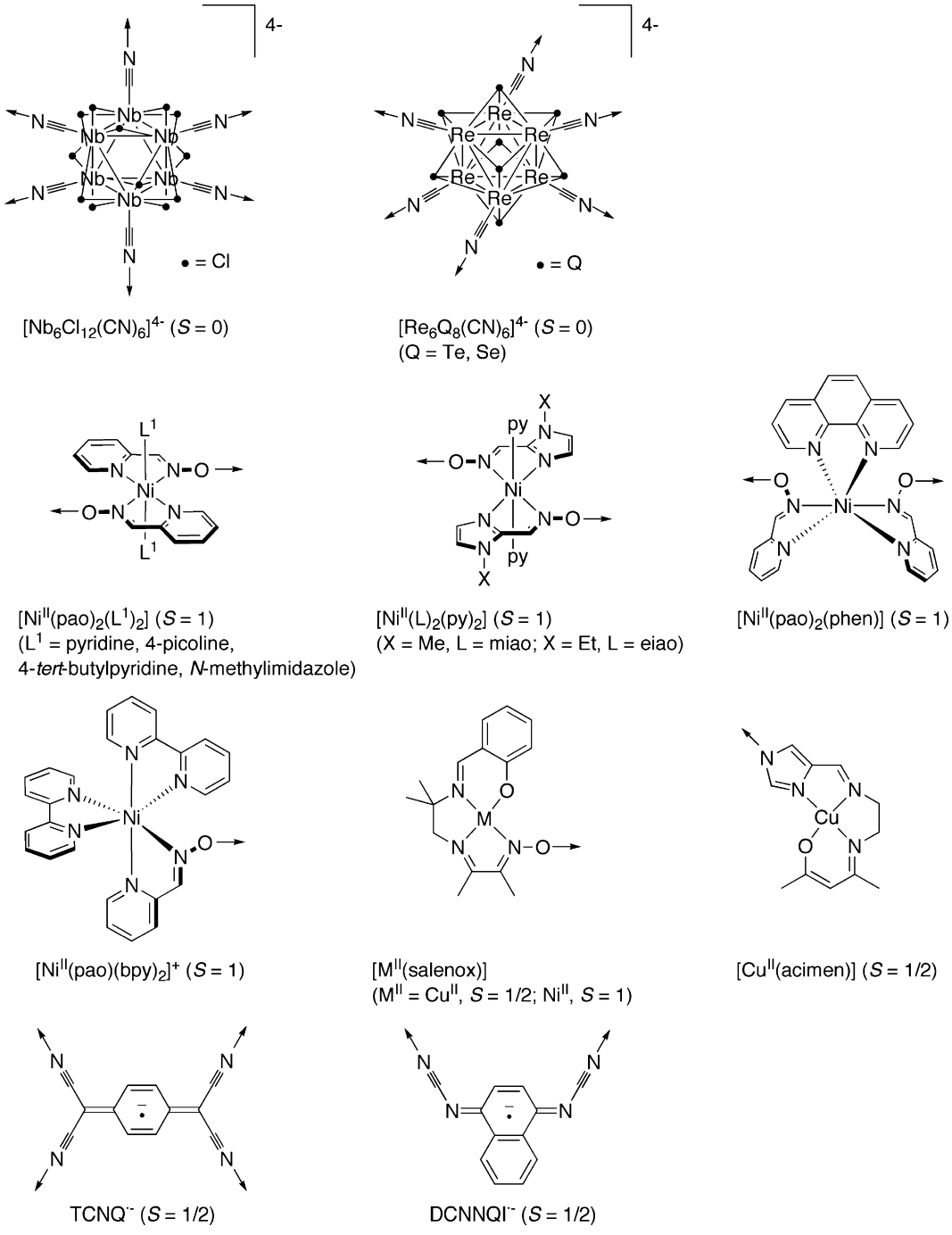

Fig. 20. (*Continued*).

compounds, and others. The cyano-bridged compounds were designed using polycyanometalates as shown in Fig. 20. A Mn:M = 1:1 assembly, $(NEt_4)_2[\{Mn^{III}(saldmen)(H_2O)\}\{Fe^{III}(CN)_6\}]$, was synthesized by Miyasaka et al. (Fig. 21) [110]. One $[Mn^{III}(saldmen)(H_2O)]^+$ group capped by H_2O is coordinated with $[Fe(CN)_6]^{3-}$, forming a discrete dinuclear compound ($Mn–N_{CN} = 2.198(9)$ Å, $Mn–N–C = 162.4(8)^\circ$), containing a hydrogen-bonded 2D network using the coordinating water molecule and crystallization solvents (H_2O and MeOH) filling in voids of packing. The magnetic interaction between Mn^{III} and low-spin Fe^{III} ion via a cyano-linkage is ferromagnetic with $J = 4.5\,cm^{-1}$ ($g_{Mn} = 2.01$, $g_{Fe} = 2.05$, $D = -9.5\,cm^{-1}$, $zJ' = 0.2\,cm^{-1}$). Interestingly, this short-range magnetic property changes by a desolvation treatment ($-2H_2O$·MeOH) into magnet behavior exhibiting a long-range order. This behavior suggests that the reconstruction of coordination/magnetic networks occurs by the desolvation of the capping solvent molecule (Fig. 22). The same group has also reported the first example of 2:1 assemblies. The compounds, $K[\{Mn^{III}(5\text{-}Rsalen)(H_2O)\}_2\{Fe^{III}(CN)_6\}]\cdot 2H_2O$ (R = Cl, Br) [111] and $(NEt_4)[\{Mn^{III}(5\text{-}Clsalen)(H_2O)\}_2\{Fe^{III}(CN)_6\}]\cdot H_2O$ [112], have been synthesized, but not structurally char-

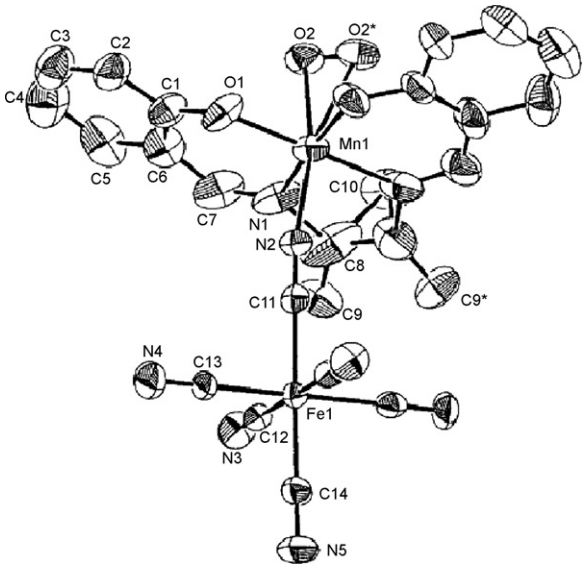

Fig. 21. Structure of $[NEt_4]_2[\{Mn^{III}(saldmen)(H_2O)\}\{Fe^{III}(CN)_6\}]$, where the H_2O molecule capping the $[Mn^{III}(saldmen)]^+$ and methyl group of saldmen^{2-} are disordering. Reproduced with permission from Ref. [110].

acterized. Later, the structure of the R = Br compounds with $M^{III} = Fe^{III}$ and Cr^{III} were reported by Long et al. (Mn–N_{CN} = 2.342(4) Å, Mn–N–C = 141.8(4)° for $M^{III} = Cr^{III}$) [113]. The compounds with $M^{III} = Fe^{III}$ also showed ferromagnetic exchange between Mn(III) and Fe(III) ions via the cyano-linkage with $J = 4.2\,cm^{-1}$ ($g_{Mn} = 2.04$, $g_{Fe} = 2.04$, $D = -7.8\,cm^{-1}$, $zJ' = -0.3\,cm^{-1}$) [111] and $J = 5.9\,cm^{-1}$ ($g_{Mn} = 2.01$, $g_{Fe} = 1.98$, $D = -6.4\,cm^{-1}$, $zJ' = -0.38\,cm^{-1}$) [112] for R = Cl and $J = 4.5\,cm^{-1}$ ($g_{Mn} = 2.02$, $g_{Fe} = 2.00$, $D = -8.5\,cm^{-1}$, $zJ' = -0.3\,cm^{-1}$) for R = Br [111], forming an $S_T = 9/2$ cluster. Meanwhile, the compound with $M^{III} = Cr^{III}$ showed antiferromagnetic exchange between Mn(III) and Cr(III) ions with $J = -6.3\,cm^{-1}$ ($g = 1.912$), forming a ferrimagnetic arrangement with an $S_T = 5/2$ ground state [113]. These compounds have the possibility to be a SMM. Long et al. also reported the SMM behavior of these compounds ($\Delta_{eff} = 25\,cm^{-1}$, $\tau_0 = 5.5 \times 10^{-10}$ s for $M^{III} = Fe^{III}$ and $\Delta_{eff} = 16\,cm^{-1}$, $\tau_0 = 6.1 \times 10^{-8}$ s for $M^{III} = Cr^{III}$ in the relation $\tau = \tau_0 \exp(\Delta_{eff}/k_B T)$) [113]. However, the dynamical parameters especially for $M^{III} = Fe^{III}$ were quite strange: Δ_{eff} is too large and τ_0 is too fast, if these are assumed as those for a SCM case. Finally, this SMM behavior was confirmed in a similar $Mn^{III}_2Fe^{III}$ trinuclear compound possessing the $S_T = 9/2$ ground state and $D_{ST} = -0.87\,cm^{-1}$ ($D_{ST}/k_B = -1.25$ K), *rac*-$(NEt_4)[\{Mn^{III}(salmen)(MeOH)\}_2\{Fe^{III}(CN)_6\}]$; Mn–$N_{CN}$ = 2.219(9) Å, Mn–N–C = 164.7(9)° (Fig. 23) [110]. For this compound, dynamic parameters of $\Delta_{eff} = 9.7\,cm^{-1}$ ($\Delta_{eff}/k_B = 14$ K), $\tau_0 = 2.5 \times 10^{-7}$ s, were obtained which are completely different from those for Long's compound, [114]. This SMM behavior was proven by detailed studies using ac and dc measurements. The single-crystal *MH* measurements using a micro-SQUID revealed a butterfly-type hysteresis with a step at ±40 mT, showing a fast tunneling relationship between $m_{ST} = \pm 9/2$ (Fig. 24). The negligibly weak inter-molecular antiferromagnetic interaction was estimated at $-0.0035\,cm^{-1}$ (−5 mK) from this tunneling field ($|J'| = g\mu_B H_{ex}/(2S_T)$). Importantly, the hysteresis loops are independent of temperature below 0.5 K. Indeed, the relaxation time is saturated at 470 s below this temperature, showing the quantum-tunneling regime. The presence of the tunneling relaxation readily explained the reduction of the energy barrier from $\Delta = |D_{ST}|(S_T^2 - 1/4) = 17.4\,cm^{-1}$ (theoretical value) to $9.7\,cm^{-1}$ (observed value).

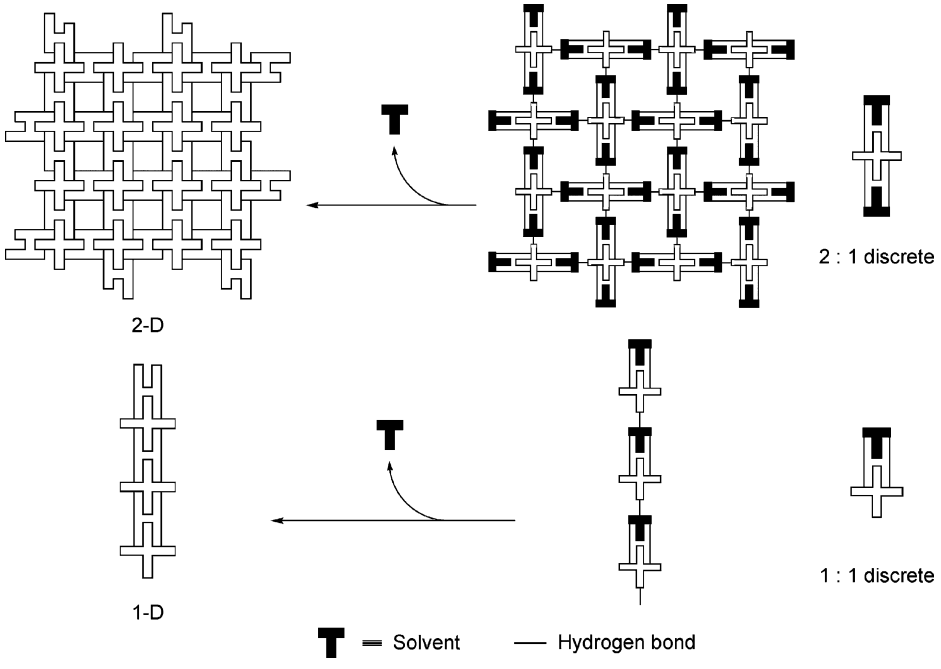

Fig. 22. Schematic representation of molecular rearrangement due to the desolvation of solvated discrete units.

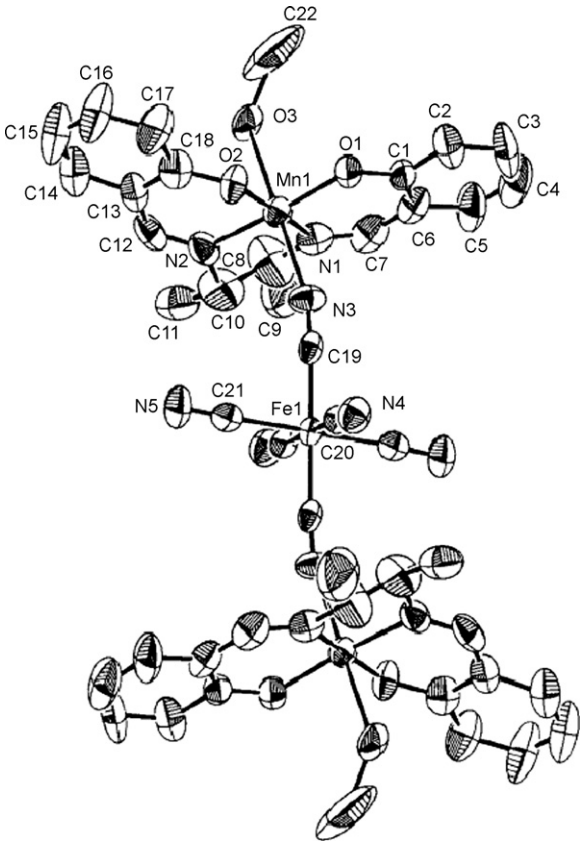

Fig. 23. Structure of *rac*-$(NEt_4)[\{Mn^{III}(salmen)(MeOH)\}_2\{Fe(CN)_6\}]$, where methyl group of $salmen^{2-}$ is disordering. Reproduced with permission from Ref. [110].

This compound also changed to a magnet by removing the capping MeOH molecule. Such a reconstruction from discrete units to a network structure was also demonstrated in a hydrogen-bonded 2:1 aggregation of monomeric species of $[Mn^{III}(5\text{-}Clsalen)(MeOH)]^+$ and $[Fe^{III}(CN)_6]^{3-}$ [115].

Two other Mn^{III}:Fe^{III} = 2:1 compounds based on $[Fe^{III}(CN)_6]^{3-}$ are known so far: *rac*-$(NEt_4)[\{Mn^{III}(salcy)(MeOH)\}_2\{Fe^{III}(CN)_6\}]$ and (*R*,*R*)-(NEt_4) $[\{Mn^{III}(salcy)(H_2O)\}_2\{Fe^{III}(CN)_6\}]$ [110].

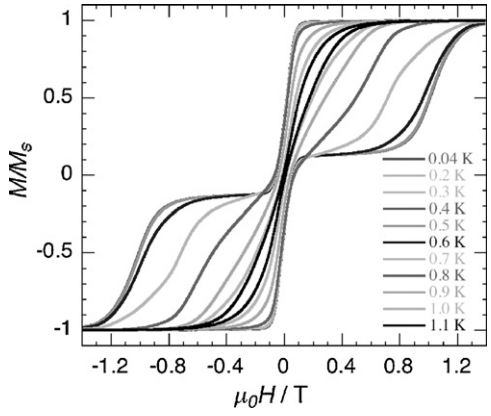

Fig. 24. Field dependence of the magnetization at temperatures below 1.1 K on an oriented single crystal of *rac*-$(NEt_4)[\{Mn^{III}(salmen)(MeOH)\}_2\{Fe^{III}(CN)_6\}]$ along the *b* axis with a sweep field rate of 0.07 T/s. Reproduced with permission from Ref. [114].

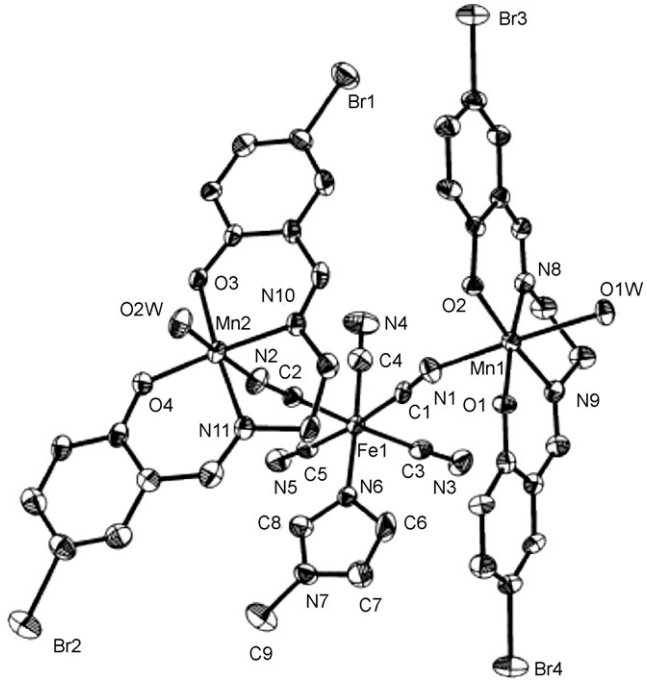

Fig. 25. A *cis*-coordinating trinuclear structure of $[\{Mn^{III}(5\text{-}Brsalen)(H_2O)\}_2\{Fe^{III}(CN)_5(1\text{-}CH_3im)\}]$. Reproduced with permission from Ref. [116].

Kou et al. synthesized five Mn^{III}:Fe^{III} = 2:1 discrete compounds employing $[Fe^{III}(CN)_5(1\text{-}CH_3im)]^{2-}$: $[\{Mn^{III}(5\text{-}Brsalen)(H_2O)\}_2\{Fe^{III}(CN)_5(1\text{-}CH_3im)\}]\cdot H_2O$, $[\{Mn^{III}(5\text{-}Clsalen)(H_2O)\}_2\{Fe^{III}(CN)_5(1\text{-}CH_3im)\}]\cdot H_2O$, $[\{Mn^{III}(5\text{-}Clsalpn)(H_2O)\}_2\{Fe^{III}(CN)_5(1\text{-}CH_3im)\}]$, $[\{Mn^{III}(5\text{-}Clsaltmen)(H_2O)\}_2\{Fe^{III}(CN)_5(1\text{-}CH_3im)\}]\cdot H_2O$, and $[\{Mn^{III}(5\text{-}Brsaltmen)(H_2O)\}_2\{Fe^{III}(CN)_5(1\text{-}CH_3im)\}]\cdot H_2O$ [116]. In all these compounds, $[Mn^{III}(SB)]^+$ is capped by a water molecule forming discrete structures. Except for the first compound, the other compounds have, basically, a similar *trans*-coordinated trinuclear arrangement (linear-type) of $[Mn^{III}–NC–Fe^{III}–CN–Mn^{III}]$. Only the first compound has a *cis*-coordinated arrangement (Fig. 25). However, all compounds showed similar magnetic properties exhibiting ferromagnetic coupling between the Mn(III) and Fe(III) ions ($J_{Mn–Fe} \approx 4.5–6\,cm^{-1}$). These data are also consistent with those observed in the compounds using $[Fe^{III}(CN)_6]^{3-}$.

Colonado et al. synthesized a compound using $[Fe^{III}(CN)_5(NO)]^{2-}$: $[\{Mn^{III}(3\text{-}MeOsalen)(H_2O)\}_2\{Fe^{III}(CN)_5(NO)\}]$ [117]. This compound is a paramagnetic species because it contains the diamagnetic $[Fe^{III}(CN)_5(NO)]^{2-}$. The 2:1 type compounds with other diamagnetic metal ions include: (*R*,*R*)-$[\{Mn^{III}(salcy)(H_2O)\}_2\{Ni^{II}(CN)_4\}]$ [118], $[\{Mn^{III}(saltmen)(H_2O)\}_2\{Hg^{II}(CN)_4\}]$ [119], and $(NEt_4)_2[\{Mn^{III}(salen)(MeOH)\}_2\{Nb_6Cl_{12}(CN)_6\}]\cdot 2MeOH$ [120].

The perfectly cyano-bridged Mn^{III}:M^{III} = 3:1 assemblies can only be seen in $[\{Mn^{III}(salen)(EtOH)\}_3\{M^{III}(CN)_6\}]$ (M^{III} = Fe^{III}, Cr^{III}) (Fig. 26) [121]. In both compounds, the

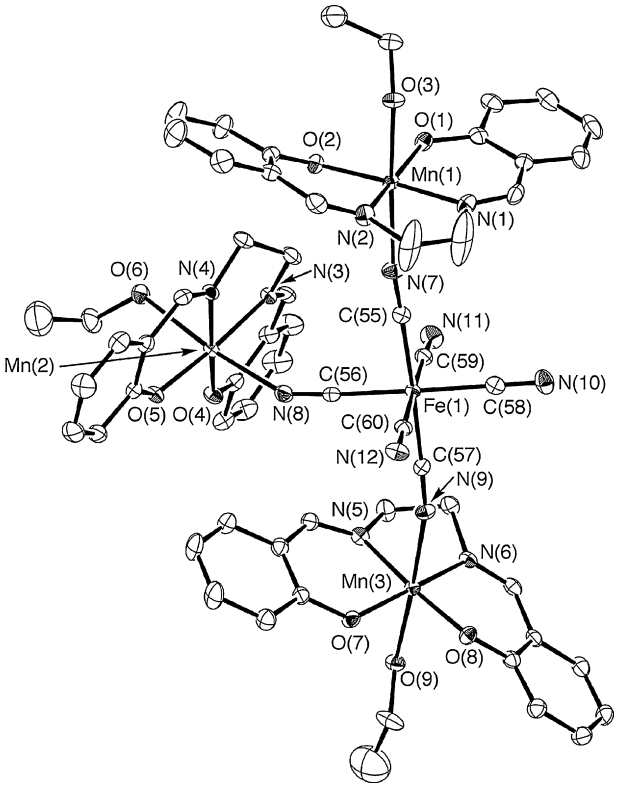

Fig. 26. Structure of $[\{Mn^{III}(salen)(EtOH)\}_3\{Fe^{III}(CN)_6\}]$. Reproduced with permission from Ref. [121].

$M(CN)_6$ moiety acts as a *meridional*-μ_3-coordinating-donor building block and binds three $[Mn(salen)(EtOH)]^+$ moieties, in which Mn–N_{CN} bond distances are very similar, in the range Mn–N ≈ 2.25–2.3 Å, but significantly different Mn-N-C angles are found (Mn_1–N–C ≈ 170°, Mn_2–N–C ≈ 150°, Mn_3–N–C ≈ 162°). A step-by-step simulation approach based on $J_1 \neq J_2 \neq J_3$ yielded an adequate parameter set of $g_{av} = 2.085$, $J_1 = J_3 = -2.78\,cm^{-1}$ (−4.0 K), and $J_2 = 3.34\,cm^{-1}$ (4.8 K) for $M^{III} = Fe^{III}$ and $g_{av} = 2.03$, $J_1 = J_2 = J_3 = -1.60\,cm^{-1}$ (−2.3 K), and $zJ' = -0.14\,cm^{-1}$ (−0.2 K) for $M^{III} = Cr^{III}$. As found in the case of $M^{III} = Fe^{III}$, the exchange interaction between Mn(III) and low-spin Fe(III) ions via the cyano-linkage is variable and dependent on the Mn^{III}–N_{CN} angle. The compound with $M^{III} = Fe^{III}$ exhibited SMM behavior.

A discrete compound using $[W^V(CN)_8]^{3-}$ with $S = 1/2$ was reported by Sieklucka and co-workers [122]: $[\{Mn^{III}(salen)(H_2O)\}_3\{W^V(CN)_8\}]\cdot H_2O$. In this compound, $[W^V(CN)_8]^{3-}$ coordinates with two $[Mn(salen)(H_2O)]^+$ moieties in a V-shape to form a $[(H_2O)Mn^{III}–NC–W^V–CN–Mn^{III}(H_2O)]^-$ unit. The other $[Mn(salen)(H_2O)]^+$ moiety coordinates with this trinuclear unit by forming a Mn^{III}–O_{Ph}–Mn^{III} bond, where O_{Ph} is a phenolate oxygen arising from one of the $[Mn(salen)(H_2O)]^+$ moieties of the trinuclear unit. Therefore, this compound has an asymmetric V-shaped form of $[(H_2O)Mn^{III}–NC–W^V–CN–Mn^{III}(H_2O)–(O_{Ph})–Mn^{III}(H_2O)]$. The temperature-dependence simulation of χT yielded $J_{Mn–W} = -0.75\,cm^{-1}$, $J_{Mn–Mn} = -1.95\,cm^{-1}$, $zJ' = -0.35\,cm^{-1}$, $g = 1.99$.

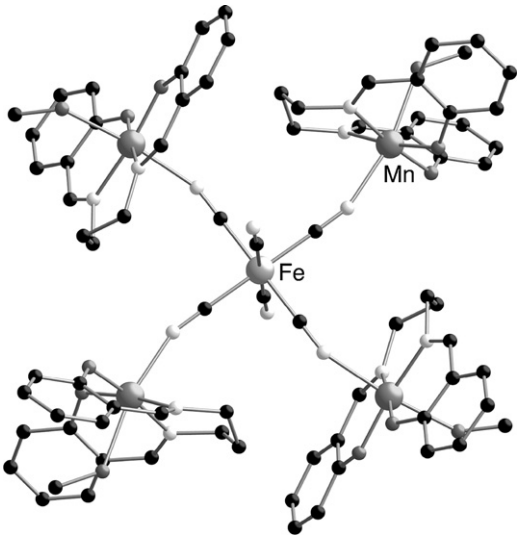

Fig. 27. Structure of $[\{Mn^{III}(salpn)(MeOH)\}_4\{Fe^{III}(CN)_6\}]ClO_4\cdot 9H_2O$ [123].

A Mn^{III}:Fe^{III} = 4:1 discrete assembly was first synthesized by the reaction of $[Mn(saltmen)(H_2O)]ClO_4$ with $(NEt_4)_3[Fe(CN)_6]$ in ethanol: $[\{Mn^{III}(saltmen)(H_2O)\}_4\{Fe^{III}(CN)_6\}]ClO_4$ [110]. A similar reaction using a set of $[Mn(saltmen)(H_2O)]ClO_4$ and $K_3[Fe(CN)_6]$ in a MeOH/water medium produced a 2D network possessing the same assembly ratio (4:1). This compound is presented in Section 5.3. Unfortunately, the first 4:1 discrete assembly was not structurally characterized, but its magnetic properties proved its chemical formula and discrete feature. The exchange between the Mn(III) and Fe(III) ions was estimated as $J = -1.60\,cm^{-1}$ with $g_{Mn} = 2.08$ and $g_{Fe} = 2.2$. In 2003, Liao et al. confirmed this Mn^{III}:Fe^{III} = 4:1 discrete assembly by investigating the structure and magnetic properties of a similar compound: $[\{Mn^{III}(salpn)(MeOH)\}_4\{Fe^{III}(CN)_6\}]ClO_4\cdot 9H_2O$ (Fig. 27) [123]. Here, the four CN^- lie in the equatorial plane of the $[Fe^{III}(CN)_6]^{3-}$ moiety and bridge four Mn ions with a bridging distance and an angle of Mn–N_{CN} = 2.261(3) Å and C–N–Mn = 160.2(3)°. The Mn ion assumed an elongated octahedral geometry, in which a MeOH molecule capped another apical position (Mn–O_{MeOH} = 2.365(3) Å). The exchange between the Mn(III) and Fe(III) ions is ferromagnetic ($J_{Mn–Fe} = 1.4\,cm^{-1}$, $g_{Mn} = 1.99$, $g_{Fe} = 2.01$).

With respect to assemblies having a higher nuclearity, there is no report on Mn^{III}:M^{III} = 5:1 discrete assemblies, but Mn^{III}:M^{III} = 6:1 assemblies, in which all of six coordination sites in $[M^{III}(CN)_6]^{3-}$ are occupied by Mn(III) ions, were reported by Xu et al. (Fig. 28) [124,125]. The compounds have the formula $[\{Mn^{III}(salen)(H_2O)\}_6\{M^{III}(CN)_6\}][M^{III}(CN)_6]\cdot 6H_2O$ ($M^{III} = Fe^{III}$, Cr^{III}), where one $[M^{III}(CN)_6]^{3-}$ is acting as a counter anion. For the compound with $M^{III} = Fe^{III}$, the χT of $17\,cm^3\,K\,mol^{-1}$ at room temperature (spin-only value: $18.76\,cm^3\,K\,mol^{-1}$) increases gradually to reach a maximum of $17.7\,cm^3\,K\,mol^{-1}$ at 14 K and then decreases sharply to $14.6\,cm^3\,K\,mol^{-1}$ at 4.9 K. The high-temperature behavior indicates that a ferromagnetic interaction between Mn(III) and Fe(III) ions is dominant. The simulation at the temperatures

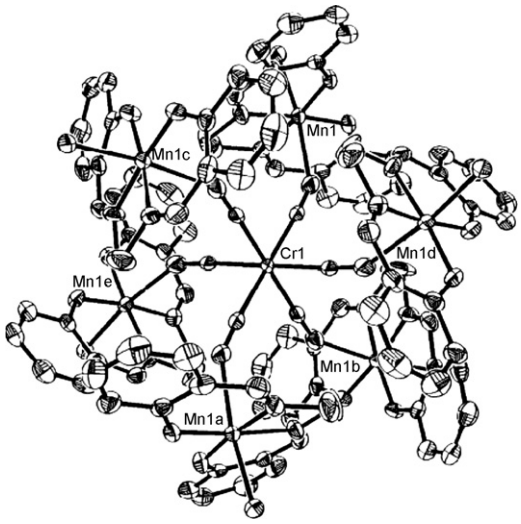

Fig. 28. Structure of the cationic part of $[\{Mn^{III}(salen)(H_2O)\}_6\{Cr^{III}(CN)_6\}]$-$[Cr^{III}(CN)_6]\cdot 6H_2O$. Reproduced with permission from Ref. [125].

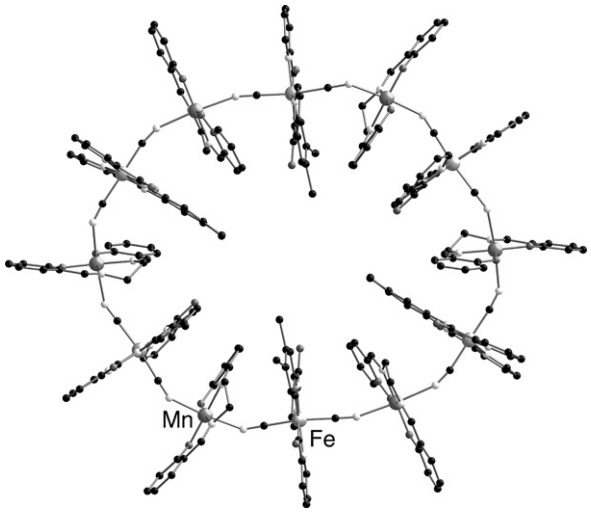

Fig. 29. Structure of $[\{Mn^{III}(salen)\}_6\{Fe^{III}(bpmb)(CN)_2\}_6]\cdot 7H_2O$ [127].

above 14 K yielded $J = 0.24\,cm^{-1}$ with $g_{Fe} = g_{Mn} = 1.92$ [125]. For the compound with $M^{III} = Cr^{III}$, a magnetic study was carried out by two groups. Xu et al. have first reported the temperature dependence of the susceptibility, but it seems to be quite strange: The μ_{eff} of $22.78\mu_B$ ($64.9\,cm^3\,K\,mol^{-1}$) at room temperature is much higher than the spin-only value of $13.19\mu_B$ ($21.75\,cm^3\,K\,mol^{-1}$) expected for the magnetically diluted eight-spin system ($6S_{Mn} = 2$, $2S_{Cr} = 3/2$), but it is nearly equal to the value of $22.3\mu_B$ ($62.16\,cm^3\,K\,mol^{-1}$) calculated for antiferromagnetic coupling between six Mn(III) ions and one Cr(III) ion in the $[\{Mn^{III}(salen)(H_2O)\}_6\{Cr^{III}(CN)_6\}]^{3+}$ unit (possessing a very strong coupling?). Furthermore, this value decreases linearly to reach a minimum at 47 K, then increases slightly to make a peak at 13 K [124]. Finally, Long et al. improved the data and quantized the exchange coupling between Mn(III) and Cr(III) ions via –NC– ($J = -2.5\,cm^{-1}$, $g = 1.86$) [126]. This behavior suggests that antiferromagnetic coupling between the Mn(III) and Cr(III) ions is dominant, consistent with other cyano-bridged Mn(III)/Cr(III) systems.

As a particular case of assembling, Kou and Sato et al. synthesized a cyano-bridged wheel-type compound, $[\{Mn^{III}(salen)\}_6\{Fe^{III}(bpmb)(CN)_2\}_6]\cdot 7H_2O$, which was selectively obtained in high yield (ca. 60%) from a mixed solution of MeOH/MeCN/H_2O (6:3:1 volume ratio) containing the starting materials, $[Mn^{III}(salen)(H_2O)]ClO_4$ and $K[Fe^{III}(bpmb)(CN)_2]$ [127]. This compound has a dodecanuclear wheel-type structure having a $[-Mn^{III}-NC-Fe^{III}-CN-]_6$ cyclic unit (Fig. 29), in which the Mn–N_{CN} distances and the Mn–N–C angles were in the range 2.258(5)–2.354(4) Å and 140.8(4)–163.3(5)°, respectively. The Mn–Fe exchange interaction via a cyanide bridge is ferromagnetic. Interestingly, this compound exhibited slow relaxation of the magnetization at low temperatures. Although the compound is an oligomeric discrete molecule anticipated for a SMM, a large cyclic wheel structure with a weak Mn···Fe coupling might be assumed as a closed quasi-1D chain anticipated for a SCM. Unfortunately, no detailed magnetic data and explanation on the relaxation process were given in the literature.

A cyano/phenoxo bridged $Mn_2^{III}M_2$ was found in $[\{Mn^{III}(acphmen)\}\{W^{V}(CN)_6(bpy)\}]_2$ (Fig. 30) [128]. This compound has a $[W^{V}-CN-Mn^{III}-(O_{Ph})_2-Mn^{III}-NC-W^{V}]$ bridging skeleton, where $-(O_{Ph})_2-$ is an out-of-plane Mn(III) acphmen dimeric form ($Mn^{III}-(O_{Ph})_2-Mn^{III}$). Both exchanges of $Mn^{III}-W^{V}$ and $Mn^{III}-Mn^{III}$ with $S_{Mn} = 2$ and $S_W = 1/2$ were ferromagnetic estimated as $J_{Mn-W} = 0.83\,cm^{-1}$ and $J_{Mn-Mn} = 0.95\,cm^{-1}$, respectively, producing an $S_T = 5$ ground state. This compound exhibited SMM behavior. Some compounds possessing a similar $[M-L-Mn^{III}-(O_{Ph})_2-Mn^{III}-L-M]$ skeleton will be introduced below.

There are Mn(III) salen compounds decorated with organometallic cyanides acting as terminal groups, [Fe(dppe)(Cp)(CN)], $[Ru(PPh_3)_2(Cp)(CN)]$, $[Fe(CO)_2(Cp)(CN)]$, and $[Cr(CO)_5(CN)]^-$ [129]. Two linear-type tetranuclear compounds with a $[M-CN-Mn^{III}-(O_{Ph})_2-Mn^{III}-NC-M]$ bridging skeleton containing an out-of-plane Mn(III) salen dimeric form ($Mn^{III}-(O_{Ph})_2-Mn^{III}$) and three trinuclear compounds with a $[M-CN-Mn^{III}-NC-M]$ bridging skeleton were synthesized: tetramers, $[\{Mn^{III}(salen)\}\{Fe(dppe)(Cp)(CN)\}]_2(SbF_6)_2$ and

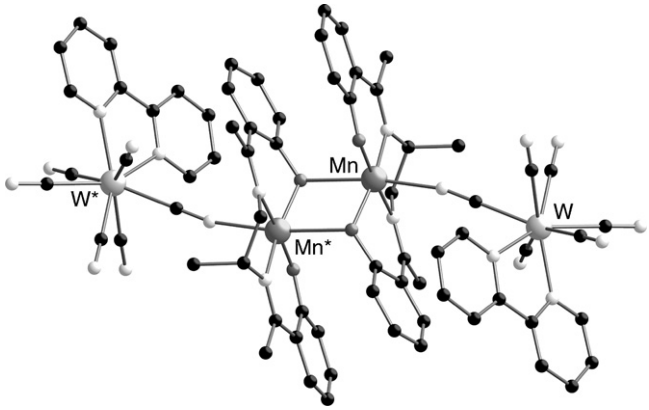

Fig. 30. Structure of $[\{Mn^{III}(acphmen)\}\{W^{V}(CN)_6(bpy)\}]_2$ [128].

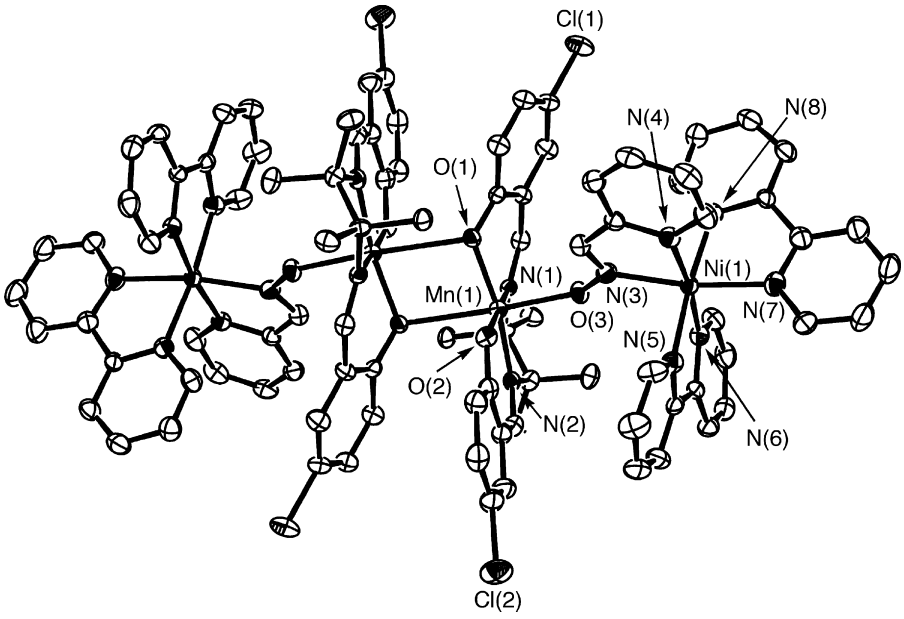

Fig. 31. Structure of $[\{Mn^{III}(5\text{-Clsaltmen})\}\{Ni^{II}(pao)(bpy)_2\}]_2(ClO_4)_4$. Reproduced with permission from Ref. [130].

$[\{Mn^{III}(salen)\}\ \{Ru(PPh_3)(Cp)(CN)\}]_2(SbF_6)_2$; trimers, $[\{Mn^{III}(salen)\}\{Fe(CO)_2(Cp)(CN)\}_2]SbF_6$, $[\{Mn^{III}(salen)\}\{Fe(dppe)(Cp)(CN)\}_2]SbF_6$, and $(NEt_4)[\{Mn^{III}(salen)\}\{Cr(CO)_5(CN)\}_2]$.

To summarize the magnetic properties on cyano-bridged compounds, the magnetic interaction between Mn(III) ion and low spin Fe(III) ion via the –NC– linkage (i.e., Mn^{III}–NC–Fe^{III}(l.s.)) shows both ferromagnetic and antiferromagnetic behavior, while that of Mn^{III}–NC–Mn^{III}(l.s.) and Mn^{III}–NC–Cr^{III} is always ferromagnetic and antiferromagnetic, respectively (this tendency can be seen in other dimensional compounds as described from the next section). Table 4 lists cyano-bridged assemblies with Mn^{III}–NC–M bridging dimensions with their exchange coupling constants. In the Mn^{III}–NC–Fe^{III}(l.s.) system, the exchange coupling is quite sensitive to the bonding feature of Mn^{III}–N–C–Fe^{III}, although the examples with the ferromagnetic coupling are more generally seen than those with the antiferromagnetic one. The nature of the magnetic interaction cannot be simply summarized as a dependency only on the Mn^{III}–N–C angle, but would also be correlated with the bent angle of Mn^{III}–N–C–M. The latter angle creates the orthogonality between an occupied dπ orbital of the Fe(III) ion and three dπ orbitals of the Mn(III) ion [111].

In recent outstanding contributions to nanosized molecular magnets, Miyasaka et al. focused on oximate-bridged assemblies of Mn(III) salen complexes employing coordination-donor metal building blocks having naked oximato groups. Among several kinds of such materials, to date, three types of such oligomeric compounds have been reported. The use of mono-oximato building blocks that act as terminal building blocks provided linear-type hetero-metal assemblies having a [M–NO–Mn^{III}–$(O_{Ph})_2$–Mn^{III}–ON–M] bridging skeleton containing an out-of-plane Mn(III) salen dimeric moiety. The first type is a family of $[\{Mn^{III}(5\text{-Rsaltmen})\}\{Ni^{II}(pao)(bpy)_2\}]_2(ClO_4)_4$ (R = H, Cl, Br, MeO) (Fig. 31) [130]. These compounds were synthesized by the assembly reaction with both $[Mn^{III}(5\text{-Rsaltmen})(H_2O)]_2(ClO_4)_2$ and $[Ni^{II}(pao)(bpy)_2]ClO_4$ in a methanol/water medium. The [Ni^{II}–NO–Mn^{III}–$(O_{Ph})_2$–Mn^{III}–ON–Ni^{II}] bridging skeleton is composed of local dimensions of $Mn–O_{oximate} \approx 2.1$ Å, Mn–O* ≈ 2.4–2.5 Å, Mn–O–N ≈ 129–132°, Mn–O–Mn* ≈ 101°, and O–Mn–O* ≈ 79°. Table 5 lists the magnetic parameters of these assemblies containing the $[Mn^{III}_2(saltmen)_2]^{2+}$ out-of-plane dimeric core. The exchange interactions in the two pathways of Ni^{II}–NO–Mn^{III} and Mn^{III}–$(O_{Ph})_2$–Mn^{III} are strongly antiferromagnetic ($J_{Mn–Ni}/k_B > -20$ K) and weakly ferromagnetic ($J_{Mn–Mn}/k_B < 1$ K), respectively, generating an $S_T = 2$ ground state. As expected from such a small low-lying state, SMM behavior was not observed at temperatures above 1.8 K.

Similar $Mn_2{}^{III}M_2{}^{II}$ assemblies having the [M–NO–Mn^{III}–$(O_{Ph})_2$–Mn^{III}–ON–M] bridging skeleton were also synthesized using a mono-Ni(II) or Cu(II) complex with 3-{2-[(2-hydroxy-benzylidene)-amino]-2-methyl-propylimino}-butan-2-one oximate ($salenox^{2-}$): $[\{Mn^{III}(5\text{-MeOsaltmen})\}\{M^{II}(salenox^{2-})\}]_2(CF_3SO_3)_2{\cdot}2H_2O$ (M = Cu, Ni) [131]. The $[M^{II}(salenox)]$ unit has a naked oximato group able to coordinate to other metal ions, so acting as a coordination-donor building block (Costes et al. was the first to report on this type of complexes (with $M = Cu^{II}$)) that acts as a bidentate unit when assembled with lanthanide metal ions (in μ-phenolato-μ-oximato fashion [132]). These two compounds are isostructural (Fig. 32). Furthermore, their solvent-free compounds ($-2H_2O$) were also stable (these compounds were characterized by single-crystal X-ray crystallography and magnetic measurements). Magnetic measurements on the compounds with $M^{II} = Cu^{II}$ revealed antiferromagnetic Mn^{III}/Cu^{II} interaction ($J_{Mn–Cu}/k_B \approx -16$ K)

Table 4
Mn^{III}—NC—M bridging dimensions and the exchange coupling constant J_{Mn-M} in cyano-bridged assemblies of Mn(III) salen complexes

Compound	Coordination donor and its spin state	Mn:M	Mn—N_{CN}	Mn—N—C	J_{Mn-M} (cm^{-1})	Reference
Discrete compounds						
$(NEt_4)_2[\{Mn(saldmen)(H_2O)\}\{Fe(CN)_6\}]$	$[Fe^{III}(CN)_6]^{3-}$, $S=1/2$	1:1	2.198(9)	162.4(8)	+4.5	[110]
$K[\{Mn(5\text{-}Clsalen)(H_2O)\}_2\{Fe(CN)_6\}]\cdot 2H_2O$	$[Fe^{III}(CN)_6]^{3-}$, $S=1/2$	2:1			+4.2	[111]
$K[\{Mn(5\text{-}Brsalen)(H_2O)\}_2\{Fe(CN)_6\}]\cdot 2H_2O$	$[Fe^{III}(CN)_6]^{3-}$, $S=1/2$	2:1	2.331(4)	142.7(3)	+4.5 (+4.6)[a]	[111,113]
$(NEt_4)[\{Mn(5\text{-}Clsalen)(H_2O)\}_2\{Fe(CN)_6\}]\cdot H_2O$	$[Fe^{III}(CN)_6]^{3-}$, $S=1/2$	2:1			+5.9	[112]
rac-$(NEt_4)[\{Mn(salmen)(MeOH)\}_2\{Fe(CN)_6\}]$	$[Fe^{III}(CN)_6]^{3-}$, $S=1/2$	2:1	2.219(9)	164.7(9)	+3.6	[110]
rac-$(NEt_4)[\{Mn(salcy)(MeOH)\}_2\{Fe(CN)_6\}]$	$[Fe^{III}(CN)_6]^{3-}$, $S=1/2$	2:1				[110]
(*R*,*R*)-$(NEt_4)[\{Mn(salcy)(H_2O)\}_2\{Fe(CN)_6\}]$	$[Fe^{III}(CN)_6]^{3-}$, $S=1/2$	2:1				[110]
$[\{Mn(5\text{-}Brsalen)(H_2O)\}_2\{Fe(CN)_5(1\text{-}CH_3im)\}]\cdot H_2O$	$[Fe^{III}(CN)_5(1\text{-}CH_3im)]^{2-}$, $S=1/2$	2:1 (*cis*)	2.236(6)	160.0(5)	+4.75(6)	[116]
					(+5.92(7))[b]	
			2.222(6)	154.3(5)		
$[\{Mn(5\text{-}Clsalen)(H_2O)\}_2\{Fe(CN)_5(1\text{-}CH_3im)\}]\cdot H_2O$	$[Fe^{III}(CN)_5(1\text{-}CH_3im)]^{2-}$, $S=1/2$	2:1	2.243(5)	149.8(5)	+4.98(10)	[116]
					(+5.86(11))[b]	
$[\{Mn(5\text{-}Clsalpn)(H_2O)\}_2\{Fe(CN)_5(1\text{-}CH_3im)\}]$	$[Fe^{III}(CN)_5(1\text{-}CH_3im)]^{2-}$, $S=1/2$	2:1	2.221(5)	165.2(5)	+6.01(8)	[116]
			2.249(5)	156.9(5)	(+6.68(8))[b]	
			(2.229(5))	(152.8(5))		
			(2.298(5))	(147.8(5))		
$[\{Mn(5\text{-}Clsaltmen)(H_2O)\}_2\{Fe(CN)_5(1\text{-}CH_3im)\}]\cdot H_2O$	$[Fe^{III}(CN)_5(1\text{-}CH_3im)]^{2-}$, $S=1/2$	2:1	2.311(3)	159.7(3)	+4.51(6)	[116]
			2.258(3)	157.8(3)	(+4.95(6))[b]	
$[\{Mn(5\text{-}Brsaltmen)(H_2O)\}_2\{Fe(CN)_5(1\text{-}CH_3im)\}]\cdot H_2O$	$[Fe^{III}(CN)_5(1\text{-}CH_3im)]^{2-}$, $S=1/2$	2:1	2.323(3)	159.4(2)	+4.68(5)	[116]
			2.266(3)	157.2(3)	(+5.10(6))[b]	
$[\{Mn(3\text{-}MeOsalen)(H_2O)\}_2\{Fe(CN)_5(NO)\}]$	$[Fe^{III}(CN)_5(NO)]^{2-}$, $S=0$	2:1	2.355(6)	146.9(6)	–	[117]
$K[\{Mn(5\text{-}Brsalen)(H_2O)\}_2\{Cr(CN)_6\}]\cdot 2H_2O$	$[Cr^{III}(CN)_6]^{3-}$, $S=3/2$	2:1	2.342(4)	141.8(4)	−6.3	[113]
(*R*,*R*)-$[\{Mn(salcy)(H_2O)\}_2\{Ni(CN)_4\}]$	$[Ni^{II}(CN)_4]^{2-}$, $S=0$	2:1	2.276(8)–2.302(8)		–	[118]
$[\{Mn(saltmen)(H_2O)\}_2\{Hg(CN)_4\}]$	$[Hg^{II}(CN)_4]^{2-}$, $S=0$	2:1	2.295(7)	173.4(8)	–	[119]
$(NEt_4)_2[\{Mn(salen)(MeOH)\}_2\{Nb_6Cl_{12}(CN)_6\}]\cdot 2MeOH$	$[Nb_6Cl_{12}(CN)_6]^{4-}$, $S=0$	2:1	2.295(3)	157.2(3)	–	[120]
$[\{Mn(salen)(EtOH)\}_3\{Fe(CN)_6\}]$	$[Fe^{III}(CN)_6]^{3-}$, $S=1/2$	3:1	2.249(2)–2.307(2)	170.7(2)	J_1: −2.78	[121]
				148.9(2)	J_2: +3.34	
				161.9(2)	J_3: −2.78	
$[\{Mn(salen)(EtOH)\}_3\{Cr(CN)_6\}]$	$[Cr^{III}(CN)_6]^{3-}$, $S=3/2$	3:1	2.234(4)–2.293(4)	168.7(4)	−1.60	[121]
				149.9(4)		
				161.5(4)		
$[\{Mn(salen)(H_2O)\}_3\{W(CN)_8\}]\cdot H_2O$	$[W^{V}(CN)_8]^{3-}$, $S=1/2$	3:1[c]	2.336(3)	153.2(3)	−0.75	[122]
			2.398(3)	149.3(3)		
$[\{Mn(saltmen)(H_2O)\}_4\{Fe(CN)_6\}]ClO_4$	$[Fe^{III}(CN)_6]^{3-}$, $S=1/2$	4:1			−1.60	[110]
$[\{Mn(salpn)(MeOH)\}_4\{Fe(CN)_6\}]ClO_4\cdot 9H_2O$	$[Fe^{III}(CN)_6]^{3-}$, $S=1/2$	4:1	2.261(3)	160.2(3)	+1.4	[123]
$[\{Mn(salen)(H_2O)\}_6\{Fe(CN)_6\}][Fe(CN)_6]\cdot 6H_2O$	$[Fe^{III}(CN)_6]^{3-}$, $S=1/2$	6:1	2.334(2)	150.74(14)	+0.24	[125]
$[\{Mn(salen)(H_2O)\}_6\{Cr(CN)_6\}][Cr(CN)_6]\cdot 6H_2O$	$[Cr^{III}(CN)_6]^{3-}$, $S=3/2$	6:1	2.322(4)	149.9(4)	−2.5[d]	[124,126]
$[\{Mn(salen)\}_6\{Fe(bpmb)(CN)_2\}_6]\cdot 7H_2O$	$[Fe^{III}(bpmb)(CN)_2]^{-}$, $S=1/2$	6:6 (ring)	2.258(5)–2.354(4)	140.8(4)–163.3(5)	F[e]	[127]
$[\{Mn(acphmen)\}\{W(CN)_6(bpy)\}]_2$	$[W^{V}(CN)_6(bpy)]^{-}$, $S=1/2$	2:2 (1:1 × 2)	2.291(3)	165.2(4)	+0.83	[128]
$[\{Mn(salen)\}\{Fe(dppe)(Cp)(CN)\}]_2(SbF_6)_2$	[Fe(dppe)(Cp)(CN)], $S=0$	2:2 (1:1 × 2)	2.154(8)	172.6(7)	–	[129]
$[\{Mn(salen)\}\{Ru(PPh_3)(Cp)(CN)\}]_2(SbF_6)_2$	$[Ru(PPh_3)_2(Cp)(CN)]$, $S=0$	2:2 (1:1 × 2)			–	[129]
$[\{Mn(salen)\}\{Fe(CO)_2(Cp)(CN)\}_2]SbF_6$	$[Fe(CO)_2(Cp)(CN)]$, $S=0$	1:2			–	[129]
$[\{Mn(salen)\}\{Fe(dppe)(Cp)(CN)\}_2]SbF_6$	[Fe(dppe)(Cp)(CN)], $S=0$	1:2			–	[129]
$(NEt_4)[\{Mn(salen)\}\{Cr(CO)_5(CN)\}_2]$	$[Cr(CO)_5(CN)]^{-}$, $S=0$				–	[129]
1D chains						
[Mn(salen)(CN)]	$[Mn^{III}(salen)(CN)_2]^{-}$, $S=1$	1:1	2.34(3)	143(2)	F[e]	[81]

Table 4 (*Continued*)

Compound	Coordination donor and its spin state	Mn:M	Mn—N_{CN}	Mn—N—C	J_{Mn-M} (cm^{-1})	Reference
			2.25(3)	147(3)		
$(NEt_4)[\{Mn(5\text{-}MeOsalen)\}_2\{Fe(CN)_6\}]$	$[Fe^{III}(CN)_6]^{3-}$, $S=1/2$	2:1	2.179(3)	146.7(4)	+6.5	[114]
$[\{Mn(R,R\text{-}salcy)(H_2O)\}_2\{Mn(R,R\text{-}salcy)\}\{Fe(CN)_6\}]\cdot 2H_2O$ and $[\{Mn(S,S\text{-}salcy)(H_2O)\}_2\{Mn(S,S\text{-}salcy)\}\{Fe(CN)_6\}]\cdot 2H_2O$	$[Fe^{III}(CN)_6]^{3-}$, $S=1/2$	3:1	Inter-tetramer: 2.398(4); intra-tetramer: 2.251(4) –2.256(4)	Inter: 148.3(3); intra: 143.0(3) –152.9(3)	Inter: −0.46; intra: −0.15	[145]
$[\{Mn(5\text{-}MeOsalen)\}\{(Tp)Fe(CN)_3\}]\cdot 2MeOH$	$[(Tp)Fe^{III}(CN)_3]^{-}$, $S=1/2$	1:1	2.364(2)	161.7(2)	+1.66	[146]
			2.320(2)	151.1(2)	+1.21	
$[Mn(salen)(H_2O)_2]_2[\{Mn(salen)(H_2O)\}\{Mn(salen)\}_2\{Mo(CN)_8\}]\cdot 0.5ClO_4\cdot 0.5OH\cdot 4.5H_2O$	$[Mo^{IV}(CN)_8]^{4-}$, $S=0$	5:1[f]	2.197(6)–2.314(6)	142.7(5)–152.0(6)	–	[122]
$[\{Mn(saltmen)(H_2O)\}\{Hg(CN)_3\}]$	$[Hg^{II}(CN)_3]^{-}$, $S=0$	1:1	2.29(1)	140(1)	–	[119]
$[Mn(salen)Ag(CN)_2]$	$[Ag^{I}(CN)_2]^{-}$, $S=0$	1:1	2.321(4)	170.4(3)	–	[68]
			2.286(4)	144.4(3)		
$(NEt_4)_2[\{Mn(acacen)\}\{Fe(CN)_6\}]$	$[Fe^{III}(CN)_6]^{3-}$, $S=1/2$	1:1	2.316(4)	152.6(3)	F[e]	[147]
$(NEt_4)[\{Mn(acacen)\}\{Fe(CN)_5(1\text{-}CH_3im)\}]\cdot 6H_2O$	$[Fe^{III}(CN)_5(1\text{-}CH_3im)]^{2-}$, $S=1/2$	1:1 (*cis*)	2.331(4)	144.4(4)	AF[g]	[116]
$[\{Mn(salen)\}\{Fe(bpb)(CN)_2\}]$	$[Fe^{III}(bpb)(CN)_2]^{-}$, $S=1/2$	1:1	2.301(3)–2.439(3)	151.8(3)–158.6(3)	AF[g]	[127]
2D networks						
$K[\{Mn(3\text{-}MeOsalen)\}_2\{Fe(CN)_6\}]\cdot 2DMF$	$[Fe^{III}(CN)_6]^{3-}$, $S=1/2$	2:1	2.290(5)	169.5(5)	F[e]	[111]
			2.415(5)	137.2(4)		
$K[\{Mn(3\text{-}MeOsalen)\}_2\{Mn(CN)_6\}]\cdot 2DMF$	$[Mn^{III}(CN)_6]^{3-}$, $S=1/2$	2:1			F[e]	[82]
$K[\{Mn(3\text{-}MeOsalen)\}_2\{Cr(CN)_6\}]\cdot 2DMF$	$[Cr^{III}(CN)_6]^{3-}$, $S=3/2$	2:1			AF[g]	[150]
$K[\{Mn(3\text{-}MeOsalen)\}_2\{Co(CN)_6\}]\cdot 2DMF$	$[Co^{III}(CN)_6]^{3-}$, $S=0$	2:1			–	[150]
$(NEt_4)[\{Mn(salen)\}_2\{Fe(CN)_6\}]$	$[Fe^{III}(CN)_6]^{3-}$, $S=1/2$	2:1	2.266(3)	167.8(3)	AF[g]	[151]
			2.337(3)	146.2(2)		
$(NEt_4)[\{Mn(5\text{-}Clsalen)\}_2\{Fe(CN)_6\}]$	$[Fe^{III}(CN)_6]^{3-}$, $S=1/2$	2:1	2.286(7)	154.4(7)	AF[g]	[112]
			2.266(7)	146.1(7)		
$[\{Mn(salen)\}_2\{Ni(CN)_4\}]\cdot 0.5H_2O$	$[Ni^{II}(CN)_6]^{2-}$, $S=0$	2:1	2.312(6)	163.8(6)	–	[153]
$[\{Mn(5\text{-}Brsalen)\}_2\{Fe(CN)_5(NO)\}]$	$[Fe^{III}(CN)_5(NO)]^{2-}$, $S=0$	2:1	2.378(2)	151.8(2)	–	[117]
$[K(18\text{-}cr\text{-}6)(2\text{-}PrOH)_2][\{Mn(acacen)\}_2\{Fe(CN)_6\}]$	$[Fe^{III}(CN)_6]^{3-}$, $S=1/2$	2:1	2.331(3)	152.0(3)	F[e]	[154]
			2.439(3)	154.8(3)		
$(NMe_4)_2[\{Mn(salen)\}_2\{Nb_6Cl_{12}(CN)_6\}]$	$[Nb_6Cl_{12}(CN)_6]^{4-}$, $S=0$	2:1	2.233(3)	173.3(1)	–	[120]
			2.365(3)			
$[\{Mn(saltmen)\}_4\{Fe(CN)_6\}]ClO_4$	$[Fe^{III}(CN)_6]^{3-}$, $S=1/2$	4:1	2.19(1)	156.1(10)	F[e]	[111]
$[\{Mn(saltmen)\}_4\{Fe(CN)_5(CH_3im)\}](ClO_4)_2$	$[Fe^{III}(CN)_5(1\text{-}CH_3im)]^{2-}$, $S=1/2$	4:1	2.197(8)	157.3(7)	2.34(7)	[116]
$[\{Mn(salen)\}_4\{Re_6Te_8(CN)_6\}]$	$[Re_6Te_8(CN)_6]^{4-}$, $S=0$	4:1	2.14(1)–2.28(1)	141.4(1)–149.5(1)	–	[155]
3D networks						
$Na[\{Mn(salen)\}_3\{Re_6Se_8(CN)_6\}]$	$[Re_6Se_8(CN)_6]^{4-}$, $S=0$	3:1	2.293(8)	138.5(7)	–	[156]
$(H_3O)_2[\{Mn(salen)\}_6\{Fe(CN)_6\}\{Nb_6Cl_{12}(CN)_6\}]\cdot 3H_2O$	$[Fe^{II}(CN)_6]^{4-}$, $S=0$ and $[Nb_6Cl_{12}(CN)_6]^{4-}$, $S=0$	6:2	2.314(4)	154.4(4)	–	[157]
			2.343(4)	147.9(4)		

[a] Long et al. have confirmed the identification of the compound already reported in Ref. [111]. See Ref. [113].
[b] The obtained parameters are varied dependent on taking into account either zJ' or ZFS of Mn(III) ion (D_{Mn}).
[c] The mixing ratio of Mn:M is 3:1, but the compound has a mixed composition.
[d] The exchange interaction was estimated in Ref. [126].
[e] The ferromagnetic interaction (F) was qualitatively evaluated.
[f] The mixing ratio of Mn:M is 5:1, but the compound has a mixed composition.
[g] The antiferromagnetic interaction (AF) was qualitatively evaluated.

Table 5
Magnetic parameters of [M—L—Mn^{III}—$(O_{Ph})_2$—Mn^{III}—L—M] and [Rad—Mn^{III}—$(O_{Ph})_2$—Mn^{III}—Rad] compounds and several Mn(III) dimeric SMMs (ns = non-SMM above 1.8 K; nd = no data in the literature)

Compound	S_T	g	J_{Mn-M} (K)	J_{Mn-Mn} (K)	zJ' (K)	D_{Mn} (K)[a]	D_{ST} (K)[b]	$\lvert D_{ST}\rvert S_T^2$ (K)	τ_0 (s)[c]	Δ_{eff} (K)[c]	Reference
$[\{Mn(saltmen)\}\{Ni(pao)(bpy)_2\}]_2(ClO_4)_4$	2	2.04(1)	−23.7(2)	+0.90(5)	−0.23(2)	nd	∼3	∼12	ns	ns	[130]
$[\{Mn(5\text{-}Clsaltmen)\}\{Ni(pao)(bpy)_2\}]_2(ClO_4)_4$	2	2.04(1)	−26.1(2)	+0.70(5)	−0.20(2)	nd	∼3	∼12	ns	ns	[130]
$[\{Mn(5\text{-}Brsaltmen)\}\{Ni(pao)(bpy)_2\}]_2(ClO_4)_4$	2	2.04(1)	−25.1(2)	+0.80(5)	−0.23(2)	nd	∼3	∼12	ns	ns	[130]
$[\{Mn(5\text{-}MeOsaltmen)\}\{Ni(pao)(bpy)_2\}]_2(ClO_4)_4$	2	1.96(1)	−24.4(2)	+0.40(5)	−0.18(2)	nd	∼3	∼12	ns	ns	[130]
$[\{Mn(5\text{-}MeOsaltmen)\}\{Cu(salenox^{2-})\}]_2(CF_3SO_3)_2{\cdot}2H_2O$	3	1.994(2)	−16.0(2)	+1.7(1)	−0.072(2)	−3.6(1)	−1.96(1)	17.6	nd	nd	[131]
$[\{Mn(5\text{-}MeOsaltmen)\}\{Cu^{II}(salenox^{2-})\}]_2(CF_3SO_3)_2$ (dried sample)	3	2.032(2)	−14.7(2)	+2.8(1)	−0.023(2)	−3.0(1)	−1.92(1)	17.3	nd	nd	[131]
$[Mn(5\text{-}MeOsaltmen)(DCNNQI)]_2{\cdot}MeOH$	3	1.95(1)	−23.0(5)	+2.0(1)	−0.23(2)		−2.1	18.9	nd	nd	[133]
$[\{Mn(5\text{-}MeOsaltmen)\}\{Ni^{II}(salenox^{2-})\}]_2(CF_3SO_3)_2{\cdot}2H_2O$	4	1.995(5)	–	+1.6(1)	−0.031(2)	−3.6(1)	−1.38(1)	22.1	2.5×10^{-7}	13.0	[131]
$[\{Mn(5\text{-}MeOsaltmen)\}\{Ni^{II}(salenox^{2-})\}]_2(CF_3SO_3)_2$ (dried sample)	4	2.05(2)	–	+1.6(1)	−0.024(2)	−3.6(1)	−1.52(1)	24.3	6.2×10^{-7}	10.5	[131]
$[Mn(saltmen)(ReO_4)]_2$	4	2.00(1)	–	+2.57	∼−0.2	−3.6	−1.63	25.5	8×10^{-9}	16	[96]
$[Mn(saltmen)(O_2CCH_3)]_2$	4	1.98	–	+1.94	0	−2.73	−1.48	23.7	nd	nd	[94]
$[Mn(saltmen)(N_3)]_2$	4	1.98		+0.86	0	−1.44	−1.42	22.7	nd	17	[94]
$[\{Mn(acphmen)\}\{W(bpy)(CN)_6\}]_2{\cdot}3H_2O$	5	1.98	+1.2	+1.37	0	nd	nd	nd	5.1×10^{-12}	32	[128]

[a] The value was obtained by the χT simulation taking into account zero-field splitting of single Mn(III) ion. For the blank, such a treatment was not performed in the work.
[b] The value was obtained by the M—H simulation for the S_T species.
[c] The values were obtained from Arrhenius equation of $\tau(T) = \tau_0 \exp(\Delta_{eff}/k_B T)$. For the blank, exact experimental values have not been given in the literature.

Fig. 32. Structure of $[\{Mn^{III}(5\text{-}MeOsaltmen)\}\{Cu^{II}(salenox^{2-})\}]_2(CF_3SO_3)_2{\cdot}2H_2O$. Reproduced with permission from Ref. [131].

via the oximato group and weak ferromagnetic Mn^{III}/Mn^{III} interaction ($J_{Mn-Mn}/k_B \approx -2$ K) via the bi-phenolato bridge leading to an $S_T = 3$ ground state. On the other hand, the diamagnetic nature of the square-planar Ni^{II} center generates an $S_T = 4$ ground state for the compounds with $M^{II} = Ni^{II}$. At low temperature, these solvated and desolvated compounds displayed SMM behavior modulated by their spin ground state. The hysteresis behavior reflected the difference of their spin ground state (Fig. 33). The anisotropic parameters of these compounds were estimated to be $D_{ST}/k_B \approx -2$ K for $M^{II} = Cu^{II}$ and $D_{ST}/k_B \approx -1.5$ K for $M^{II} = Ni^{II}$, allowing one to estimate the energy gap for the magnetization relaxation $\Delta = |D_{ST}|S_T^2 \approx 18$ and 24 K, respectively. The observed respective Δ_{eff} values were, however, much smaller than these calculated values: that for $M^{II} = Cu^{II}$ could not be estimated from the temperature range above 1.8 K and that for $M^{II} = Ni^{II}$ was approximately 13 K. The origin of the reduction of Δ_{eff} is due to QTM. Indeed, the ac susceptibility measurements at several dc fields demonstrated the suppression of QTM in the magnetization relaxation process, which yielded Δ_{eff} close to the calculated value: $\Delta_{eff}/k_B \approx 16$ K under 4000 Oe for the compounds with $M^{II} = Cu^{II}$ and at 22 K under 500 Oe for the compounds with $M^{II} = Ni^{II}$. These studies demonstrated very well that it is possible to chemically tune the SMM properties of targeted complexes by modifying the decorating additional metal building unit without change of the structural skeleton.

The compounds noted hereafter are not hetero-metal assemblies, but are closely related to the above tetranuclear compounds. The present compounds are $[Mn^{III}(5\text{-}MeOsaltmen)(DCNNQI)]_2{\cdot}MeOH$ and $[Mn^{III}(5\text{-}MeOsaltmen)(DCNNQI)]_2{\cdot}2CH_2Cl_2{\cdot}2CH_3CN$, which are

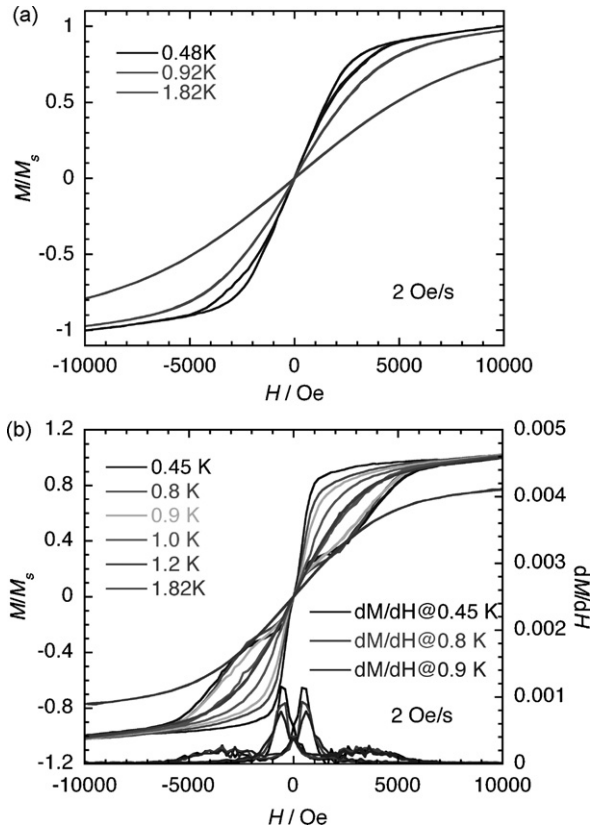

Fig. 33. Field dependence of the magnetization on a single crystal of $[\{Mn^{III}(5\text{-MeOsaltmen})\}\{Cu^{II}(salenox^{2-})\}]_2(CF_3SO_3)_2\cdot 2H_2O$ (a) and $[\{Mn^{III}(5\text{-MeOsaltmen})\}\{Ni^{II}(salenox^{2-})\}]_2(CF_3SO_3)_2\cdot 2H_2O$ (b). Reproduced with permission from Ref. [131].

decorated by a monoanionic organic radial DCNNQI molecule [133]. The bridging scheme is $[Rad–Mn^{III}–(O_{Ph})_2–Mn^{III}–Rad]$ (Fig. 34), forming a linear tetra-spin system of ($S_{rad1} = 1/2$, $S_{Mn1} = 2$, $S_{Mn2} = 2$, $S_{rad2} = 1/2$), similar to the tetranuclear compounds above.

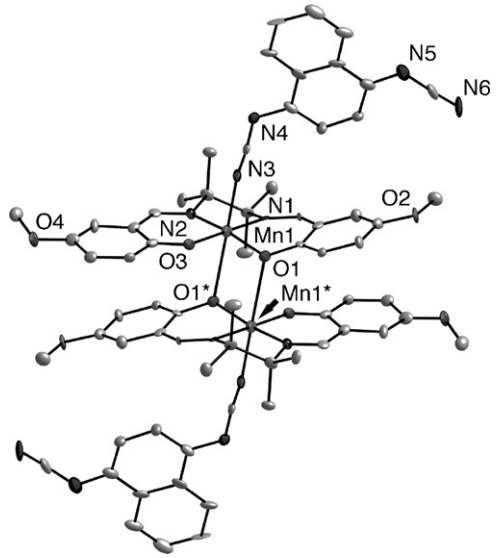

Fig. 34. Structure of $[Mn^{III}(5\text{-MeOsaltmen})(DCNNQI)]_2$ MeOH. Reproduced with permission from Ref. [133].

Interestingly, although these two compounds have a very similar molecular structure, the packing forms of the respective compounds are completely different (this difference can be distinguished by their crystallization solvents, S = MeOH or $2CH_2Cl_2\cdot 2CH_3CN$). The former with S = MeOH is nearly discrete, but the latter with $S = 2CH_2Cl_2\cdot 2CH_3CN$ constructs a one-dimensional aggregation by forming a dimeric stacking between inter-molecular DCNNQI moieties. Due to the diamagnetic nature of the DCNNQI dimer, the compound formally possesses an $S_T = 4$ ground state. However, the inter-molecular interactions through the DCNNQI dimers and space prohibited that the compound is a SMM. While, in the former (S = MeOH), strong antiferromagnetic exchange between the Mn(III) ion and DCNNQI radical ($J_{Mn–rad}/k_B \approx -23$ K) and weak ferromagnetic exchange between the Mn(III) ions ($J_{Mn–Mn}/k_B \approx 2$ K) generated an $S_T = 3$ ground state, and this compound was a SMM with $\Delta/k_B \approx 19$ K ($D_{ST}/k_B = -2.1$ K).

The second family of oximate-bridged oligomers includes compounds having a $[Mn^{III}–ON–Ni^{II}–NO–Mn^{III}]$ bridging skeleton. This family and its magnetic properties become an extremely important part of discussion on the SCM behavior of 1D chains comprised of this type of trinuclear unit (see next section). The $Mn_2^{III}Ni^{II}$ trinuclear compounds, $[\{Mn^{III}(5\text{-Rsaltmen})\}_2\{Ni^{II}(pao)_2(phen)\}](ClO_4)_2$ (R = Cl, Br) (Fig. 35), were synthesized by the assembly reaction of $[Mn(5\text{-Rsaltmen})(H_2O)]_2(ClO_4)_2$ with $[Ni(pao)_2(phen)]$ in a methanol/water medium [93]. In the molecule, the Mn(III) ion is quasi-square pyramidal due a negligible weak interaction between Mn···R (R = Cl and Br in the 5-Rsaltmen ligands). dc magnetic measurements of these compounds confirmed their $S_T = 3$ ground state ($J_{Mn–Ni}/k_B \approx -24$ K) and strong uni-axial anisotropy ($D_{ST}/k_B \approx -2.4$ K). The ac magnetic susceptibility revealed a characteristic of SMM behavior with $\tau_0 \approx 1 \times 10^{-7}$ s and $\Delta_{eff}/k_B \approx 18$ K ($\Delta = |D_{ST}|S_T^2 = 21$ K).

An imidazolate-bridged $Mn_2^{III}Cu_2^{II}$ compound, $[\{Mn^{III}(salen)\}\{Cu^{II}(acimen)\}]_2(BPh_4)_2$, was synthesized by Matsumoto et al. [134]. Its bridging skeleton of $[Cu^{II}–im–Mn^{III}–(O_{Ph})_2–Mn^{III}–im–Cu^{II}]$ is comprised of an imidazolate-bridge linkage between the Cu(II) and Mn(III) ions ($Cu^{II}–im–Mn^{III}$) and the bi-phenolate bridge of out-of-plane Mn(III) salen dimer ($Mn^{III}–(O_{Ph})_2–Mn^{III}$) (Fig. 36). Despite that there is no significant quantitative evaluation of the low-temperature behavior, the magnetic data of this compound suggest the presence of ferromagnetic exchange between the Mn(III) ions via the bi-phenolate linkage, in addition to antiferromagnetic exchange between the Mn(III) and Cu(II) ions via the imidazolate linkage ($J_{Mn–Cu} = -1.68\ cm^{-1}$).

5.2. One-dimensional chains including single-chain magnets

Since the discovery of single-chain magnets (SCMs) at the beginning of this century, hetero-metallic 1D chains based on Mn(III) salen complexes have attracted a great deal of attention. As mentioned in Section 2.2, this is because the linear arrangement of Mn(III) salen complexes can arrange the respective Jahn–Teller axes to form an easy axis of the

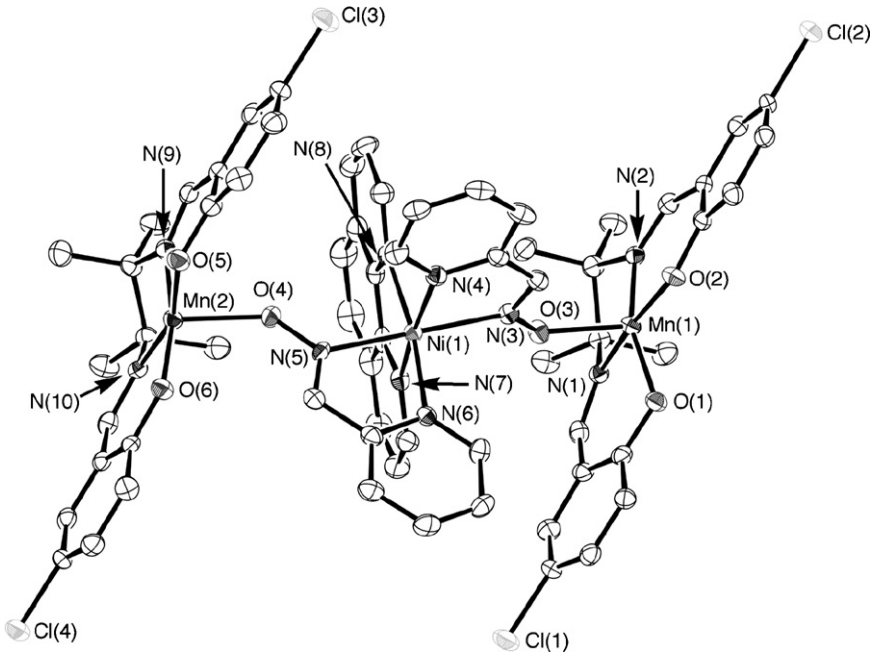

Fig. 35. Structure of Mn^{III}—Ni^{II}—Mn^{III} trinuclear compound, $[\{Mn^{III}(5\text{-Clsaltmen})\}_2\{Ni^{II}(pao)_2(phen)\}](ClO_4)_2$. Reproduced with permission from Ref. [93].

magnetization parallel to the chain direction (see Fig. 2). This design of SCMs was proposed by Miyasaka et al. [135] and he and Clérac et al. presented an $Mn_2^{III}Ni^{II}$ chain, $[\{Mn(saltmen)\}_2\{Ni(pao)_2(py)_2\}](ClO_4)_2$, possessing a $[-Mn^{III}-ON-Ni^{II}-NO-Mn^{III}-(O_{Ph})_2-]$ repeat unit in 2002 (Fig. 37) [37]. This compound is the first ferromagnetic-type SCM. The temperature dependence of χT decreases gradually from 300 K to reach a minimum at approximately 90 K and then increases abruptly at low temperatures. At low temperature, this one-dimensional arrangement was described as a chain composed of ferromagnetically coupled anisotropic $S_T = 3$ units. The $S_T = 3$ state of each unit is induced by the strong antiferromagnetic coupling in the oximate-bridged Mn^{III}–Ni^{II}–Mn^{III} trinuclear unit ($J_{Mn-Ni}/k_B = J/k_B \approx -20$ K). The ferromagnetic coupling between the trinuclear units via a bi-phenolate bridge ($J'/k_B \approx +0.7$ K) forms a regular chain of ferromagnetically coupled units at low temperatures (<10 K). The low-temperature single crystal *MH* measurements conducted with a micro-SQUID setup revealed the existence of strong uniaxial anisotropy of the chain with $D_{ST}/k_B \approx -2.5$ K for the repeating unit (Fig. 38) [136]. These data led to the conclusion that this compound behaves as an Ising-type chain at low temperature. Indeed, the simulation of the low-temperature χT behavior using an Ising model deduced an energy value to create domain wall (Δ_ξ) consistent with $4J'S_T^2$ (Fig. 39). Furthermore, this simulation showed a negligibly small interchain interaction ($J''/k_B \approx -0.047$ K) and an average chain

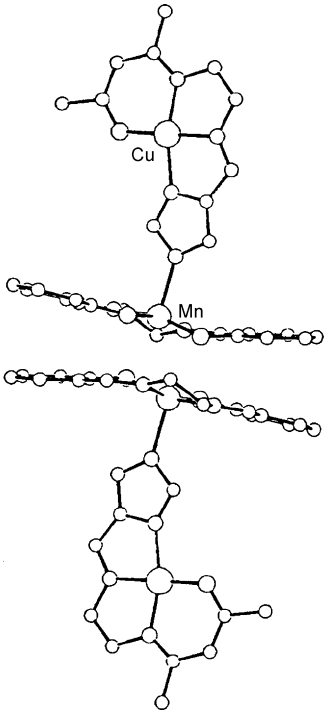

Fig. 36. Structure of $[\{Mn^{III}(salen)\}\{Cu^{II}(acimen)\}]_2(BPh_4)_2$. Reproduced with permission from Ref. [134].

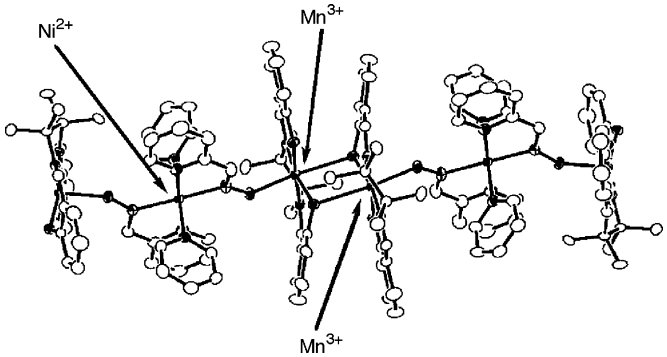

Fig. 37. One-dimensional chain structure of $[\{Mn^{III}(saltmen)\}_2\{Ni^{II}(pao)_2(py)_2\}](ClO_4)_2$. Reproduced with permission from Ref. [37].

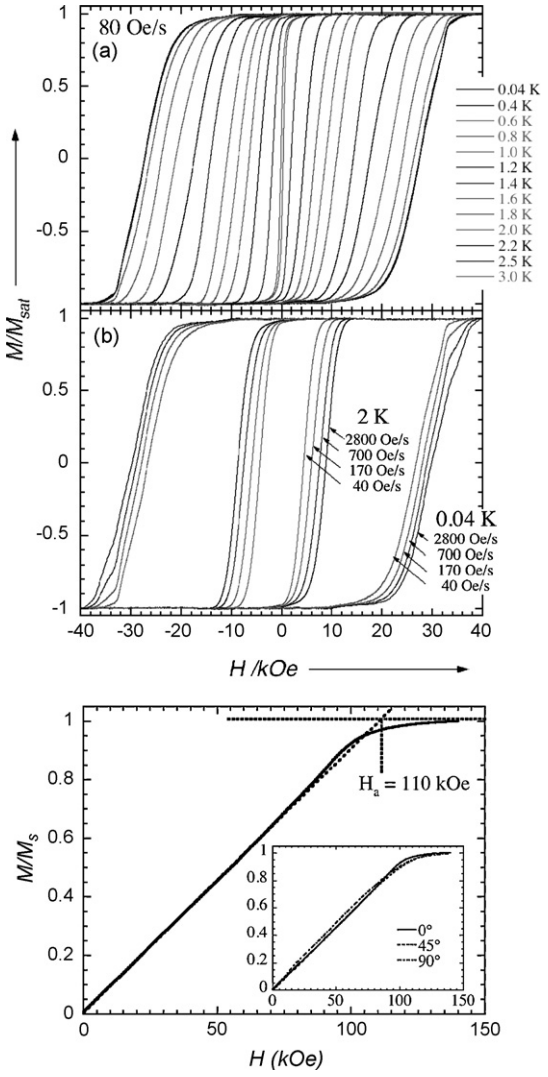

Fig. 38. Field dependence of the magnetization measured on a single crystal of $[\{Mn(saltmen)\}_2\{Ni(pao)_2(py)_2\}](ClO_4)_2$: (top) when the magnetic field is applied parallel to the chain direction at different temperature with 80 Oe/s field sweep rate (a) and at 2 and 0.04 K at different field sweep rates (b), (bottom) when the magnetic field is applied perpendicular to the chains at 1.5 K, where the intersection between the two dotted lines gives the anisotropy field. *Inset*: Similar measurements than the main figure at three angles in the plan normal to the easy axis. The main figure is at 50°. Reproduced with permission from Refs. [136,138].

length of 140 nm. The slow relaxation of the magnetization was demonstrated well by ac and dc magnetic measurements at low temperatures (Fig. 40). The relaxation parameters are: $\tau_0 = 5.5 \times 10^{-11}$ s and $\Delta_{eff}/k_B \approx 72$ K. They explained this Δ_{eff} by using an equation $\Delta_1 = 8J'S_T^2 + |D_{ST}|S_T^2$ [136,137]. Interestingly, they found a crossover between infinite chain regime and finite chain regime in the relaxation dynamics, where Δ_{eff} changed to $\Delta_2 = 4J'S_T^2 + |D_{ST}|S_T^2$ in the latter case [136].

This SCM behavior was confirmed in a family of analogous $Mn_2^{III}Ni^{II}$ chains, $[\{Mn^{III}(saltmen)\}_2\{Ni^{II}(pao)_2(L^1)_2\}](A)_2$ (L^1 = pyridine, 4-picoline, 4-*t*-butylpyridine, *N*-methylimidazole; $A^- = ClO_4^-$, BF_4^-, PF_6^-, ReO_4^-), by varying the L^1 ligands and the counter A^- anions to change the inter-chain environment but not the chain bridging motif for

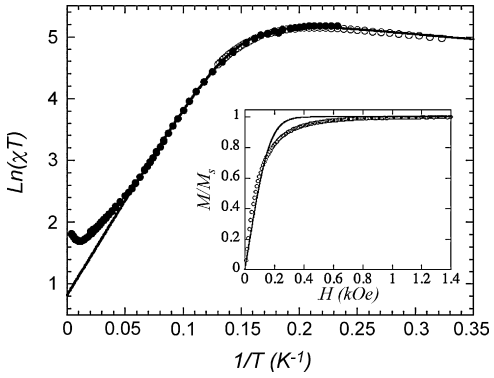

Fig. 39. Semilog plot of χT vs. $1/T$. *Inset*: Field dependence of the magnetization (normalized at the saturation value) at 4 K and with a field sweep rate of 0.14 kOe/s. Solid lines correspond to the fit using the Ising expressions. Reproduced with permission from Ref. [136].

fixing intra-chain parameters S_T, D, J and J'. All compounds showed identical behavior almost independent of the inter-chain environment [138]. Recently, they synthesized another group of $Mn_2^{III}Ni^{II}$ chain compounds that exhibit similar SCM behavior, $[\{Mn^{III}(saltmen)\}_2\{Ni^{II}(L)_2(py)_2\}](A)_2$ (L = miao$^-$, A = ClO_4^-, PF_6^-; L = eiao$^-$, A = ClO_4^-) [139]. The unit exchange in the Ni^{II} moiety allowed tuning of the exchange coupling J' between the trimer $[Mn^{III}–Ni^{II}–Mn^{III}]$ units (i.e., interaction of $Mn^{III}\cdots Mn^{III}$) without significant change of anisotropy. The most important point is that they demonstrated a linear correlation between J' and the energy barrier of the magnetization reversal (Δ_{eff}) among these $Mn_2^{III}Ni^{II}$ compounds including the discrete trinuclear compounds introduced in the former section (Fig. 41). This result proved that the

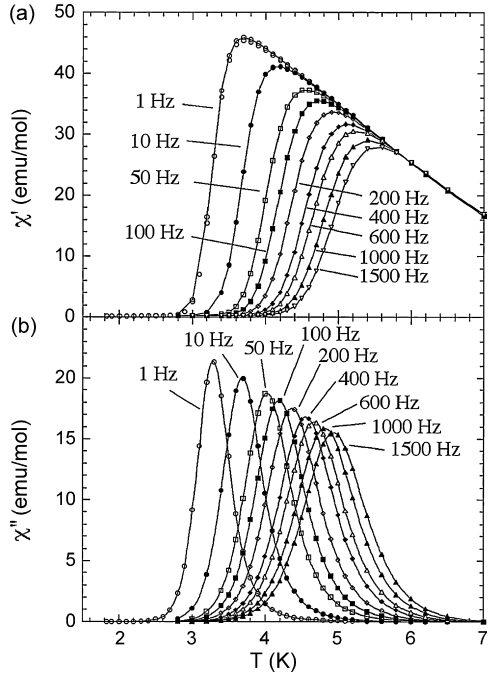

Fig. 40. Temperature and frequency dependence of the (a) real (χ') and (b) imaginary (χ'') part of the ac susceptibility. The solid lines are guides for the eyes. Reproduced with permission from Ref. [37].

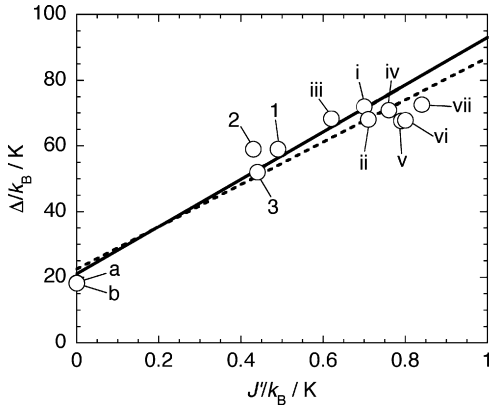

Fig. 41. Correlation of effective energy barrier for magnetization relaxation (Δ) with exchange coupling between trinuclear units (J') in the family of $Mn_2^{III}Ni^{II}$ SCMs, **1**–**3** and **i**–**vii**, and SMMs, **a** and **b**. The solid and dashed lines represent the least-squares fit with $\Delta/k_B = 22.5 + 64.4J'/k_B$ and the expected line of $\Delta/k_B = 21 + 72J'/k_B$, respectively, where the Δ_A/k_B value of 21 K was assumed from the data of compounds **a** and **b**. (**i**) $[\{Mn(saltmen)\}_2\{Ni(pao)_2(py)_2\}](ClO_4)_2$; (**ii**) $[\{Mn(saltmen)\}_2\{Ni(pao)_2(4\text{-pic})_2\}](ClO_4)_2$ (4-pic = 4-picoline); (**iii**) $[\{Mn(saltmen)\}_2\{Ni(pao)_2(t\text{-Bupy})_2\}](ClO_4)_2$ (*t*-Bupy = 4-*tert*-butylpyridine); (**iv**) $[\{Mn(saltmen)\}_2\{Ni(pao)_2(N\text{-Meim})_2\}](ClO_4)_2$ (*N*-Meim = *N*-methylimidazole); (**v**) $[\{Mn(saltmen)\}_2\{Ni(pao)_2(py)_2\}](BF_4)_2$; (**vi**) $[\{Mn(saltmen)\}_2\{Ni(pao)_2(py)_2\}](PF_6)_2$; (**vii**) $[\{Mn(saltmen)\}_2\{Ni(pao)_2(py)_2\}](ReO_4)_2$; (**a**) $[\{Mn(5\text{-Clsaltmen})\}_2\{Ni(pao)_2(phen)\}](ClO_4)_2$; (**b**) $[\{Mn(5\text{-Brsaltmen})\}_2\{Ni(pao)_2(phen)\}](ClO_4)_2$. Reproduced with permission from Ref. [139].

magnetization relaxation dynamics of these ferromagnetic-type SCMs is well described generalizing the Glauber model and introducing finite anisotropy.

Further characteristic physical properties of this $Mn_2^{III}Ni^{II}$ SCM system were investigated by physicists research groups: High-field and high-frequency EPR study [140], NMR study [141], effect of pressure on SCMs [142], and quantum behavior at extremely low temperatures [143].

A cyano-bridged SCM based on a Mn(III) salen complex has also been reported by Miyasaka and Clérac et al. The compound is comprised of $[Mn^{III}(5\text{-MeOsalen})]^+$ and $[Fe^{III}(CN)_6]^{3-}$ in a 2:1 formulation ratio: $(NEt_4)[\{Mn^{III}(5\text{-MeOsalen})\}_2\{Fe^{III}(CN)_6\}]$ (Fig. 42) [114]. The chain possesses a $[-Mn^{III}-NC-Fe^{III}-CN-Mn^{III}-(O_{Ph})_2-]$ repeat unit including two types of bridges, a cyano-bridge (–NC–) and a bi-phenolate bridge ($-(O_{Ph})_2-$), connection between the Mn^{III} and Fe^{III} ions and the two Mn^{III} ions, respectively. Both bridges mediated ferromagnetic interactions. With decreasing temperature, the χT versus T curve increased gradually from 6.8 $cm^3\,K\,mol^{-1}$ at 300 K to reach a maximum of 49.0 $cm^3\,K\,mol^{-1}$ at 2.2 K (followed by a slight decrease to 46.0 $cm^3\,K\,mol^{-1}$ at 1.82 K). The simulation of χT above 10 K using a Heisenberg trinuclear unit ($S_{Mn1} = 2$, $S_{Fe} = 1/2$, $S_{Mn2} = 2$) taking into account inter-trimer interactions yielded an adequate parameter set of $g_{av} = 2.03$, $J_{Mn-Fe}/k_B = +6.5$ K, and $J'/k_B = +0.07$ K, where J' is the exchange coupling between the trimer units, supporting a ferromagnetic chain scheme of $S_T = 9/2$ repeat spins. dc magnetic measurements of a single crystal using micro-SQUID and Hall-probe magnetometers revealed uni-axial anisotropy ($D_{ST}/k_B = -0.94$ K) with an easy axis lying along the chain direction. When the external field was applied perpendicular to the chains, a linear increase with the magnetization without hysteresis was observed (Fig. 43b). When the external field was applied parallel to the chains, large hysteresis loops were observed (Fig. 43a). Thus, the low-temperature χT behavior was well simulated with an Ising model with $\Delta_\xi = 4J'S_T^2 = 6.1$ K (i.e., $J'/k_B = 0.08$ K, in excellent agreement with the value estimated from the simulation of high-temperature χT). The average chain length was approximately 60 nm. The investigation of its dynamical behavior revealed two regimes of SCM behavior with a crossover at 1.4 K. Above 1.4 K, $\tau_{01} = 3.7 \times 10^{-10}$ s and $\Delta\tau_1/k_B = 31$ K, and below 1.4 K, $\tau_{02} = 3 \times 10^{-8}$ s and $\Delta\tau_2/k_B = 25$ K. These two energy barriers were explained well by correlations of $\Delta_1 = 8J'S_T^2 + |D_{ST}|S_T^2$ and $\Delta_2 = 4J'S_T^2 + |D_{ST}|S_T^2$, respectively.

More recently, the same group reported that an alternating chain of a Mn(III) salen complex and the TCNQ radical exhibits SCM behavior [79]. This is an exciting result. The well-known family of alternating chain compounds composed of Mn(III) porphyrin and TCNQ, TCNE, or their derivatives was previously studied by Miller et al. and had already displayed similar behavior [144], but SCM behavior could not be proven because of the presence of structural fluctuations due to the partial elimination of crystallization solvents that may cause spin-glass-like behavior. The present compound, $[Mn^{III}(5\text{-TMAMsaltmen})(TCNQ)](ClO_4)_2$, had no crystallization solvent and was very stable in air (Fig. 44) [79]. This compound has a zigzag chain structure packed with adjacent chains with an inter-chain Mn···Mn

Fig. 42. One-dimensional chain structure of $(NEt_4)[\{Mn^{III}(5\text{-MeOsalen})\}_2\{Fe^{III}(CN)_6\}]$. Reproduced with permission from Ref. [114].

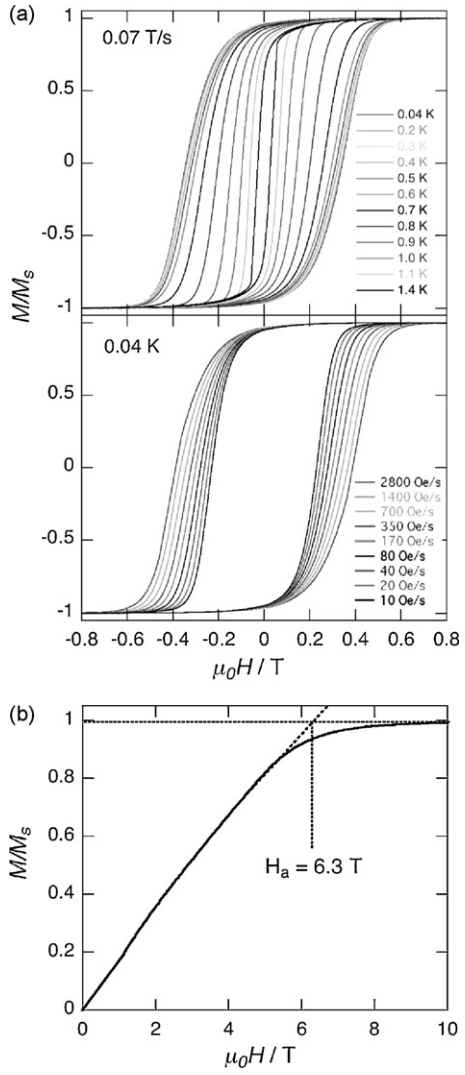

Fig. 43. Field dependence of the normalized magnetization (M/M_S) on a single crystal of $(NEt_4)[\{Mn^{III}(5\text{-MeOsalen})\}_2\{Fe^{III}(CN)_6\}]$, in which the external field was applied parallel (a) and perpendicular (b) to the chain direction (Fig. 41b was measured at 1.5 K). Reproduced with permission from Ref. [114].

distance of over 8 Å, reminiscent of what was observed in the family of Mn^{III}(porphyrin)–TCNE or –TCNQ compounds reported previously by Miller et al. Indeed, χT behavior is very similar to that of the family of Mn^{III}(porphyrin)–TCNE or –TCNQ compounds, indicating a strong antiferromagnetic exchange coupling ($J/k_B \approx -96$ K) between the Mn^{III} ion and TCNQ radical. The fact that the correlation between the structure (especially, the angle of Mn^{III}–N–C) and the exchange coupling followed a manner observed in the family of Mn^{III}(porphyrin)–TCNE or –TCNQ compounds supported the similarity of these compounds. Nevertheless, the absence of magnetic ordered phase or spin-glass behavior was established by heat capacity calorimetry measurements that exhibit no abnormal C_p between 0.5 and 10 K (Fig. 45a). Therefore, the observation of field hysteresis of the magnetization below 3.5 K (with a coercive field up to 14 kOe at 1.8 K) (Fig. 45b) was due to the slow relaxation of the magnetization. Single crystal magnetization measurements demonstrated the presence of uni-axial symmetry of this compound, indicating the Ising-type nature of this compound. The temperature dependence of the relaxation time displayed two activated regimes above and below 4.5 K with $\tau_{01} = 2.1 \times 10^{-10}$ s, $\Delta_{\tau 1} = 94.1$ K and $\tau_{02} = 6.8 \times 10^{-8}$ s and $\Delta_{\tau 2} = 67.7$ K, respectively. Thus, the detailed analysis of these dynamics properties allowed an unambiguous demonstration of the SCM behavior in this Mn(III)–TCNQ system. It is important that the observed energy barriers are ruled out of consideration using $\Delta\tau_1 = 8JS_T^2 + |D_{ST}|S_T^2$ and $\Delta\tau_2 = 4JS_T^2 + |D_{ST}|S_T^2$, because of $|D_{ST}/J| < 4/3$ [137].

As another topic, Zuo and Song et al. synthesized helical chains exhibiting 3D ferrimagnetic behavior employing chiral Mn(III) salen complexes, $[Mn^{III}(R,R\text{-salcy})(H_2O)_2]ClO_4$ and $[Mn^{III}(S,S\text{-salcy})(H_2O)_2]ClO_4$ [145]. Their compounds are $[\{Mn^{III}(R,R\text{-salcy})(H_2O)\}_2\{Mn^{III}(R,R\text{-salcy})\}\{Fe^{III}(CN)_6\}]\cdot 2H_2O$ and $[\{Mn^{III}(S,S\text{-salcy})(H_2O)\}_2\{Mn^{III}(S,S\text{-salcy})\}\{Fe^{III}(CN)_6\}]\cdot 2H_2O$ (Fig. 46). These compounds are enantiomers and crystallized in the chiral space group $P2_12_12_1$, producing left-hand and right-hand helical chains, respectively. In the chain, two *trans*-positioned cyanide groups of the $[Fe^{III}(CN)_6]^{3-}$ unit bridge the $[Mn^{III}(salcy)]^+$ unit

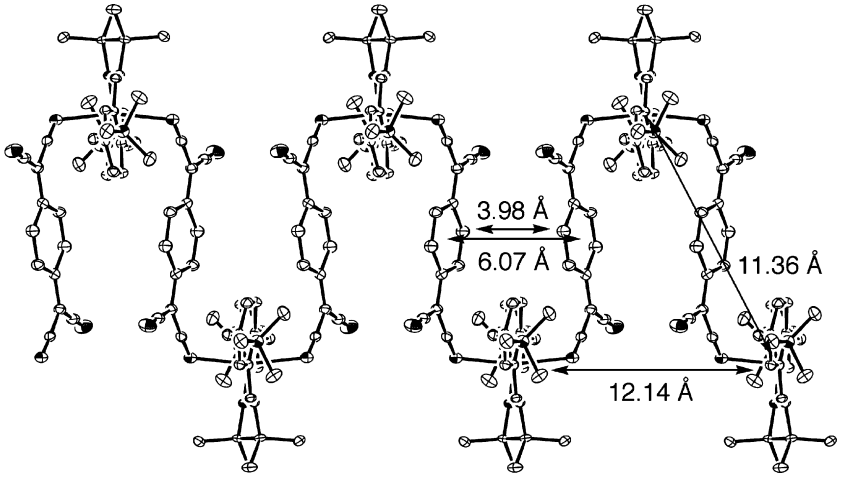

Fig. 44. One-dimensional zigzag chain structure of $[Mn^{III}(5\text{-TMAMsaltmen})(TCNQ)](ClO_4)_2$. Reproduced with permission from Ref. [79].

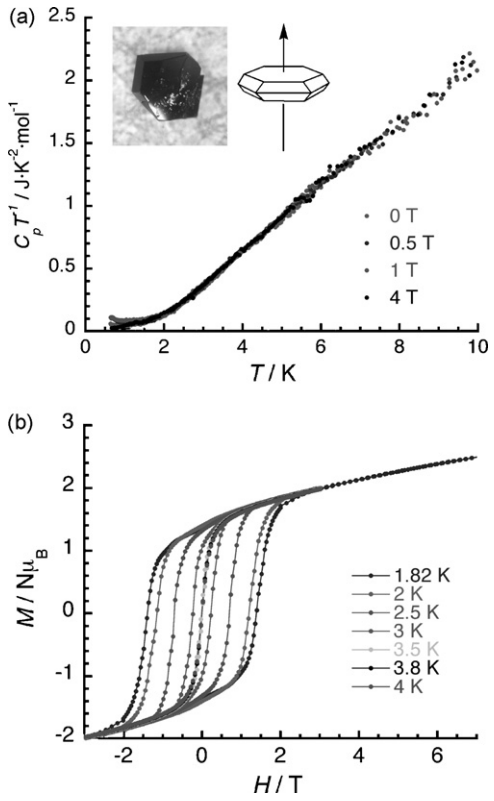

Fig. 45. C_pT^{-1} vs. T on a single crystal (a) and field dependence of the magnetization on a polycrystalline sample (b) of [Mn(5-TMAMsaltmen)(TCNQ)](ClO$_4$)$_2$. Reproduced with permission from Ref. [79].

to form a chain having a [–Mn^{III}–NC–Fe^{III}–CN–] repeat unit (Mn$_1$–N$_{CN1}$ = 2.398(4) Å, Mn$_1$–N$_{CN2}$ = 2.251(4) Å, Mn$_1$–N$_1$–C$_1$ = 148.3(3)°, and Mn$_1$–N$_2$–C$_2$ = 151.6(3)°). Two equatorial *cis*-positioned cyanide groups coordinate respectively to the capped [Mn^{III}(salcy)(H$_2$O)]$^+$ moieties (Mn$_2$–N$_{CN3}$ = 2.255(4) Å, Mn$_2$–C$_3$–N$_3$ = 143.0(3)°, Mn$_3$–N$_{CN4}$ = 2.256(4) Å, and Mn$_3$–N$_4$–C$_4$ = 152.9(3)°), consequently assuming a [Mn$_3$Fe] repeating chain. Two cyanide groups remain non-coordinated. The near inter-chain M···M distances are approximately 5 Å. From a simulation study on temperature dependence of χT, the intra- and inter-tetrameric exchange constants (J and J_c) were $J = -0.46\,cm^{-1}$ and $J_c = -0.15\,cm^{-1}$ (with $g = 1.96$ and TIP = $7.35 \times 10^{-3}\,cm^3\,mol^{-1}$), displaying ferrimagnetic chain behavior. These compounds finally exhibited a 3D long-range order at $T_c = 3$ K.

An alternating zigzag chain composed of [Mn^{III}(5-MeOsalen)]$^+$ and [(Tp)Fe^{III}(CN)$_3$]$^-$ also exhibited a 3D long-range order, but metamagnetic nature due to the presence of weak inter-chain antiferromagnetic interaction ($H_c = 3600$ Oe) [146]. The compound is [{Mn^{III}(5-MeOsalen)}{(Tp)Fe^{III}(CN)$_3$}]·2MeOH (Mn–N$_{CN1}$ = 2.364(2) Å, Mn–N$_1$–C$_1$ = 161.7(2)°, Mn–N$_{CN2}$ = 2.320(2) Å, Mn–N$_2$–C$_2$ = 151.1(2)°) (Fig. 47). The intra-chain Mn···Fe exchange and inter-chain interaction were $J_{Mn-Fe1} = 1.66\,cm^{-1}$, $J_{Mn-Fe2} = 1.21\,cm^{-1}$, $zJ = -0.038\,cm^{-1}$ in a fitting of $\chi T - T$ and MH plots taking into account ZFS ($D_{Mn} = -0.95\,cm^{-1}$).

The reaction of [Mn^{III}(salen)]$^+$ with [Mo^{IV}(CN)$_8$]$^{4-}$ (diamagnetic) produced a 1D chain of [Mn^{III}(salen)(H$_2$O)$_2$]$_2$[{Mn^{III}(salen)(H$_2$O)}{Mn^{III}(salen)}$_2${Mo^{IV}(CN)$_8$}]·0.5ClO$_4$·0.5OH·4.5H$_2$O, where the [Mn3^{III}Mo^{IV}]$^-$ unit constructed a chain skeleton by forming an out-of-plane dimeric bridge [122]. Chain compounds with other diamagnetic metal ions include: [{Mn^{III}(saltmen)(H$_2$O)}{Hg^{II}(CN)$_3$}] [119] and [{Mn^{III}(salen)}{Ag^{I}(CN)$_2$}] [68].

Finally, we have a brief comment for compounds based on [Mn^{III}(acacen)]$^+$. The [Mn^{III}(acacen)]$^+$ group is not a "salen" complex, but acts as a similar coordination-acceptor building block. An alternating chain using this unit, (NEt$_4$)$_2$[{Mn^{III}(acacen)}{Fe^{III}(CN)$_6$}], was synthesized by Miyasaka et al. (Fig. 48) [147]. This compound has a *trans*-coordinated snaky-chain structure consisting of [–Mn^{III}–NC–Fe^{III}–CN–] repeat units with dimensions of Mn–N = 2.316(4) Å and Mn–N–C = 152.6(3)°, in which the Fe ion is positioned at the inversion center and the [Mn^{III}(acacen)]$^+$ moiety lies on a mirror plane. The exchange interaction between the Mn(III) and Fe(III) ions was ferromagnetic, but was not quantitatively evaluated in the literature. The *cis*-coordinated chain can be seen in (NEt$_4$)[{Mn^{III}(acacen)}{Fe^{III}(CN)$_5$(1-CH$_3$im)}]·6H$_2$O (Fig. 49), in which Mn–N = 2.331(4) Å and Mn–N–C = 144.4(4)° [116]. While the former *trans*-coordinated compound exhibited Mn–Fe ferromagnetic coupling, this compound exhibited Mn–Fe antiferromagnetic coupling, forming an intra-chain ferrimagnetic spin arrangement. The presence of weak inter-chain antiferromagnetic interaction yielded a metamagnet ($T_N \sim 4$ K and H_c = 1700–2000 Oe).

Kou and Sato et al. also reported an alternating chain of [{Mn^{III}(salen)}{Fe^{III}(bpb)(CN)$_2$}], where the Mn–N$_{CN}$ distances were in the range 2.301(3)–2.439(3) Å and the Mn–N–C angles were in the range 151.8(3)–158.6(3)° [127]. The χT–T and MH data were interpreted by the presence of Mn–Fe antiferromagnetic coupling, but no ferrimagnetic short-range order was detected through the whole temperature range.

5.3. Two-dimensional network studies

High-dimensional compounds synthesized by the reaction of Mn(III) salen complexes with polycyanometallates are of interest because their bulk magnetic properties are mediated by a long-range spin order via the cyano-bridge. Therefore, this work was started in 1990s with the intent to design molecule-based magnets as Prussian blue analogues. Several 2D network compounds using polycyanometallates have been reported and two types of 2:1 and 4:1 compounds identified from the Mn:M ratio. Both types of compounds were first synthesized by Miyasaka et al. [111,148].

In the Mn:M = 2:1 compound, each Mn ion is surrounded by an equatorial salen ligand and two axial nitrogen atoms from a polycyanometallate unit such as [M^{III}(CN)$_6$]$^{3-}$, the four M–CN groups of which coordinate to the Mn ions of [Mn(SB)]$^+$ units, forming a two-dimensional network having [–Mn^{III}–NC–M–CN–]$_4$ cyclic repeat units. This is the common skeleton in the Mn:M = 2:1 compound. If the

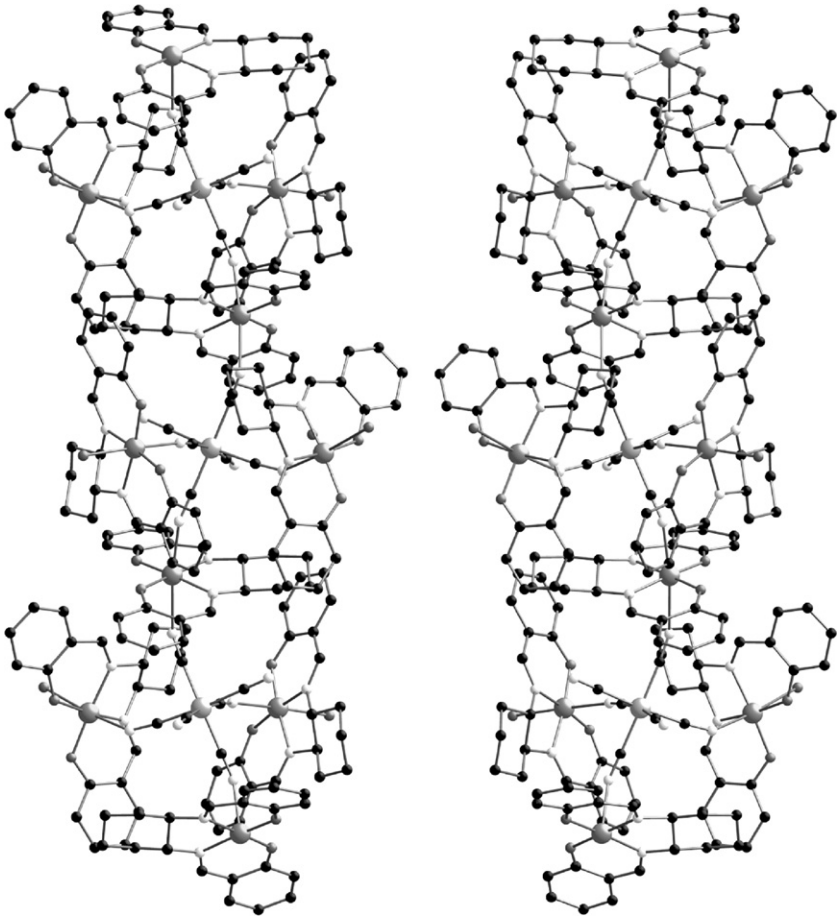

Fig. 46. Structures of the left- and right-handed helical chains of $[\{Mn^{III}(R,R\text{-salcy})(H_2O)\}_2\{Mn^{III}(R,R\text{-salcy})\}\{Fe^{III}(CN)_6\}]\cdot 2H_2O$ (*R* isomer, left) and $[\{Mn^{III}(S,S\text{-salcy})(H_2O)\}_2\{Mn^{III}(S,S\text{-salcy})\}\{Fe^{III}(CN)_6\}]\cdot 2H_2O$ (*S* isomer, right), respectively [145].

M center has an inversion center, there are two kinds of Mn–N bond in the network. Two coordination-naked NC– groups face the perpendicular direction of layers, sometimes having interactions with counter ions or crystallization solvents. Most systems have counter ions and/or crystallization solvents between layers. A Mn:Fe = 2:1 compound, $K[\{Mn^{III}(3\text{-MeOsalen})\}_2\{Fe^{III}(CN)_6\}]\cdot 2DMF$, also forms a similar 2D network [111,148]. However, the K^+ ion is held into the center of the octameric ring by forming a KO_8 complex as seen in K^+-crown-ether complexes. Therefore, this compound constructs a neutral network (Fig. 50). The bond and angles forming the network are: Mn–N_1 = 2.290(5) Å, Mn–N_2 = 2.415(5) Å, Mn–N_1–C_1 = 169.5(5)°, and Mn–N_2–C_2 = 137.2(4) Å. The existence of two kinds of Mn–N bond makes it difficult to evaluate exactly the exchange between Mn(III) and Fe(III) ions via a CN group. However, in this compound, the exchanges via both pathways were evaluated to be ferromagnetic. As expected, these local exchanges finally provide intra-layer long-range ordering, but it is reversed with inter-layer antiferromagnetic interaction as seen in a metamagnet. Nevertheless, structural fluctuations caused from the partial elimination of crystallization solvents (DMF molecules) located between layers made it possible to present ferromagnet behavior (canting ferromagnet) with field hysteresis of the magnetization (Fig. 51). This magnetic behavior was confirmed by heat capacity measurements [149]. The metal substituted analogues, $K[\{Mn^{III}(3\text{-MeOsalen})\}_2\{M^{III}(CN)_6\}]\cdot 2DMF$ (M^{III} = Mn^{III} [82], Cr^{III}, Co^{III} [150]), were also prepared and magnetically investigated. Except for the paramagnetic compound with M^{III} = Co^{III} (S = 0), the exchange between Mn(III) and M(III) ions were observed to be ferromagnetic for M^{III} = Mn^{III} (S = 1) and antiferromag-

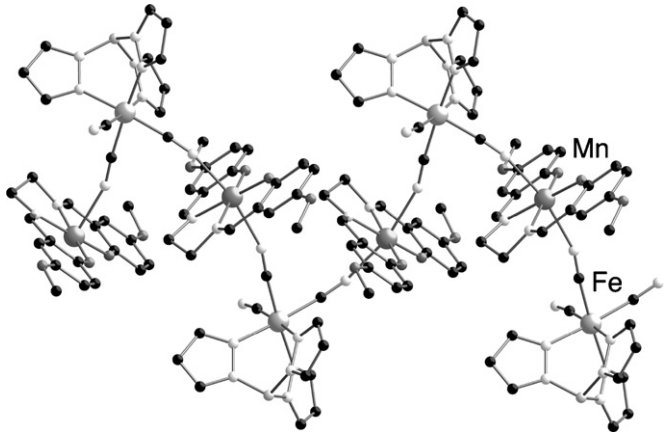

Fig. 47. One-dimensional zigzag chain of $[\{Mn^{III}(5\text{-MeOsalen})\}\{(Tp)Fe^{III}(CN)_3\}]\cdot 2MeOH$ [146].

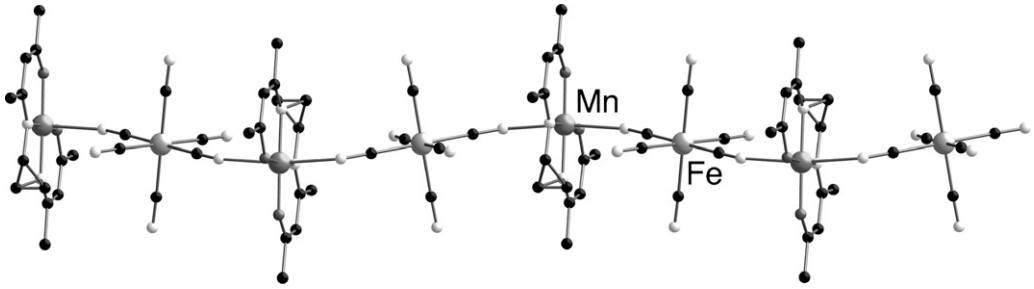

Fig. 48. One-dimensional chain structure of $(NEt_4)_2[\{Mn^{III}(acacen)\}\{Fe^{III}(CN)_6\}]$ [147].

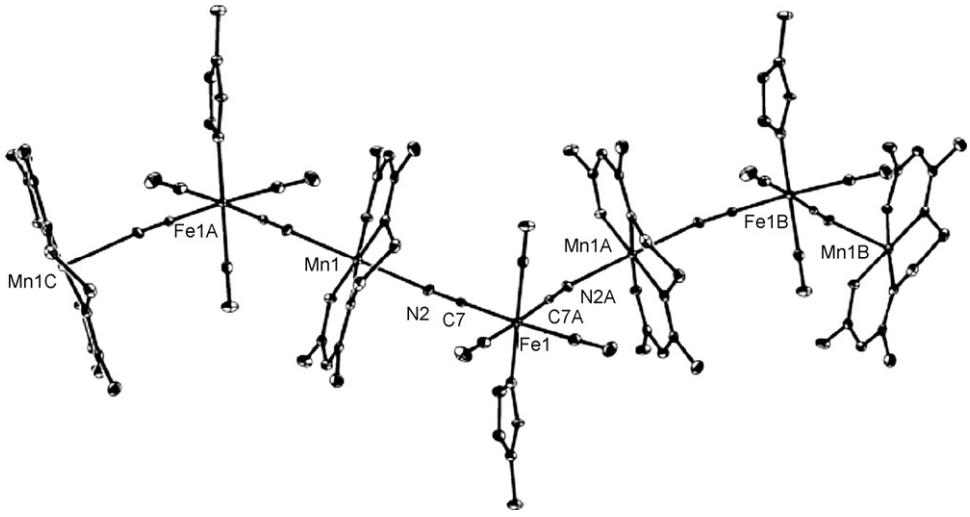

Fig. 49. One-dimensional chain structure of $(NEt_4)[\{Mn^{III}(acacen)\}\{Fe^{III}(CN)_5(1\text{-}CH_3im)\}]\cdot 6H_2O$. Reproduced with permission from Ref. [116].

netic for $M^{III} = Cr^{III}$ ($S = 3/2$). The inter-layer interactions in both compounds are expected to be antiferromagnetic as seen in $M^{III} = Fe^{III}$. The compound with $M^{III} = Mn^{III}$ was a typical metamagnet ($T_N = 16$ K), but the compound with $M^{III} = Cr^{III}$ was a ferrimagnet ($T_c = 11$ K) due to the inter-layer spin canting possibly caused by structural fluctuations (a small cusp was observed at ca. 9 K in its susceptibility) [150]. Interestingly, the compound with $M^{III} = Mn^{III}$ exhibited a negative magnetization in remnant

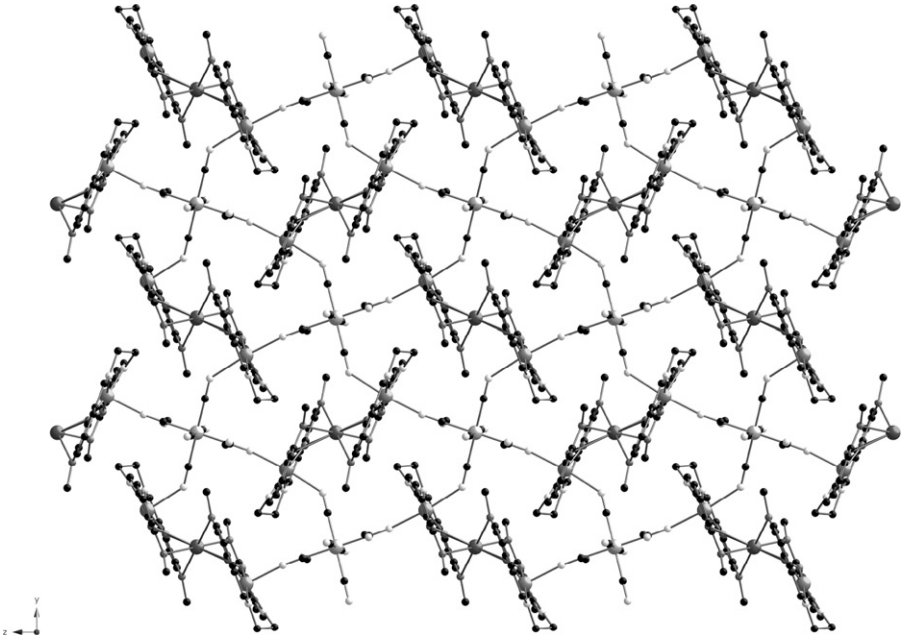

Fig. 50. Two-dimensional network structure of $K[\{Mn^{III}(3\text{-}MeOsalen)\}_2\{Fe^{III}(CN)_6\}]\cdot 2DMF$ [111].

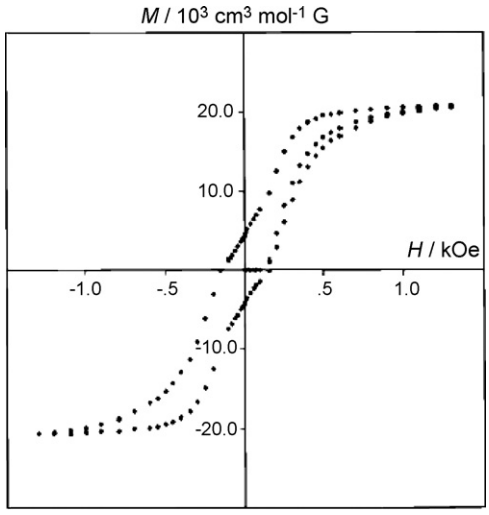

Fig. 51. Hysteresis loop (M ($N\mu_B$) vs. H) at 4.5 K for crystalline sample of $K[\{Mn^{III}(3\text{-MeOsalen})\}_2\{Fe^{III}(CN)_6\}]\cdot 2DMF$. Reproduced with permission from Ref. [111].

magnetization and zero-field cooled magnetization at very weak external fields [82].

$(NEt_4)[\{Mn^{III}(salen)\}_2\{Fe^{III}(CN)_6\}]$ (bonds and angles: Mn–N_1 = 2.266(3) Å, Mn–N_2 = 2.337(3) Å, Mn–N_1–C_1 = 167.8(3)°, and Mn–N_2–C_2 = 146.2(2) Å) (Fig. 52) [151] and $(NEt_4)[\{Mn^{III}(5\text{-Clsalen})\}_2\{Fe^{III}(CN)_6\}]$ (bonds and angles: Mn–N_1 = 2.286(7) Å, Mn–N_2 = 2.266(7) Å, Mn–N_1–C_1 = 154.4(7)°, and Mn–N_2–C_2 = 146.1(7) Å) [112] having a typical anionic network with the $[-Mn^{III}-NC-M-CN-]_4$ cyclic repeat units had intra-layer ferrimagnet order at 7.7 and 10.3 K, respectively, but the latter became finally a metamagnet at low temperatures below T_N = 4 K due to inter-layer antiferromagnetic interactions. The former displayed a sharp peak in both in-phase (χ') and out-of-phase (χ'') ac susceptibilities at T_c, illustrating typical 3D magnet behavior (above 1.8 K) (Fig. 53a). However, heat capacity measurements revealed the presence of another phase transition at 0.78 K [152]. In addition, the existence of strong magnetic anisotropy was confirmed through single-crystal magnetic measurements. Although the Jahn–Teller axes of the Mn(III) ions lie on a layer, at temperatures below T_c, the easy axis is directed perpendicular to the layer (Fig. 53b).

Three other compounds with Mn:M = 2:1 formula will be introduced. The use of a square-planar $[Ni^{II}(CN)_4]^{2-}$ building block (which is diamagnetic) instead of $[M^{III}(CN)_6]^{3-}$ produced a similar distorted square-glide network: $[\{Mn^{III}(salen)\}_2\{Ni^{II}(CN)_4\}]\cdot 0.5H_2O$ (Mn–N_{CN} = 2.312(6) Å, Mn–N–C = 163.8(6)°) (Fig. 54) [153]. From the magnetic data, two characteristics were suggested. One is that the Mn^{III} ion was assumed to have low-spin S = 1 character. Another is that the $[Mn^{III}(salen)]^+$ units were antiferromagnetically coupled through the diamagnetic $[Ni^{II}(CN)_4]^{2-}$ unit with $J = -3.2\,cm^{-1}$. These characters may be still doubtful. The former character might be due to the interconversion of cyanide bridge from Ni^{II}–CN–Mn^{III} to Ni^{II}–NC–Mn^{III}. Indeed, the [NC–Mn^{III}–CN] moiety is expected to show low-spin character. A similar network compound using $[Fe^{III}(CN)_5(NO)]^{2-}$ was also synthesized: $[\{Mn^{III}(5\text{-Brsalen})\}_2\{Fe^{III}(CN)_5(NO)\}]$ is a paramagnet with S_{Mn} = 2 [117]. The reaction of $[Mn^{III}(acacen)]^+$ with [K(18-

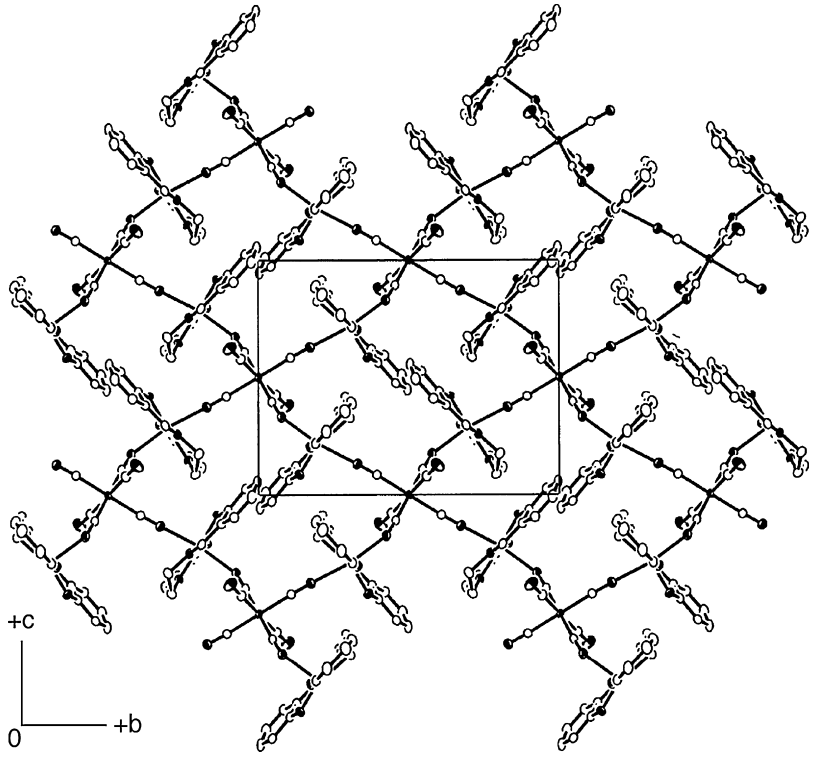

Fig. 52. Two-dimensional network structure of $(NEt_4)[\{Mn^{III}(salen)\}_2\{Fe^{III}(CN)_6\}]$. Reproduced with permission from Ref. [151].

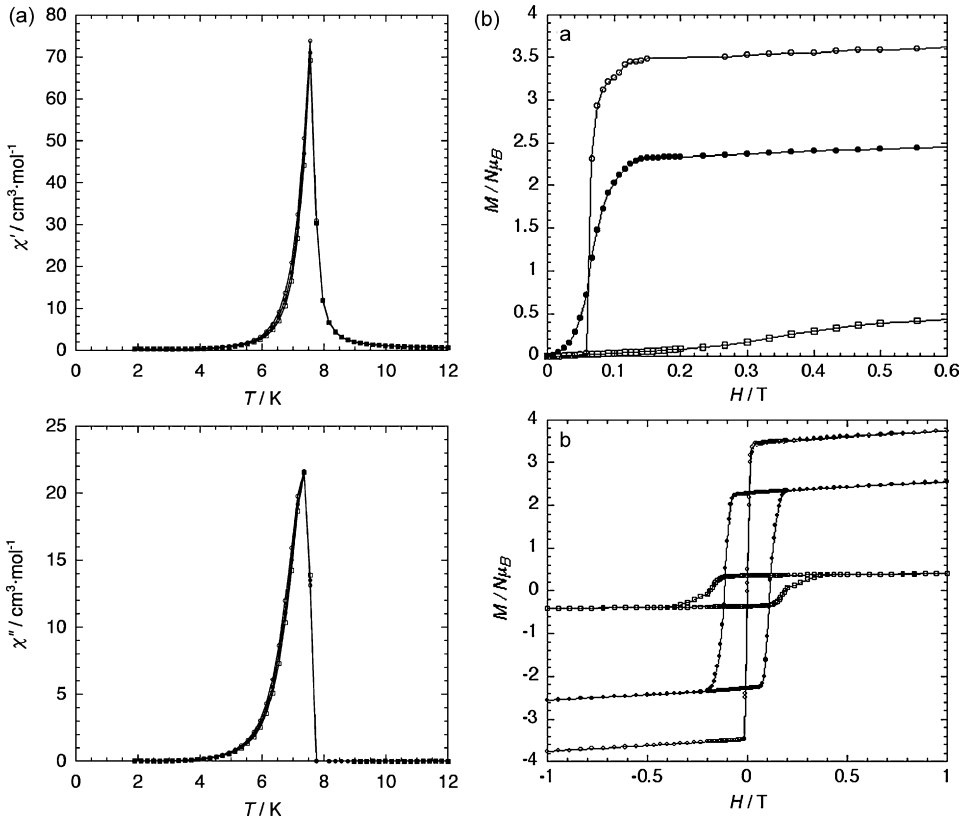

Fig. 53. Some magnetic data of $(NEt_4)[\{Mn^{III}(salen)\}_2\{Fe^{III}(CN)_6\}]$. (a) Temperature and frequency dependence of the real (χ') and imaginary (χ'') parts of the ac susceptibility: (◯) 800 Hz; (●) 1000 Hz; (□) 1200 Hz. (b) Field dependence of the magnetization on a direction-arranged single crystal when the external field was applied as *a*//H* (◯), *b//H* (□), and *c//H* (●), where the initial magnetization curve (a) and hysteresis loop at 1.9 K (b). Reproduced with permission from Ref. [152].

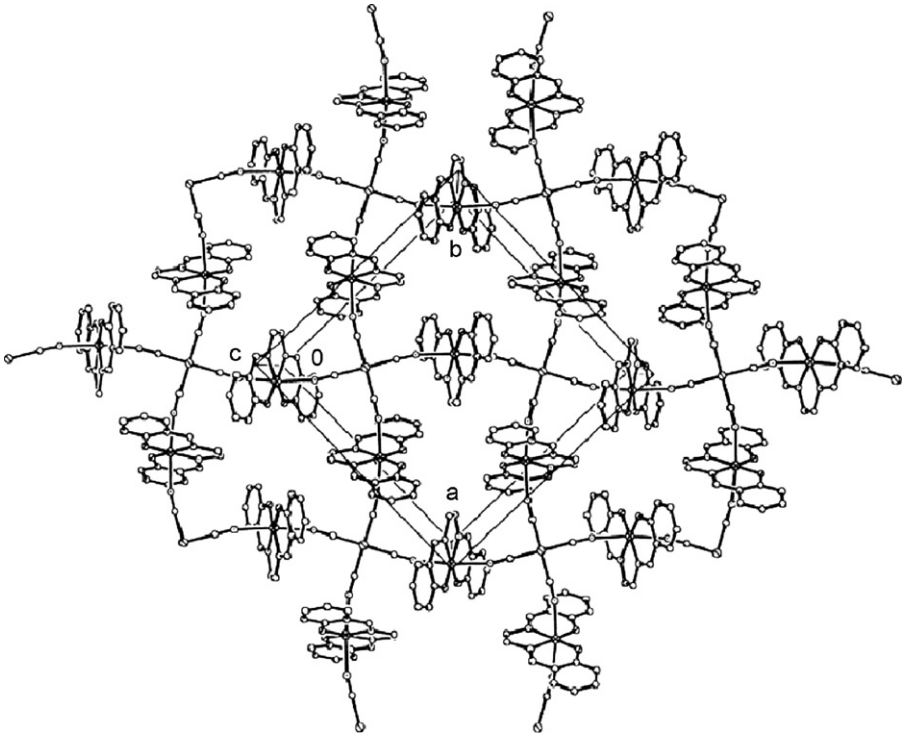

Fig. 54. Two-dimensional network structure of $[\{Mn^{III}(salen)\}_2\{Ni^{II}(CN)_6\}]\cdot 0.5H_2O$. Reproduced with permission from Ref. [153].

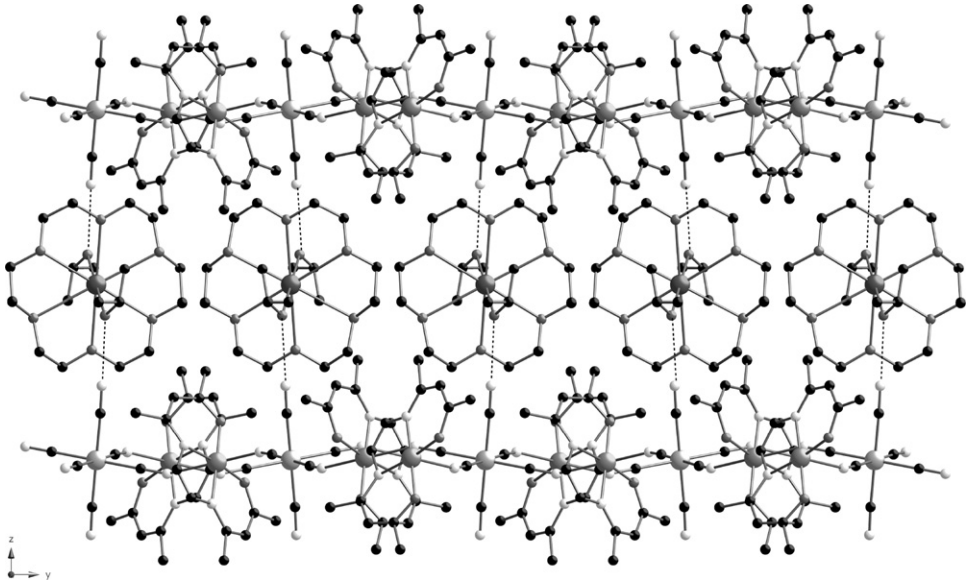

Fig. 55. Projections of hybrid layered structure of $[K(18\text{-cr-}6)(2\text{-PrOH})_2][\{Mn^{III}(acacen)\}_2\{Fe^{III}(CN)_6\}]$ onto the *bc* plane (left) and the *ac* plane (right) [154].

cr-6)$(H_2O)_2]_3[Fe(CN)_6]$ yielded a similar network compound: $[K(18\text{-cr-}6)(2\text{-PrOH})_2][\{Mn^{III}(acacen)\}_2\{Fe^{III}(CN)_6\}]$ (18-cr-6 = 18-crown-6-ether; bond and angles: Mn–N_1 = 2.331(3) Å, Mn–N_2 = 2.439(3) Å, Mn–N_1–C_1 = 152.0(3)°, and Mn–N_2–C_2 = 154.8(3)°) [154]. The interesting structural aspect can be seen in the formation of inter-layer stacking. The counter cations of $[K(18\text{-cr-}6)(2\text{-PrOH})_2]^+$ form 1D columns between the layers of $[\{Mn^{III}(acacen)\}_2\{Fe^{III}(CN)_6\}]^-$ by connecting through hydrogen-bonds between the 2-PrOH group and the naked –CN group of the layers (Fig. 55). The coexistence of intra-layer ferromagnetic order and inter-layer antiferromagnetic order provided metamagnetic behavior (T_N = 5.0 K and H_c = 1200 Oe).

The first Mn:Fe = 4:1 network compound was found in $[\{Mn^{III}(saltmen)\}_4\{Fe^{III}(CN)_6\}]ClO_4$ (Fig. 56) [111]. In this compound, Fe and two cyanide (*trans*-position) groups lie on a fourfold rotation axis, and each of the four equatorial CN^- ligands coordinates axially to a Mn from a $[Mn^{III}(saltmen)]^+$ moiety, forming a four-blade propeller-like unit (Mn–N_{CN} = 2.19(1) Å and Mn–N–C = 156.1(10)°). This symmetrical pentanuclear unit interacts with four neighboring units by forming an out-of-plane dimeric moiety in the $[Mn^{III}(saltmen)]^+$ moieties as shown in Section 4, consequently constructing a 2D network having a dodecanuclear $[-Mn^{III}-(O_{Ph})_2-Mn^{III}-NC-Fe^{III}-CN-]_4$ cyclic repeat unit. Therefore, the Mn(III) ion has a distorted square bipyramidal geometry, in which the two apical sites are occupied by the nitrogen atom from $[Fe^{III}(CN)_6]^{3-}$ and the phenoxy oxygen atom from an adjacent $[Mn^{III}(saltmen)]^+$ moiety, displaying a Jahn–Teller distortion with distances of Mn–N_{CN} = 2.19(1) Å and Mn–O_{Ph} = 2.847(9) Å. The temperature dependence of χT of this compound displayed ferromagnetic exchange in both pathways of Mn–NC–Fe and Mn–$(O_{Ph})_2$–Mn, finally exhibiting a 3D magnetic order at low temperature below T_c = 4.5 K. A compound having a similar repeat unit was then synthesized using $[Fe^{III}(CN)_5(CH_3im)]^{2-}$ by Kou et al.: $[\{Mn^{III}(saltmen)\}_4\{Fe^{III}(CN)_5(CH_3im)\}](ClO_4)_2$ (Mn–N_{CN} = 2.197(8) Å, Mn–O_{Ph} = 2.844(8) Å, Mn–N–C = 157.3(7)°) [116]. The dc magnetic measurements displayed similar magnetic properties (J = 2.34(7) cm^{-1}, g = 2.04(2), zJ' = 0.036(4) cm^{-1}) exhibiting a long-range order at T_c = 4.8 K.

The use of polycyano polymetal clusters instead of $[M(CN)_6]^{3-}$ produced two kinds of 2D networks. One is $(NMe_4)_2[\{Mn^{III}(salen)\}_2\{Nb_6Cl_{12}(CN)_6\}]$, where $[Nb_6Cl_{12}(CN)_6]^{4-}$ is an octahedral edge-bridged niobium cyano-chloride cluster [120]. Using four equatorial NC– groups, this compound forms a distorted square-glide 2D network (Fig. 57). Another is $[\{Mn^{III}(salen)\}_4\{Re_6Te_8(CN)_6\}]$, where $[Re_6Te_8(CN)_6]^{4-}$ is a face-capped octahedral rhenium cyano-tellurium cluster [155]. In this compound, all six cyanide groups of $[Re_6Te_8(CN)_6]^{4-}$ are shared by $[Mn^{III}(salen)]^+$, four of which form a network like a twisted rope and the other two of which have a terminal $[Mn^{III}(salen)]^+$ unit. The twisted ropes interconnected through the terminal $[Mn^{III}(salen)]^+$ units, form a 2D network. The magnetic interactions in these compounds are diluted because of using diamagnetic clusters, but their structures are very interesting. In particular, to use such large clusters in the assemblies with Mn(III) salen complexes would make it possible to design higher-dimensional structures. Indeed, such an assembly yielded a Prussian blue-type 3D network described in the next section.

5.4. Three-dimensional networks

There is no report of complete coordinated 3D networks using simple polycyano metallate ions such as $[M(CN)_6]^{3-}$, but there are two compounds based on polycyano polymetal clusters. $Na[\{Mn^{III}(salen)\}_3\{Re_6Se_8(CN)_6\}]$ has been synthesized by Kim et al., where $[Re_6Se_8(CN)_6]^{4-}$ is a face-capped octahedral rhenium cyano-selenium cluster similar to $[Re_6Te_8(CN)_6]^{4-}$ [156]. The six cyanide groups of

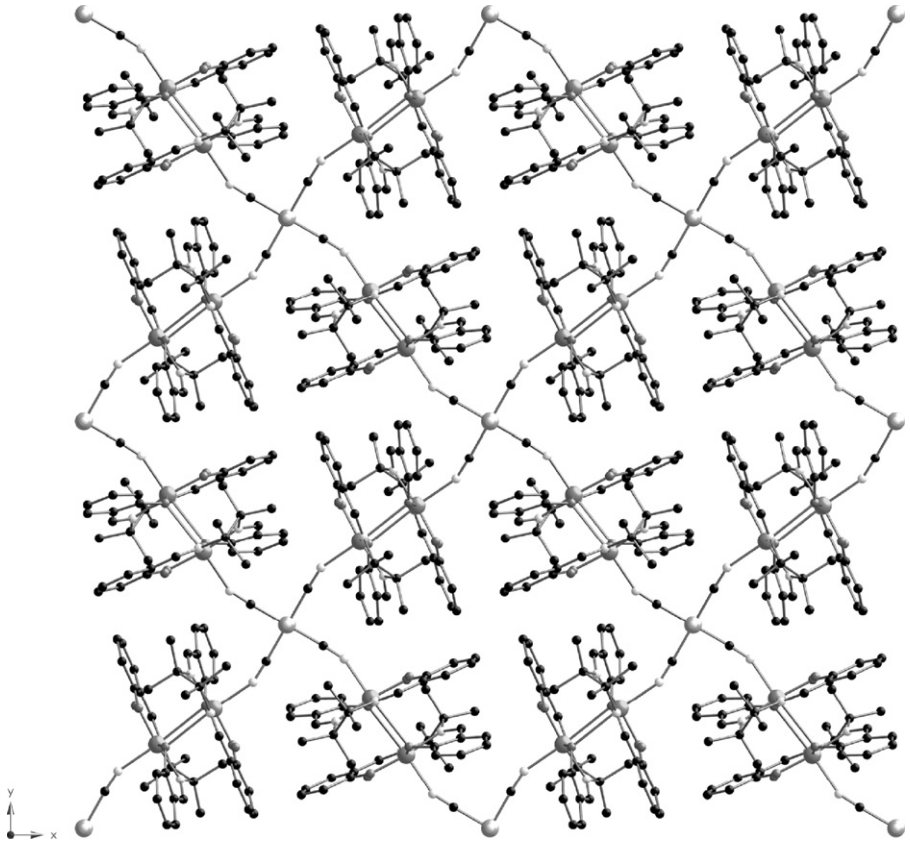

Fig. 56. Two-dimensional network structure of $[\{Mn^{III}(saltmen)\}_4\{Fe^{III}(CN)_6\}]ClO_4$ [111].

$[Re_6Se_8(CN)_6]^{4-}$ coordinate to three $[Mn^{III}(salen)]^+$ moieties without breaking coordination bond of Re–CN–Mn^{III}–NC–Re, forming a complete coordinated 3D framework like a Prussian blue (Fig. 58). The compound crystallized in the high symmetry rhombohedral space group $R\bar{3}c$. The authors demonstrated that changing Q (Te or Se) in a $[Re_6Q_8(CN)_6]^{4-}$ cluster can control the dimensionality in making infinite framework materials. Another 3D compound is $(H_3O)_2[\{Mn^{III}(salen)\}_6\{Fe^{II}(CN)_6\}\{Nb_6Cl_{12}(CN)_6\}]\cdot 3H_2O$ reported by Lachgar et al. [157]. In this compound, two kinds of units, $[Fe^{II}(CN)_6]^{4-}$ and $[Nb_6Cl_{12}(CN)_6]^{4-}$, built nodes connected by $[Mn^{III}(salen)]^+$ moieties via Fe^{II}–CN–Mn^{III}–NC–Nb linkage. Each node coordinates to six $[Mn^{III}(salen)]^+$ moieties, forming a Prussian blue-like 3D framework (Fig. 59). The compound crystallized in the rhombohedral space group $R\bar{3}$. Despite the fact that $[Fe^{II}(CN)_6]^{4-}$ and $[Nb_6Cl_{12}(CN)_6]^{4-}$

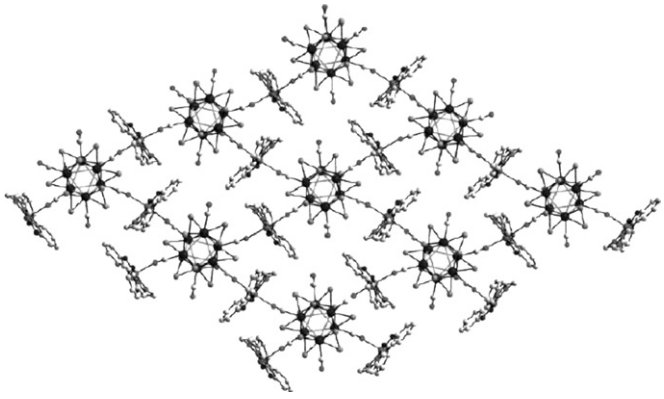

Fig. 57. Two-dimensional network structure of $(NMe_4)_2[\{Mn^{III}(salen)\}_2\{Nb_6Cl_{12}(CN)_6\}]$. Reproduced with permission from Ref. [120].

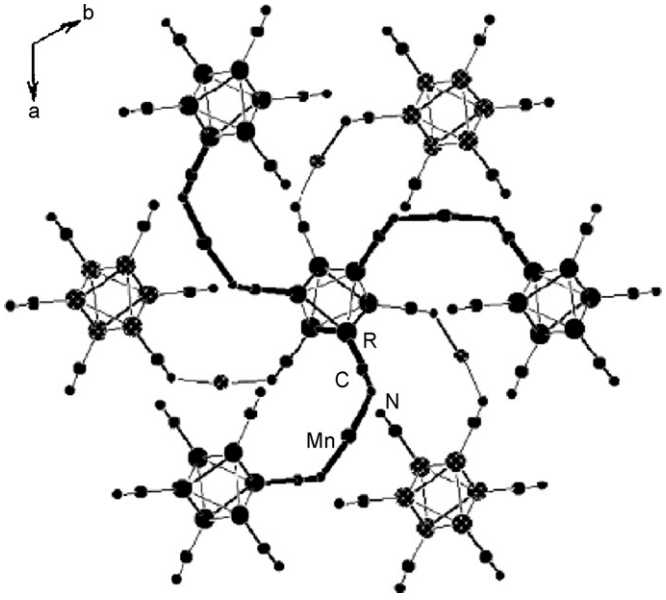

Fig. 58. Three-dimensional network in $Na[\{Mn^{III}(salen)\}_3\{Re_6Se_8(CN)_6\}]$. A Re_6Se_8 unit surrounded by six $[Mn^{III}(salen)]^+$ units which are linked to other six Re_6Se_8 units. Reproduced with permission from Ref. [156].

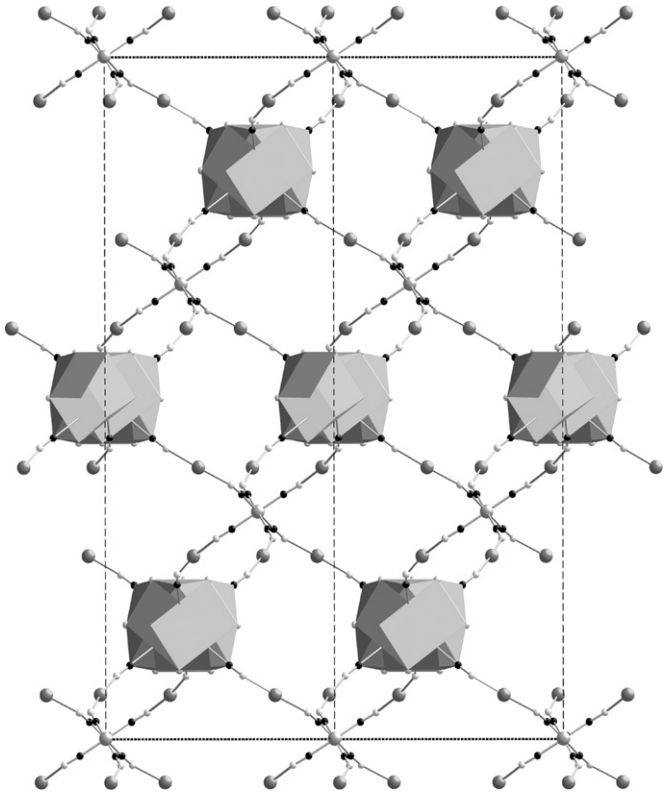

Fig. 59. (a) A projection of the overall structure of $(H_3O)_2[\{Mn^{III}(salen)\}_6\{Fe^{II}(CN)_6\}\{Nb_6Cl_{12}(CN)_6\}]\cdot 3H_2O$. (b) A schematic diagram showing the pseudocubic lattice and the connectivity between $[Fe^{III}(CN)_6]^{4-}$ and $[Nb_6Cl_{12}(CN)_6]^{4-}$ nodes through $[Mn^{III}(salen)]^+$ [157].

are both diamagnetic, the temperature-dependent effective moment displayed a contribution from ferromagnetic exchange. However, the origin of this contribution is not yet completely understood.

6. Final remarks

In the design of molecular-based magnetic materials, the synthetic strategy using an assembly of "a coordination-donor building block" and "a coordination-acceptor building block" is an effective way to discover new magnetic materials, and concomitantly, to develop materials chemistry and physics in the past decade. As summarized in this review, the family of Mn salen complexes is an excellent candidate for such coordination-acceptor building blocks. In particular, Mn(III) complexes with the *quasi-planar form* of the salen ligand acts as a *trans*-bi-coordination-acceptor unit (linear-type linker). Since the coordination-acceptor sites in this form correspond to the elongated Jahn–Teller axis, the coordination ability and mode (e.g., bond distance) are sensitively affected by: (i) equatorial ligand fields from the salen ligand used, (ii) the coordination-donor ability or ligand field of a given axial ligand, and (iii) packing effects of the assembled compounds. For example, as seen Mn(III) salen complexes/hexacyanometallate ($[M^{III}(CN)_6]^{3-}$) family, the assembled forms are of great variety, with dimensionality from discrete to 2D network and in various Mn:M formulation ratios from 1:1 to 6:1 dependent on Schiff-base ligands, solvents, and counter ions used. These assemblies reveal various intriguing magnetic properties involving well-defined superparamagnetism and bulk magnetism.

Here, there should be emphasis on superparamagnetism in Mn(III) salen assemblies. The Mn(III) salen complexes act not only as a simple paramagnetic building blocks but also as a uniaxial anisotropic building block useful for design of SMM or SCM, which generates a relative large anisotropy of $D_{Mn}/k_B \approx -1$ to -8 K. The Jahn–Teller axis corresponds to the magnetic easy axis. When these complexes are assembled into a linear form with a *trans*-bridging ligand or *trans*-coordination-donor unit, the individual Mn^{III} Jahn–Teller axes are necessarily aligned to the bridging direction. This synthetic strategy is especially useful for the design of SCMs, leading to a simple system with an easy axis of the magnetization parallel to the chain direction. The SCM system dramatically varies its magnetic properties dependent on intra-chain exchange. Therefore, the family of chains constructed using tunable Mn(III) salen complexes in the above synthetic manner provides useful data to understand the mechanism of the SCM system.

Finally, we would like to stress that further studies on assemblies of Mn salen complexes would increase the possibility of discovering new magnetic materials.

Acknowledgements

This paper is dedicated to present and past members of the Miyasaka research group and to our collaborators, whose efforts contributed to the advancement of our research on magnetic assemblies based on Mn(III) salen complexes. H.M. thanks PRESTO and CREST projects of JST, and a Grant-in-Aid for Scientific Research on Priority Areas ("Chemistry of Coordination Space," Grant No. 18033042) from the Ministry of Education, Culture, Sports, Science, and Technology, Japan, which have financially supported recent our research.

References

[1] K. Wieghardt, Angew. Chem. Int. Ed. Engl. 28 (1989) 1153.
[2] R. Manchanda, G.W. Brudvig, R.H. Crabtree, Coord. Chem. Rev. 144 (1995) 1.
[3] V.L. Pecoraro, M.J. Baldwin, A. Gelasco, Chem. Rev. 94 (1994) 807.
[4] E.J. Lanson, V.L. Pecoraro, in: E.J. Lanson, V.L. Pecoraro (Eds.), Introduction to Manganese Enzymes, VCH, New York, 1992, p. 1.
[5] G.C. Dismukes, Y. Siderer, Proc. Natl. Acad. Sci. U.S.A. 78 (1981) 274.
[6] J.C. de Paula, G.W. Brudvig, J. Am. Chem. Soc. 107 (1985) 2643.
[7] W.F. Beyer Jr., L. Fridrich, Biochemistry 24 (1985) 6460.
[8] W.F. Beyer Jr., I. Frodovich, Manganese in Metabolism and Enzyme Function, Academic Press, New York, 1989, p. 193.
[9] M.L. Ludwig, K.A. Pattridge, W.C. Stallings, Metabolism and Enzyme Function, Academic Press, New York, 1989, p. 405.
[10] A. Willing, H. Follman, G. Auling, Eur. J. Biochem. 170 (1988) 603.
[11] J.W. Gohdes, W.H. Armstrong, Inorg. Chem. 27 (1988) 1841.
[12] T. Katsuki, Coord. Chem. Rev. 140 (1995) 189.
[13] J.R. Chipperfield, J. Clayton, S.A. Khan, S. Woodward, Dalton Trans. (2000) 1087.
[14] W. Zhang, J.L. Loebach, S.R. Wilson, E.N. Jacobsen, J. Am. Chem. Soc. 112 (1990) 2801.
[15] E.N. Jacobsen, in: I. Ojima (Ed.), Catalytic Asymmetric Synthesis, VCH, New York, 1993, p. 159.

[16] K. Noda, N. Hosoya, R. Irie, Y. Ito, T. Katsuki, Synlett (1993) 469.
[17] Z. Li, K.R. Conster, E.N. Jacobsen, J. Am. Chem. Soc. 115 (1993) 5326.
[18] M. Palucki, P. Hanson, E.N. Jacobsen, Tetrahedron Lett. 33 (1992) 7111.
[19] K. Noda, N. Hosoya, K. Yanai, R. Irie, T. Katsuki, Tetrahedron Lett. 35 (1994) 1887.
[20] O. Kahn, Molecular Magnetism, VCH, New York, 1993.
[21] (a) M. Ohashi, T. Koshiyama, T. Ueno, M. Yanase, H. Fujii, Y. Watanabe, Angew. Chem. Int. Ed. 42 (2003) 1005;
(b) J.R. Carey, S.K. Ma, T.D. Pfister, D.K. Garner, H.K. Kim, J.A. Abramite, Z. Wang, Z. Guo, Y. Lu, J. Am. Chem. Soc. 126 (2004) 10812;
(c) T. Ueno, M. Ohashi, M. Kono, K. Kondo, A. Suzuki, T. Yamane, Y. Watanabe, Inorg. Chem. 43 (2004) 2852;
(d) T. Ueno, T. Koshiyama, M. Ohashi, K. Kondo, M. Kono, A. Suzuki, T. Yamane, Y. Watanabe, J. Am. Chem. Soc. 127 (2005) 6556.
[22] N.A. Law, T.E. Machonkin, J.P. McGorman, E.J. Larson, J.W. Kampf, V.L. Pecoraro, J. Chem. Soc., Chem. Commun. (1995) 2015.
[23] H. Asada, M. Fujiwara, T. Matsushita, Polyhedron 19 (2000) 2039.
[24] D. Feichtinger, D.A. Plattner, Chem. Eur. J. 7 (2001) 591.
[25] D. Feichtinger, D.A. Plattner, Angew. Chem. Int. Ed. Engl. 36 (1997) 1718.
[26] D.A. Plattner, D. Feichtinger, J. El-Bahroui, O. Wiest, Int. J. Mass Spectrom. 195/196 (2000) 351.
[27] D. Feichtinger, D.A. Plattner, J. Chem. Soc., Perkin Trans. 2 (2000) 1023.
[28] J. Du Bois, J. Hong, E.M. Carreira, M.W. Day, J. Am. Chem. Soc. 118 (1996) 915.
[29] C.J. Chang, W.B. Connick, D.W. Low, M.W. Day, H.B. Gray, Inorg. Chem. 37 (1998) 3107.
[30] N. Svenstrup, A. Bøgevig, R.G. Hazell, K.A. Jørgensen, J. Chem. Soc., Perkin Trans. 1 (1999) 1559.
[31] A.S. Jepsen, M. Roberson, R.G. Hazell, K.A. Jørgensen, Chem. Commun. (1998) 1599.
[32] H. Iwamoto, M. Tsuchimoto, S. Ohba, Acta Crystallogr. C 56 (2000) e187.
[33] E. Gallo, E. Solari, N. Re, C. Floriani, A. Chiesi-Villa, C. Rizzoli, J. Am. Chem. Soc. 119 (1997) 5144.
[34] M.R. Bermejo, A. Garcia-Deibe, J. Sanmartin, A. Sousa, N. Aurangzeb, C.E. Hulme, C.A. McAuliffe, R.G. Pritchard, M. Watkinson, J. Chem. Soc., Chem. Commun. (1994) 645.
[35] (a) G. Christou, D. Gatteschi, D.N. Hendrickson, R. Sessoli, MRS Bull. 25 (2000) 66;
(b) D. Gatteshi, R. Sessoli, Angew. Chem. Int. Ed. 42 (2003) 268;
(c) S.K. Ritter, Chem. Eng. News 82 (2004) 29;
(d) D. Gatteschi, R. Sessoli, J. Villain, Molecular Nanomagnets, Oxford University Press, 2006.
[36] A. Caneschi, D. Gatteschi, N. Lalioti, C. Sangregorio, R. Sessoli, G. Venturi, A. Vindigni, A. Rettori, M.G. Pini, M.A. Novak, Angew. Chem. Int. Ed. 40 (2001) 1760.
[37] R. Clérac, H. Miyasaka, M. Yamashita, C. Coulon, J. Am. Chem. Soc. 124 (2002) 12837.
[38] S. Mitra, Prog. Inorg. Chem. 22 (1977) 309.
[39] B.N. Figgis, Trans. Faraday Soc. 56 (1960) 1553.
[40] H.J. Gerritsen, E.S. Sabinsky, Phys. Rev. 132 (1963) 1507.
[41] B.J. Mennedy, K.S. Murray, Inorg. Chem. 24 (1985) 1552.
[42] E.J. Lanson, V.L. Pecoraro, J. Am. Chem. Soc. 113 (1991) 3810.
[43] E. Lanson, M.S. Lah, X. Li, J.A. Bonadies, V.L. Pecoraro, Inorg. Chem. 31 (1992) 373.
[44] N. Aurangzeb, C.A. McAuliffe, R.G. Pritchard, M. Watkinson, Acta Crystallogr. C 49 (1993) 1945.
[45] C.E. Hulme, M. Watkinson, M. Haynes, R.G. Pritchard, C.A. McAuliffe, N. Jaiboon, B. Beagley, A. Sousa, M.R. Bermejo, M. Fondo, J. Chem. Soc., Dalton Trans. (1997) 1805.
[46] H. Torayama, T. Nishide, H. Asada, M. Fujiwara, T. Matsushita, Polyhedron 17 (1998) 105.
[47] N.A. Law, J.W. Kampf, V.L. Pecoraro, Inorg. Chim. Acta 297 (2000) 252.
[48] M.R. Bermejo, A. Castiñeiras, J.C. Garcia-Monteagudo, M. Rey, A. Sousa, M. Watkinson, C.A. McAuliffe, R.G. Pritchard, R.L. Beddoes, J. Chem. Soc., Dalton Trans. (1996) 2935.
[49] M. Watkinson, M. Fondo, M.R. Bermejo, A. Sousa, C.A. McAuliffe, R.G. Pritchard, N. Jaiboon, N. Aurangzeb, M. Naeem, J. Chem. Soc., Dalton Trans (1999) 31.
[50] M. Maneiro, M.R. Bermejo, M. Fondo, A.M. González, J. Sanmartín, J.C. García-Monteagudo, R.G. Pritchard, A.M. Tyryshkin, Polyhedron 20 (2001) 711.
[51] Y. Ciringh, S.W. Gordon-Wylie, R.E. Norman, G.R. Clark, S.T. Weintraub, C.P. Horwitz, Inorg. Chem. 36 (1997) 4968.
[52] T.M. Rajendiran, M.L. Kirk, I.A. Setyawati, M.T. Caudle, J.W. Kampf, V.L. Pecoraro, Chem. Commun. (2003) 824.
[53] D. Huang, X. Zhang, H. Zhu, C. Chen, Q. Liu, Acta Crystallogr. E 57 (2001) m441.
[54] T.M. Rajendiran, M.T. Caudle, M.L. Kirk, I. Setyawati, J.W. Kampf, V.L. Pecoraro, J. Biol. Inorg. Chem. 8 (2003) 283.
[55] H.S. Maslen, T.N. Waters, J. Chem. Soc., Chem. Commun. (1973) 760.
[56] S.-F. Si, J.-K. Tang, D.-Z. Liao, Z.-H. Jiang, S.-P. Yan, J. Mol. Struct. 606 (2002) 87.
[57] N. Aurangzeb, C.E. Hulme, C.A. McAuliffe, R.G. Pritchard, M. Watkinson, M.R. Bermejo, A. Sousa, J. Chem. Soc., Chem. Commun. (1994) 2193.
[58] C. Chen, D. Huang, X. Zhang, F. Chen, H. Zhu, Q. Liu, C. Zhang, D. Liao, L. Li, L. Sun, Inorg. Chem. 42 (2003) 3540.
[59] J.A. Bonadies, M.L. Kirk, M.S. Lah, D.P. Kessissoglou, W.E. Hatfield, V.L. Pecoraro, Inorg. Chem. 28 (1989) 2037.
[60] J.E. Davies, B.M. Gatehous, K.S. Murray, J. Chem. Soc., Dalton Trans. (1973) 2523.
[61] N. Aurangzeb, C.E. Hulme, C.A. McAuliffe, R.G. Pritchard, M. Watkinson, A. Garcia-Deibe, M.R. Bermejo, A. Sousa, J. Chem. Soc., Chem. Commun. (1992) 1524.
[62] K.-L. Zhang, Y. Xu, C.-G. Zheng, Y. Zhang, Z. Wang, Z.-Z. You, Inorg. Chim. Acta 318 (2001) 61.
[63] S. Biswas, K. Mitra, C.H. Schwalbe, C.R. Lucas, S.K. Chattopadhyay, B. Adhikary, Inorg. Chim. Acta 358 (2005) 2473.
[64] F. Akhtar, M.G.B. Drew, Acta Crystallogr. B 38 (1982) 612.
[65] W. Chiang, D.M. Ho, D. Van Engen, M.E. Thompson, Inorg. Chem. 32 (1993) 2886.
[66] H.-L. Shyu, H.-H. Wei, Y. Wang, Inorg. Chim. Acta 290 (1999) 8.
[67] S. Sailaja, K.R. Reddy, M.V. Rajasekharan, C. Hureau, E. Riviére, J. Cano, J.-J. Girerd, Inorg. Chem. 42 (2003) 180.
[68] A. Panja, N. Shaikh, P. Vojtísek, S. Gao, P. Banerjee, N. J. Chem. 26 (2002) 1025.
[69] K.R. Reddy, M.V. Rajasekharan, J.-P. Tuchagues, Inorg. Chem. 37 (1998) 5978.
[70] H. Li, Z.J. Zhong, C.-Y. Duan, X.-Z. You, T.C.W. Mak, B. Wu, Inorg. Chim. Acta 271 (1998) 99.
[71] M. Yuan, S. Gao, H.-L. Sun, G. Su, Inorg. Chem. 43 (2004) 8221.
[72] Q. Shi, R. Cao, X. Li, J. Luo, M. Hong, Z. Chen, N. J. Chem. 26 (2002) 1397.
[73] (a) J.A. Schlueter, J.L. Manson, K.A. Hyzer, U. Geiser, Inorg. Chem. 43 (2004) 4100;
(b) J.L. Manson, C.D. Incarvito, A.L. Rheingold, J.S. Miller, J. Chem. Soc., Dalton Trans. (1998) 3705;
(c) S.R. Batten, P. Jensen, C.J. Kepert, M. Kurmoo, B. Moubaraki, K.S. Murray, D.J. Price, J. Chem. Soc., Dalton Trans. (1999) 2987;
(d) A. Claramunt, A. Escuer, F.A. Mautner, N. Sanz, R. Vicente, J. Chem. Soc., Dalton Trans. (2000) 2627;
(e) B.-W. Sun, S. Gao, B.-Q. Ma, D.-Z. Niu, Z.-M. Wang, J. Chem. Soc., Dalton Trans. (2000) 4187;
(f) J.W. Raebiger, J.L. Manson, R.D. Sommer, U. Geiser, A.L. Rheingold, J.S. Miller, Inorg. Chem. 40 (2001) 2578;
(g) A. Escuer, F.A. Mautner, N. Sanz, R. Vicente, Inorg. Chem. 39 (2000) 1668;
(h) S.R. Marshall, C.D. Incarvito, J.L. Manson, A.L. Rheingold, J.S. Miller, Inorg. Chem. 39 (2000) 1969;
(i) P.M. van der Werff, S.R. Batten, P. Jensen, B. Moubaraki, K.S. Murray, Inorg. Chem. 40 (2001) 1718;
(j) H.-H. Lin, S. Mohanta, C.-J. Lee, H.-H. Wei, Inorg. Chem. 42 (2003) 1584;

(k) J.L. Manson, A.M. Arif, C.D. Incarvito, L.M. Liable-Sands, A.L. Rheingold, J.S. Miller, J. Solid State Chem. 145 (1999) 369;
(l) S. Dalai, P.S. Mukherjee, E. Zangrando, N.R. Chaudhuri, N. J. Chem. 26 (2002) 1185.
[74] (a) H. Miyasaka, K. Nakata, K. Sugiura, M. Yamashita, R. Clérac, Angew. Chem. Int. Ed. 43 (2004) 707;
(b) H. Miyasaka, K. Nakata, L. Lecren, C. Coulon, Y. Nakazawa, T. Fujisaki, K. Sugiura, M. Yamashita, R. Clérac, J. Am. Chem. Soc. 128 (2006) 3770.
[75] M.R. Bermejo, M. Fondo, A. García-Deibe, A.M. González, A. Sousa, J. Sanmartín, C.A. McAuliffe, R.G. Pritchard, M. Watkinson, V. Lukov, Inorg. Chim. Acta 293 (1999) 210.
[76] N. Matsumoto, N. Takemoto, A. Ohyoshi, H. Okawa, Bull. Chem. Soc. Jpn. 61 (1988) 2984.
[77] H. Byrd, R.S. Buff, J.M. Butler, G.M. Gray, J. Chem. Crystallogr. 33 (2003) 515.
[78] H. Oshio, E. Ino, T. Ito, Y. Maeda, Bull. Chem. Soc. Jpn. 68 (1995) 889.
[79] H. Miyasaka, T. Madanbashi, K. Sugimoto, Y. Nakazawa, W. Wernsdorfer, K. Sugiura, M. Yamashita, C. Coulon, R. Clérac, Chem. Eur. J. 12 (2006) 7028.
[80] N. Petersen, J.W. Raebiger, J.S. Miller, J. Solid State Chem. 159 (2001) 403.
[81] N. Matsumoto, Y. Sunatsuki, H. Miyasaka, Y. Hashimoto, D. Luneau, J.-P. Tuchagues, Angew. Chem. Int. Ed. 38 (1999) 171.
[82] N. Re, E. Gallo, C. Floriani, H. Miyasaka, N. Matsumoto, Inorg. Chem. 35 (1996) 5964.
[83] M. Tsuchimoto, H. Iwamoto, M. Kojima, S. Ohba, Chem. Lett. (2000) 1156.
[84] W. Willing, R. Chridtophersen, U. Müller, K. Dehnicke, Z. Anorg. Allg. Chem. 555 (1987) 16.
[85] S.C. Critchlow, M.E. Lerchen, R.C. Smith, N.M. Doherty, J. Am. Chem. Soc. 110 (1988) 8071.
[86] D.M.-T. Chan, M.H. Chisholm, K. Folting, J.C. Huffman, N.S. Marchant, Inorg. Chem. 25 (1986) 4170.
[87] M.H. Chisholm, D.M. Hoffman, J.C. Huffman, Inorg. Chem. 22 (1983) 2903.
[88] W. Liese, K. Dehnicke, I. Walker, J. Strähle, Z. Naturforsch. 34B (1979) 693.
[89] N. Svenstrup, A. Bøgevig, R.G. Hazell, K.A. Jørgensen, J. Chem. Soc., Perkin Trans. (1999) 1559.
[90] D. Martínez, M. Motevalli, M. Watkinson, Acta Crystallogr. C 58 (2002) m258.
[91] A. Panja, N. Shaikh, M. Ali, P. Vojtísek, P. Banerjee, Polyhedron 22 (2003) 1191.
[92] V.L. Pecoraro, W.M. Butler, Acta Crystallogr. C 42 (1986) 1151.
[93] H. Miyasaka, T. Nezu, K. Sugimoto, K. Sugiura, M. Yamashita, R. Clérac, Chem. Eur. J. 11 (2005) 1592.
[94] Z. Lu, M. Yuan, F. Pan, S. Gao, D. Zhang, D. Zhu, Inorg. Chem. 45 (2006) 3538.
[95] H. Miyasaka, R. Clérac, T. Ishii, H.-C. Chang, S. Kitagawa, M. Yamashita, J. Chem. Soc., Dalton Trans. (2002) 1528.
[96] H. Miyasaka, R. Clérac, W. Wernsdorfer, L. Lecren, C. Bonhomme, K. Sugiura, M. Yamashita, Angew. Chem. Int. Ed. 43 (2004) 2801.
[97] Y. Sato, H. Miyasaka, N. Matsumoto, H. Okawa, Inorg. Chim. Acta 247 (1996) 57.
[98] S. Saha, D. Mal, S. Koner, A. Bhattacherjee, P. Gütlich, S. Mondal, M. Mukherjee, K. Okamoto, Polyhedron 23 (2004) 1811.
[99] R. Karmakar, C.R. Choudhury, G. Bravic, J.-P. Sutter, S. Mitra, Polyhedron 23 (2004) 949.
[100] N. Matsumoto, Z.J. Zhang, H. Okawa, S. Kida, Inorg. Chim. Acta 160 (1989) 153.
[101] M. Mikuriya, Y. Yamato, T. Tokii, Bull. Chem. Soc. Jpn. 65 (1992) 1466.
[102] A. Garcia-Deibe, A. Sousa, M.R. Bermejo, P.P. MacRory, C.A. McAuliffe, R.G. Pritchard, M. Hellowell, J. Chem. Soc., Chem. Commun. (1991) 728.
[103] K. Oyaizu, T. Nakagawa, E. Tsuchida, Inorg. Chim. Acta 305 (2000) 184.
[104] X. Li, V.L. Pecoraro, Inorg. Chem. 28 (1989) 3403.
[105] M.J. Baldwin, N.A. Law, T.L. Stemmler, J.W. Kampf, J.E. Penner-Hahn, V.L. Pecoraro, Inorg. Chem. 38 (1999) 4801.
[106] (a) J.B. Goodenough, Phys. Rev. 100 (1955) 564;
(b) J. Kanamori, J. Phys. Chem. Solids 10 (1959) 87.
[107] (a) C. Sangregorio, T. Ohm, C. Paulsen, R. Sessoli, D. Gatteschi, Phys. Rev. Lett. 78 (1997) 4645;
(b) S.M.J. Aubin, N.R. Dilley, L. Pardi, J. Krzystek, M.W. Wemple, L.-C. Brunel, M.B. Maple, G. Christou, D.N. Hendrickson, J. Am. Chem. Soc. 120 (1998) 4991.
[108] (a) W. Wernsdorfer, N. Aliaga-Alcalde, D.N. Hendrickson, G. Christou, Nature 416 (2002) 406;
(b) R. Tiron, W. Wernsdorfer, D. Foguet-Albiol, N. Aliaga-Alcalde, G. Christou, Phys. Rev. Lett. 91 (2003) 227203;
(c) R. Tiron, W. Wernsdorfer, N. Aliaga-Alcalde, G. Christou, Phys. Rev. B 68 (2003) 140407.
[109] L. Lecren, W. Wernsdorfer, Y.-G. Li, A. Vindigni, H. Miyasaka, R. Clérac, J. Am. Chem. Soc. 129 (2007) 5045.
[110] H. Miyasaka, H. Ieda, N. Matsumoto, N. Re, R. Crescenzi, C. Floriani, Inorg. Chem. 37 (1998) 255.
[111] H. Miyasaka, N. Matsumoto, H. Okawa, N. Re, E. Gallo, C. Floriani, J. Am. Chem. Soc. 118 (1996) 981.
[112] H. Miyasaka, N. Matsumoto, N. Re, E. Gallo, C. Floriani, Inorg. Chem. 36 (1997) 670.
[113] H.J. Choi, J.J. Sokol, J.R. Long, Inorg. Chem. 43 (2004) 1606.
[114] M. Ferbinteanu, H. Miyasaka, W. Wernsdorfer, K. Nakata, K. Sugiura, M. Yamashita, C. Coulon, R. Clérac, J. Am. Chem. Soc. 127 (2005) 3090.
[115] H. Miyasaka, H. Okawa, A. Miyazaki, T. Enoki, J. Chem. Soc., Dalton Trans. (1998) 3991.
[116] W.-W. Ni, Z.-H. Ni, A.-L. Cui, X. Liang, H.-Z. Kou, Inorg. Chem. 46 (2007) 22.
[117] M. Clemente-León, E. Coronado, J.R. Galán-Mascarós, C.J. Gómez-García, Th. Woike, J.M. Clemente-Juan, Inorg. Chem. 40 (2001) 87.
[118] T. Akitsu, Y. Takeuchi, Y. Einaga, Acta Crystallogr. E 61 (2005) m502.
[119] H. Miyasaka, N. Matsumoto, Chem. Lett. (1997) 427.
[120] H. Zhou, C.S. Day, A. Lachgar, Chem. Mater. 16 (2004) 4870.
[121] H. Miyasaka, H. Takahashi, T. Madanbashi, K. Sugiura, R. Clérac, H. Nojiri, Inorg. Chem. 44 (2005) 5969.
[122] P. Przychodzen, K. Lewinski, M. Balanda, R. Pelka, M. Rams, T. Wasiutynski, C. Guyard-Duhayon, B. Sieklucka, Inorg. Chem. 43 (2004) 2967.
[123] S.-F. Si, J.-K. Tang, Z.-Q. Liu, D.-Z. Liao, Z.-H. Jiang, S.-P. Yan, P. Cheng, Inorg. Chem. Commun. 6 (2003) 1109.
[124] X. Shen, B. Li, J. Zou, Z. Xu, Y. Yu, S. Liu, Trans. Met. Chem. 27 (2002) 372.
[125] X. Shen, B. Li, J. Zou, H. Hu, Z. Xu, J. Mol. Struct. 657 (2003) 325.
[126] H.J. Choi, J.J. Sokol, J.R. Long, J. Phys. Chem. Solids 65 (2004) 839.
[127] Z.-H. Ni, H.-Z. Kou, L.-F. Zhang, C. Ge, A.-L. Cui, R.-J. Wang, Y. Li, O. Sato, Angew. Chem. Int. Ed. 44 (2005) 7742.
[128] J.H. Yoo, J.H. Lim, H.C. Kim, C.S. Hong, Inorg. Chem. 45 (2006) 9613.
[129] R. Appelt, H. Vahrenkamp, Inorg. Chim. Acta 350 (2003) 387.
[130] H. Miyasaka, T. Nezu, K. Sugimoto, K. Sugiura, M. Yamashita, R. Clérac, Inorg. Chem. 43 (2004) 5486.
[131] C. Kachi-Terajima, H. Miyasaka, A. Saitoh, N. Shirakawa, M. Yamashita, R. Clérac, Inorg. Chem. 46 (2007) 5861.
[132] (a) J.P. Costes, F. Dahan, A. Dupuis, J.P. Laurent, N. J. Chem. 21 (1997) 1211;
(b) J.P. Costes, F. Dahan, A. Dupuis, J.P. Laurent, J. Chem. Soc., Dalton Trans. (1998) 1307;
(c) J.P. Costes, F. Dahan, A. Dupuis, J.P. Laurent, Inorg. Chem. 39 (2000) 169;
(d) J.P. Costes, F. Dahan, A. Dupuis, Inorg. Chem. 39 (2000) 5994.
[133] C. Kachi-Terajima, H. Miyasaka, K. Sugiura, R. Clérac, H. Nojiri, Inorg. Chem. 45 (2006) 4381.
[134] N. Matsumoto, H. Okawa, S. Kida, T. Ogawa, A. Ohyoshi, Bull. Chem. Soc. Jpn. 62 (1989) 3812.
[135] H. Miyasaka, R. Clérac, Bull. Chem. Soc. Jpn. 78 (2005) 1725.
[136] C. Coulon, R. Clérac, L. Lecren, W. Wernsdorfer, H. Miyasaka, Phys. Rev. B 69 (2004) 132408.
[137] C. Coulon, H. Miyasaka, R. Clérac, Struct. Bond 122 (2006) 163.

[138] H. Miyasaka, R. Clérac, K. Mizushima, K. Sugiura, M. Yamashita, W. Wernsdorfer, C. Coulon, Inorg. Chem. 42 (2003) 8203.
[139] A. Saitoh, H. Miyasaka, M. Yamashita, R. Clérac, J. Mater. Chem. 17 (2007) 2002.
[140] Y. Oshima, H. Nojiri, K. Asakura, T. Sakai, M. Yamashita, H. Miyasaka, Phys. Rev. B 73 (2006) 214435.
[141] J. Kishine, T. Watanabe, H. Deguchi, M. Mito, T. Sakai, T. Tajiri, M. Yamashita, H. Miyasaka, Phys. Rev. B 74 (2006) 224419.
[142] M. Mito, H. Deguchi, T. Tajiri, S. Takagi, M. Yamashita, H. Miyasaka, Phys. Rev. B 72 (2005) 144421.
[143] W. Wernsdorfer, R. Clérac, C. Coulon, L. Lecren, H. Miyasaka, Phys. Rev. Lett. 95 (2005) 237203.
[144] (a) K. Sugiura, S. Mikami, M.T. Johnson, J.S. Miller, K. Iwasaki, K. Umishita, S. Hino, Y. Sakata, J. Mater. Chem. 10 (2000) 959;
(b) M.T. Johnson, A.M. Arif, J.S. Miller, Eur. J. Inorg. Chem. 6 (2000) 1781.
[145] H.-R. Wen, C.-F. Wang, Y.-Z. Li, J.-L. Zuo, Y. Song, X.-Z. You, Inorg. Chem. 45 (2006) 7032.
[146] S. Wang, M. Ferbinteanu, M. Yamashita, Inorg. Chem. 46 (2007) 610.
[147] N. Re, E. Gallo, C. Floriani, H. Miyasaka, N. Matsumoto, Inorg. Chem. 35 (1996) 6004.
[148] H. Miyasaka, N. Matsumoto, H. Okawa, N. Re, E. Gallo, C. Floriani, Angew. Chem. Int. Ed. Engl. 34 (1995) 1446.
[149] Y. Miyazaki, Q.-S. Yu, T. Matsumoto, H. Miyasaka, N. Matsumoto, M. Sorai, Thermochim. Acta 431 (2005) 133.
[150] H. Miyasaka, H. Okawa, N. Matsumoto, Mol. Cryst. Liq. Cryst. 335 (1999) 303.
[151] H. Miyasaka, H. Ieda, N. Matsumoto, K. Sugiura, M. Yamashita, Inorg. Chem. 42 (2003) 3509.
[152] Y. Miyazaki, T. Sakakibara, H. Miyasaka, N. Matsumoto, M. Sorai, J. Therm. Anal. Cal. 81 (2005) 603.
[153] A.-H. Yuan, X.-P. Shen, Q.-J. Wu, Z.-X. Huang, Z. Xu, J. Coord. Chem. 55 (2002) 411.
[154] H. Miyasaka, H. Okawa, A. Miyazaki, T. Enoki, Inorg. Chem. 37 (1998) 4878.
[155] Y. Kim, S.-M. Park, W. Nam, S.-J. Kim, Chem. Commun. (2001) 1470.
[156] Y. Kim, S.-M. Park, S.-J. Kim, Inorg. Chem. Commun. 5 (2002) 592.
[157] J. Zhang, A. Lachgar, J. Am. Chem. Soc. 129 (2007) 250.